HUMAN SCALP HAIR: GEOMETRY, BIOCHEMISTRY, GROWTH PARAMETERS AND MECHANICAL CHARACTERISTICS

Kwezikazi Mkentane
MKNKWE002

A Thesis Presented for the Degree of
Doctor of Philosophy (Trichology & Cosmetic Science) in the Department of Medicine, University of Cape Town

Supervisor: Associate Professor Nonhlanhla P. Khumalo
Co-supervisor: Associate Professor Lester M. Davids
*****

December 2016

TABLE OF CONTENTS

ACKNOWLEDGEMENTS

I would like to thank the following people and institutions for their invaluable support throughout my doctoral degree journey; The National Research Foundation, the University of Cape Town's post grad funding office and the Medical Research Council for funding my doctoral studies.

The university's postgraduate community and academic staff for their research and admin support.

My supervisors; Associate Professors Nonhlanhla P. Khumalo and Lester M. Davids for their guidance and mentorship.

Dr Jeanne Rossouw for introducing me to molecular biology. May her soul rest in peace.

Mr Mohammed Jaffer and colleagues at the university's Electron Microscopy Unit for all their assistance with acquiring TEM ad SEM micrographs.

Dr Helene Nieuwoudt and Professor Martin Kidd from Stellenbosch University for the assistance with the analyses of FTIR data.

All Redox 'Labsters' past and present, for the camaraderie, humour and comments we have exchanged over a good spread of eats at our journal clubs and lab meetings.

The Kidson and Prince Laboratory members for their help with techniques and reagents.

My colleagues at The Hair and Skin Research lab, especially Miss Ntombenhle Sishi, Drs Jennifer Van Wyk and Malebogo Ngoepe for their invaluable support with various aspects of my project.

My family and friends for their support, patience and encouragement throughout the most demanding 4 years of my life thus far.

My beloved, for his love and support; the past 3 years would have been all the more challenging without your prayers, encouragement and humour. Kea leboga Motshweneng.

My mother, for her continuous support and prayers. Enkosi Mandulini.

And lastly, to God, the creator of all life for expressing His thoughts through me. Thank you for giving the grace for every assignment.

~ I love you God, You make me strong. You are a bedrock under my feet, the castle on which I live...~

ABBREVIATIONS

AA:	Amino Acids
ATR:	Attenuate total reflectance
CMC:	Cell membrane complex
DA:	Discriminative analysis
FFA:	Free fatty acids
FLM:	Fluorescence Light Microscopy
FTIR:	Fourier Transform Infrared
ISD:	Interscale distance
IQR:	Interquartile range
Min:	minutes
MPA:	Mega Pascal
MSE:	mean error squared
OPLS	Orthogonal partial least squares
SEM:	Scanning Electron Microscopy
SPVA:	Sulfo-phospho-vanillin assay
TEM:	Transmission Electron Microscopy
USA:	United States of America

SYMBOLS

α:	alpha
β:	beta
℃:	degrees celsius
δ:	delta
Ø:	diameter
g:	grams
ml:	millilitre
µ:	micro
cm^{-1}:	wavenumber

ABSTRACT

Scalp hair is increasingly being used as a testing substrate for toxins and for monitoring treatment adherence. The biochemistry of human hair is assumed to be similar, however, a recent study reported higher lipid content in African hair. The effect of hair curvature, if any, on drug incorporation (e.g. lipid soluble drugs) is unknown. Racial description of hair morphology is unscientific. A geometric classification of hair into 8 groups (I-straight to VIII-tightly curly) was recently proposed, however its reliability has not been confirmed.

The aim of this thesis was to investigate the reliability of the geometric classification (and to assess whether it could be improved) and to investigate relationships between hair morphology and other hair characteristics.

Virgin hair was collected from 128 volunteers using a standardized protocol. Geometric measurements to classify hair were carried out using published templates. Reliability was assessed using Kappa statistics.

Characteristics assessed included mechanical properties (miniature tensile tester), growth rate and hair density (TrichoScan® trichogram), biochemistry (Vanillin assay for lipids and Fourier Transform Infrared adsorption for lipids and amino acids) and imaging (Electron and Fluorescent Light Microscopy).

For geometric classification, the inter-observer agreement was poor for 8-groups (k=0.418) but improved for 6-groups (k=0.671). The intra-observer agreement also improved [ranges: k=0.444 to 0.648 (8-groups) and k=0.599 to 0.836 (6-groups)]. The yield strength of all hair groups was higher than usually reported for racially grouped samples. Curly hair groups had lower growth rates and tensile strengths. The TrichoScan based growth rate was fastest for the straightest (0.72 ± 0.3 cm/month) and slowest for the curliest (0.39 ± 0.2 cm/month) hair.

When the relationship between biochemistry and geometry was investigated, the analysis of FTIR spectra suggested a correlation with biochemistry (internal lipid content) for the extremes (i.e. straight versus curly) for both the 8 and 6-group hair classification while the inverse was observed for absorption of both amide I and II bands. A supervised statistical approach applied to 4 hair groups using the FTIR data improved classification success from (36.85% and 36.0% with the 8 and 6 groups) to

79% (range: 69% – 88%), which needs confirmation but would be more objective than using race as a visual descriptor for hair testing in Medical and Forensic Science.

This thesis therefore proposes a geometric classification with fewer groups (6, based kappa statistics of geometric measurements and 4, based on biochemistry); it is also the first, that we are aware of, to report correlations between hair geometry, biochemistry and physical properties on the same samples.

LIST OF FIGURES

LIST OF TABLES

CHAPTER ONE

1 INTRODUCTION AND LITERATURE REVIEW

Human hair plays an important role in psychosocial communication by functioning as a symbol of youth, beauty and health. Scalp hair is also an easy marker and expression of ethnic origin, culture and positioning within a society. Natural hair morphology varies widely across the world possibly due to diversity arising from heredity and environmental factors[1]. Human scalp hair has thermoregulatory, sensory and decorative (social communication) functions. Modification and maintenance of scalp hair has thus contributed significantly to a multibillion dollar cosmetic industry. Some of the often overlooked functions of scalp hair include protection against electromagnetic radiation, transportation of pheromones and sebum (from the skin surface)[2] as well as aiding in cleansing the skin surface of squames, dirt and parasites[2]. Hair is increasingly being used in forensic[3–5] and medical science to assess exposure to toxins[6–8] and monitor adherence to therapies, such as antiretroviral treatment [9–13]. Hair can also be investigated for its use as a substrate for biomarkers for stress[14–17] and testing for diabetes[18,19].

1.1 Human Scalp Hair Morphogenesis

The hair shaft is produced by the hair follicle portion of the pilosebaceous unit. The earliest evidence of human hair in the growing foetus is observed on the eyebrows and upper lip at 9 weeks[20]; by 12 weeks, all hair follicles across the body have started developing[20] into lanugo that is usually replaced just before (or soon after) birth[21,22]. The pilosebaceous unit starts as an invagination of the epidermis into the dermis and results from epidermal cells that cluster together, forming a placode over dermal fibroblast aggregates[23–25].These dermal fibroblasts are the precursors of the hair follicle dermal papilla (DP)[26,27].An experiment by Higgins *et al.* illustrated the induction of de novo hair follicles from cultured dermal papilla spheroids, providing evidence that the dermal papilla has all the necessary information for the induction of a hair follicle[27].The quantity of dermal cells has also been shown to influence hair size, morphology and cycling of the hair follicle and the reduction of these cells is reported

to lead to a decline in follicular numbers [26].Following interactions between the epidermal and mesenchymal cells, the dermal aggregates grow down as buds into the dermis and give rise to the epithelial portion of the hair follicle, which goes through eight morphological stages of induction to maturation as illustrated in Figure 1-1.

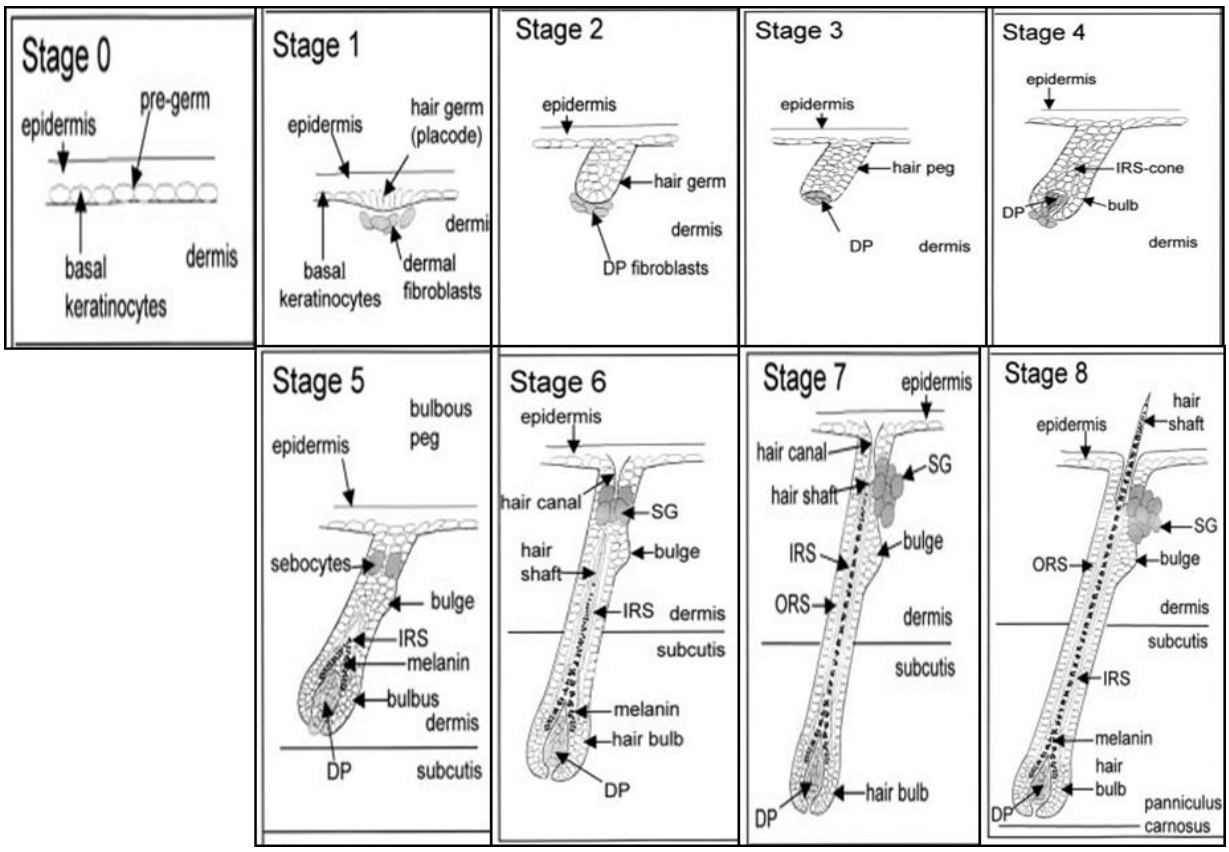

Figure 1-1 Schematic diagrams of hair follicle morphogenesis[24].

Using immunohistochemistry of murine hair, Paus *et al*. (1999) extensively described the physical changes that the hair follicle undergoes during morphogenesis[24]. During stage 1, the hair germ appears as an epidermal thickening with an increase in the number of dermal fibroblasts below the hair germ, coupled by a change in the orientation of the dermal fibroblasts. The hair germ then becomes elongated and has a convex proximal end and the dermal fibroblasts condense to form a cap below the hair germ at stage 2. A characteristic feature of stage 3 is a hair peg with a concave basal border and central keratinocytes that have a columnar arrangement. These columnar keratinocytes are organized radially to the follicular axis. In stage 4, the hair peg thickens further, becomes bulb-like and the inner root sheath (IRS) is formed. The dermal papilla (DP) cells are arranged in an elongated orientation and are partially

(50%) enclosed by the hair peg, becoming oval-shaped and almost completely enclosed at stage 5.

In addition to the changes to the DP at stage 5, the IRS is elongated halfway up the hair follicle, the bulge region appears, the first sebum producing cells, the sebocytes are observed and the first melanin granules are also seen in the pre-cortex. The sebocytes then form the sebaceous gland at stage 6 and hair canal is visible at this stage. The IRS starts developing at stage 6 and is reported to surround the hair shaft and grows up to the level of the hair canal and the DP becomes thinner and is completely enclosed by the hair matrix. The hair follicle matrix is comprised of a pool of cells that give rise to about 8 different cell lineages which can develop into the different components of the hair follicle (Figure 1-2). In the last two stages of hair follicle morphogenesis, the sebaceous gland localizes at the posterior wall of the hair follicle and the hair follicle acquires its maximum length, reaching the subcutaneous layer. The tip of the hair shaft leaves the IRS and enters the hair canal and emerges through the epidermis[24].

The schematic diagram in Figure 1-2 illustrates the 8 different cell lineages that eventually give rise to or provide the necessary environment for the transient and permanent portions of the hair follicle. The hair matrix cells around the bulb, the transient part of the hair follicle, are reported to be highly proliferative [23] and a single hair follicle produces 5-10μg of protein every 24hours[28] after a tightly regulated process called keratinization.

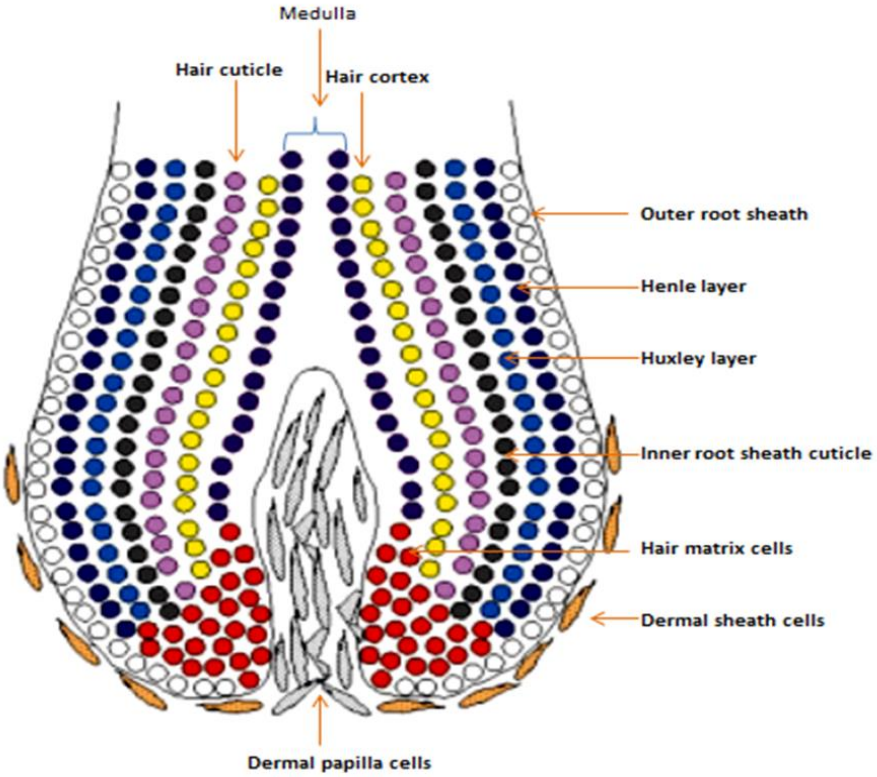

Figure 1-2 Schematic diagram showing the different cell lineages that give rise to the cycling hair follicle[28]

Keratinization, in the context of hair, is the protein synthesis process that eventually leads to a mature hair shaft[29]. During keratinization, cortical cells (keratinocyte cell of the cortex) terminally differentiate and are completely filled with keratin intermediate filaments and matrix, a complex that is further stabilized by disulphide linkages, and a transglutaminase enzyme[28,30]. The building blocks for the process of keratinization are fibrillar keratin intermediate filaments (KIFs) and matrix proteins or keratin associated proteins (KAPs)[30–33]. Intermediate filaments are named after their intermediate size between micro actin filaments and tubulin macro filaments[34].

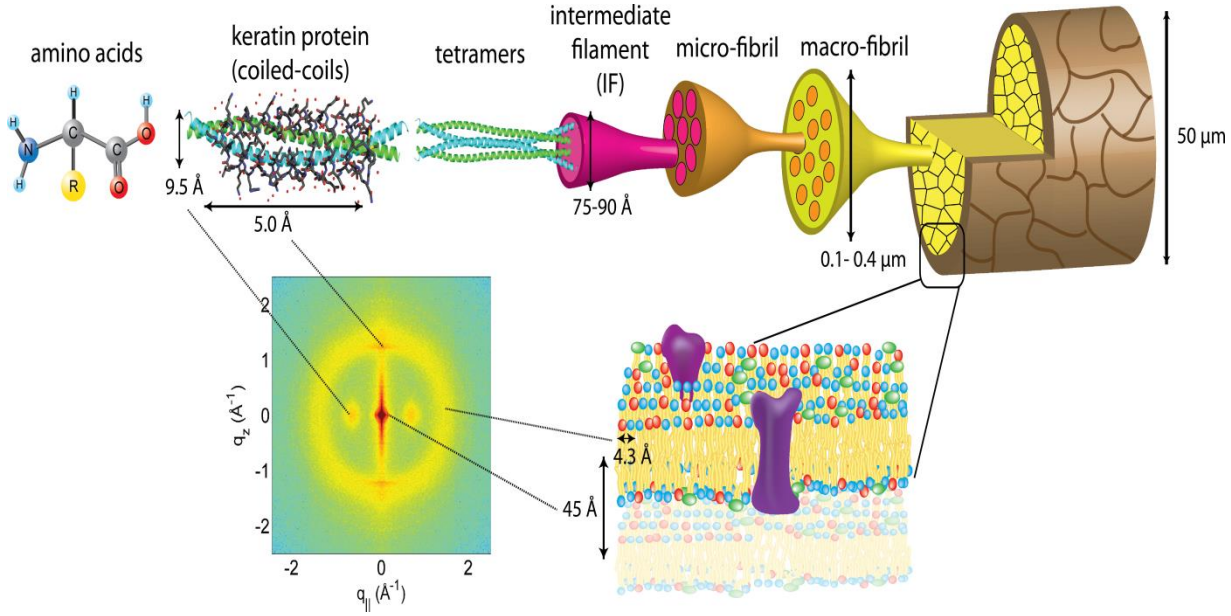

Figure 1-3 The hierarchical structure of the hair shaft[35].

Figure 1-3 is a hierarchical illustration of the hair shaft, showing the constituents that contribute to the different components and their X- Ray diffraction patterns[35]. Intermediate filament keratins are fibrous alpha proteins that can be classified into two groups according to their isoelectric points; Type I (acidic,40 - 50 kilo Daltons (kDa) and Type II keratins (neutral to basic keratins, 55-65kDa), with 9 and 11 members in each group respectively[36,37].

Intermediate filaments have low-sulphur content, while the matrix that surrounds them is sulphur-rich. The hair matrix is composed of high sulphur proteins (HSP), high glycine tyrosine (HGT) proteins, and non-high sulphur/high glycine tyrosine proteins. These are collectively called keratin associated proteins (KAPs). Matrix proteins have no helical content and have a molecular weight of 10-28 kDa. The time it takes for a keratinocyte cell to be completely keratinized upon entering the keratinization zone is said to be 48hrs [28].

The hair follicle is comprised of three main sections; the lower segment consisting of the bulb and supra-bulb (bulge),the middle segment (isthmus), and the upper segment (infundibulum) as shown in Figure 1-4[38]. Within the infra-infundibulum section is the Inner root sheath (IRS), a component that has been described as the mould of the hair

shaft[39,40]. The inner root sheath is made up of the four layers; the Companion, Henley's and Huxley's layers as well as the inner root sheath cuticle. The IRS ends at the opening of the sebaceous gland. The sebaceous gland forms part of the isthmus region and has been suggested to release proteases that lead to the degradation of the IRS[28,41] allowing the mature hair shaft to be covered in protective sebum as it makes an exit in the region of the infundibulum. The three innermost cell layers; the medulla, the cortex and the cuticle cells are what ultimately constitute the permanent hair shaft that emerges out of the epidermis (Figure 1-4). These components are discussed under section 1.4.

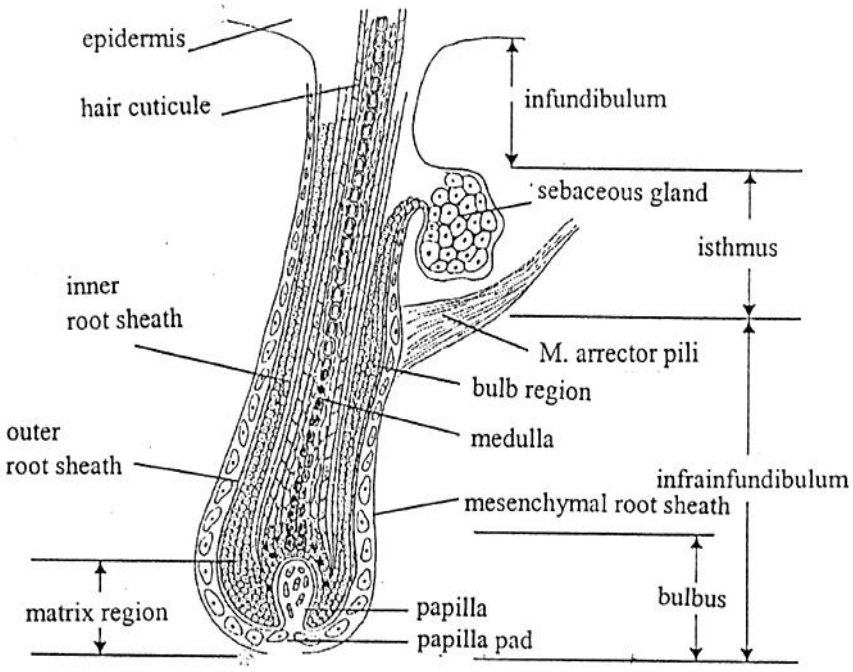

Figure 1-4 The different zones of growth and structural organization in the hair follicle[38].

1.1.1 The Hair Cycle

Throughout a lifetime, the hair follicle is constantly cycling[21,42] going through periods of growth, regression, rest and shedding. These are termed Anagen, Catagen, Telogen and Exogen as shown in Figure 1-5. Thermoregulation may have been the evolutionary force that resulted in adaption to seasonal variation and a cycling hair follicle[43].

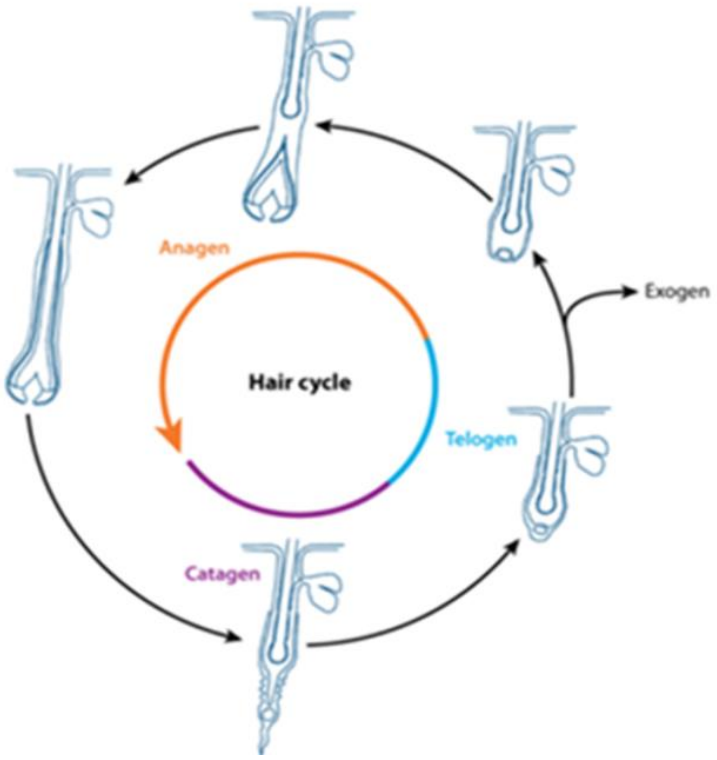

Figure 1-5 A schematic illustration of the stages of the hair cycle. The level and shape of the DP changes at the various stages[44]

Anagen: The anagen phase is a period where the hair is actively growing, the terminative epithelial cells of the bulb continuously proliferate, undergo programmed cell death and terminally differentiate, becoming fully keratinized[29,45]. This phase of the hair cycle is the longest for scalp hair follicles, lasting 3 - 5 years [44]. During this phase, hair follicles continuously produce hair fibres at a rate of 0.3 to 0.5mm/day[46,47].

Catagen: This phase is the regression phase of the hair cycle where the transient part of the HF undergoes apoptosis[42,48,49] and the DP is retracted upwards to the surface, stopping at the level of the stem cell niche when it reaches the resting phase. The Catagen phase is brief and lasts for 2-3 weeks[42,46].

Telogen: The resting phase lasts 2 – 4 months[46,48]. In this phase of the hair cycle, the dermal papilla retracts upwards to the level of the sebaceous gland and just below the stem cell bulge[46]. This positions the hair bulb perfectly for the stem cells to migrate to populate the hair matrix, giving rise once again to all the cell lineages of the transient portion of the hair follicle, marking the beginning of another anagen phase[44,48,50,51].

Exogen: The Exogen phase has been defined as the shedding of the club hair at the end of the resting phase[25,52]. Hair shedding is described as being independent of the hair cycle and occurs without any influence from the anagen phase[48,53].

The length of each phase in the hair cycle is regulated and varies according to body site; very short on the forehead, longer on the eyebrows or eyelashes and longest on the scalp[22,39]. Further, each HF or follicular unit has its own hair cycle clock[47,54,55]. The exact mechanisms of how hair cycle clocks are regulated have not been elucidated[24] but contributions from the dermal papilla are hypothesized[47].

Two different types of hairs are present across the bodies of children and adults (i.e. vellus and terminal).Vellus hairs are fine and usually not pigmented and cover most of the body and often invisible (e.g. on the cheeks), while terminal hairs are large and pigmented[39].Terminal hair follicles tend to go deep into tissue while vellus hair follicles are superficial. The transition between vellus and terminal, arising from hormonal changes, is classically seen at the onset of puberty [21,22,53,56]. In males, androgens are reported to convert vellus hair to terminal hair on the beard and other sites during puberty. Interestingly, androgens can also turn terminal head hair into vellus hair in genetically predispose individuals resulting in common male pattern baldness; this phenomenon has been called the Androgen paradox[56].

1.2 Morphology of human scalp hair

Various factors that contribute to the morphology of the hair fibre have been reported over the years. In a 1938 review by Trotter[57], Duclert (in 1824) is quoted as having suggested that hair curl depends on the shape of the hair follicle[57]. The explanation for this thought was given by Grotte in 1867.In 1882 T.P.A Stuart also attributed the curl pattern of negroid hair to a hair follicle that displayed curvature and reported that the curvature is a fourth of a circle, which was less than Grotte's observation that it was a half-circle[57]. In 1889, Fritsch observed that the dermal papilla was the structure in the hair bulb that determined hair morphology. He showed that kidney-shaped

dermal papillae resulted in flattened hair and that Europeans usually had round dermal papillae while Africans sometimes had what he called “twin-papillae”[57].

In 1897, J. Pohl Pincus looked at histological sections of Caucasian hair and saw that the hair was dived in 3 parts; an upper part of the deepest third section where cells appeared to be well-organised and fused together, a middle section that had uniform circular cross-section. The last section he observed to be superficial, and seemed to abruptly change in shape where it met with the middle. He also observed that at this position, the inner root sheath disappeared.

In recent times, these observations were confirmed by other researchers[40,58,59]. Using computer-aided reconstruction of scalp biopsy samples, Lindelof demonstrated that hair emerged from follicles at a right angle to the surface of the scalp for Asian hair and at an acute angle for African hair resulting in straight and curly hair respectively[59], while Thibaut *et al*.2005 observed that hair follicles collected from African volunteers were curved with a retro-curvature and that their bulbs were bent[40]. More recently, Thibaut *et al*. also showed, using immunohistochemistry, that the proliferation of hair matrix cells was asymmetrical in curved hair follicles[40,60]. Another recent study used mouse models to show that the size and shape of the dermal papilla dictates hair shaft morphology and thickness and that the depletion of DP cells results in smaller hair fibres[26].

1.3 Hair Classification Methods

Hair morphology and other visible physical characteristics have widely been used by anthropologists as one of the key distinguishing characteristics in allocating racial groups[57]. However, natural hair morphology varies widely across the world possibly due to diversity arising from heredity and environmental factors[61]. Further, curvature within racial groups (especially Caucasian) is not uniform[62,63]. This makes race an unreliable surrogate for hair curl. Various hair classification approaches have been proposed in different fields.

1.3.1 Classifications by anthropologists

In 1938, Trotter compiled a comprehensively inventory of hair classification systems that existed in that period, their origins and applications[57]. Trotter and earlier workers described the nature of hair as the hair's appearance, behaviour or habit. The observed habits were that hair tends to either hang straight, wave deeply or have curls that form ringlets[57]. Trotter cites Herodutus as being the first person to make inferences of race based on hair appearance or morphology when he divided Xerxes' army into straight and "woolly" hair groups[57]. In 1878 Topinards published an essay on the classification of human races using hair morphology as the main differentiator of external physical characteristics and the shape of the skull and skin colour only as secondary differentiators[57]. In 1853 Browne observed and made drawings of hair cross-sections and assigned mankind into three different species based on the shape of the hair cross-section[57]. These species he defined as follows:

A: The "cylindrical piled hair" cross-section, represented by a person of Indian descent.

B: The "oval piled hair" cross-section, represented by a white man.

C: The "eccentrically – elliptical piled", represent by a person of Negroid descent.

In addition to describing the cross-sections of the hair types that he drew, Browne also described the (microscopic and macroscopic) characteristics of the various hairs. His work was later supported by the work of Pruner-Bey in 1863, who examined the microscopic characteristics of hair cross-sections, correlated these with macroscopic observations and found that the flatter the hair tended to be, the more it would roll up', whereas the more round it was, the more inclined it was to be straight and 'smooth'. In 1860 Geoffroy Saint-Hilarie assigned racial groups based on how the hair exited the scalp surface, whether at an angle or straight[57].

Workers like Ranke (1890), however reviewed preceding hair-centred racial classifications and concluded that it was inadequate to distinguish races, as was skin pigmentation[57].

1.3.2 Classifications for the Cosmetic Industry

1.3.2.1 *The LOIS System*©

The LOIS system© classifies hair according to total strand shape in relation to the letters that spell out LOIS [64] as shown in Figure 1-6. Using this system, hairs that "bend, have right angles, with little or no curvature" are classified as L, while straight hair with no bends or curvature looks like the capital letter "I" and is thus classified as I. Hair groups with more curvature are classified as either "O" or "S"; the letter "S" also describes wavy hair, while the letter "O" describes hair fibres whose curvature tends to roll up into one or several zeros. People that have more than one obvious hair group are then described by a combination of letters[64]. A shortcoming of the LOIS system© is that it subjective and does not define guidelines about hair length requirements for the classification, and thus wavy hair that rolls up into a circle can be classified as an S or an O.

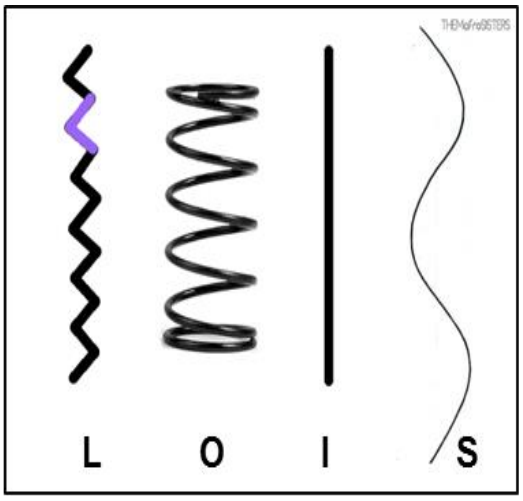

Figure 1-6 The LOIS hair classification[64]

1.3.2.2 *Andre Walker Hair Classification*

The Andre Walker hair classification (Figure 1-7) is widely used in the informal cosmetic industry and it classifies hair form into four main categories, 1 to 4, with the straightest hair being Type 1 and the hair with the greatest curvature being Type 4.

Figure 1-7 The Andre Walker hair typing system[65].

Each category is then subdivided into two or three descriptive sub-categories, which are subjectively described as straight and thin or kinky and 'wiry' as being soft, shiny, difficult to hold curl and fragile and tightly coiled respectively [66]. Further, this classification does not give length guidelines.

1.3.3 Geometric Hair Classifications

Over the years, modern researchers have increasingly heeded to Ranke's[57] assessment that race is an incorrect descriptor of hair curvature and others have echoed to call that use of race should be abandoned[67,68], a move that has resulted in

an attempt to develop more objective geometric classifications of hair morphology[63,69–71].

1.3.3.1 *Hrdy, Bailey& Schliebe Curve Diameter Classification*

The first objective hair classification was introduced by Hrdy who assessed hair form variation in seven populations (Bougainville, East Africa, Northwest European, Malaita, Sioux, Japan and Ifugao)[71]. Hrdy assessed the average diameter, medullation, scale count, kinking, average curvature, ratio of maximum to minimum curvature, crimp and ratio of natural to straight hair length then compared within and between population variations using F-tests. He found that the average curvature and ratio of curvature were the two most important variables in describing hair form. Using correlation matrices, Hrdy observed a strong correlation between curling variables (kinking, average curvature, ratio of maximum to minimum curvature, crimp and ratio of natural to straight length) while a weak correlation was observed between scale count and the curling variables.

Using principal component analysis (PCA), Hrdy found that 3 components (curling, size and regularity of curl) accounted for 80% of the variance in the data[71]. He also observed that the average curvature varied between populations and that it had the greatest contribution in differentiating between groups[71]. Bailey and Schliebe[70] later investigated the precision of this approach by measuring the hair curvature of 30 strands (6cm long) from the same individual three times on a template of circles of known radii (Figure 1-8). The two scientists also investigated the differences in average hair curvature within a limited genetic pool of 5 male members of the same family and found that there were distinct population distributions[70].

The relationship between ethnic origin and hair morphology was later investigated by De La Mettrie *et al*. in an experiment that included 1442 volunteers from 18 different countries[63]. De La Mettrie *et al*. and showed the distribution of hair morphology variation across the world[63] .

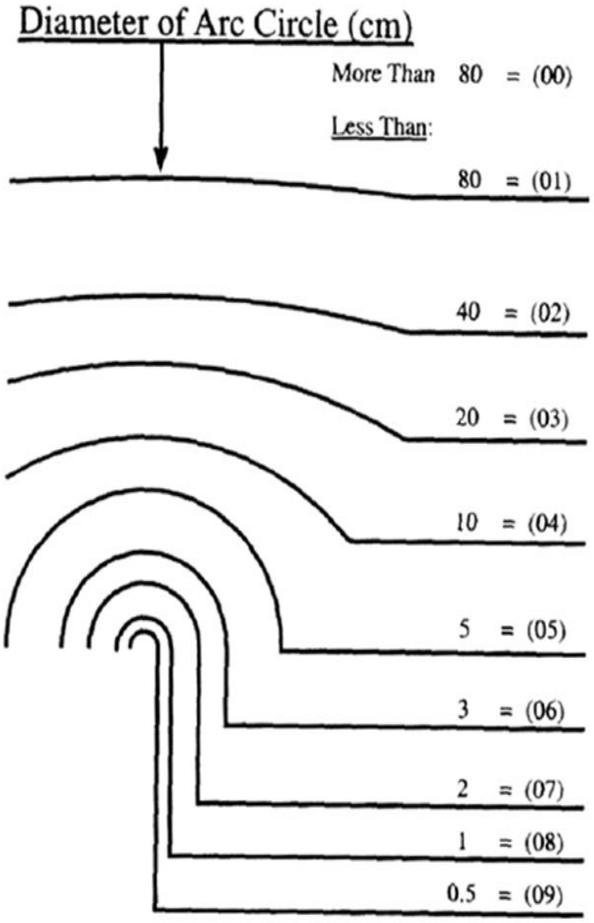

Figure 1-8 A geometric classification template based on curvature measurements by Bailey & Schliebe. Diagram taken from Ogle & Fox[72].

1.3.3.2 *De Mettrie et al. Geometric Classification*

The hair classification study showed the distribution of hair morphology variation across the world[63]. This study was later extended to a total of over 2500 volunteers from 26 countries[69]. The results of this study was an 8-group hair classification method that classifies hair using 3 geometric parameters; curve diameter, number of waves and the number of twists present in 5cm of wavy to curly hair. With this extended study, Loussouarn *et al*. suggested that it was possible to classify the worldwide variability of human hair morphology into 8 main groups without reference to racial origin.

This hair classification method completely eliminates race as a descriptor for hair morphology and instead classifies hair as type I through to type 8. Type I describes

straight hair, whether it originates from an Asian or Caucasian person. Curly hair ranges from type IV to VIII [63,69]. This new hair classification method raises questions about whether or not these 8 categories correlate with hair characteristics that have previously been assigned to racial groups. Some of these characteristics include the biochemistry, mechanical and microscopic details of hair fibre traits. No study has published testing the new geometric classification's reliability. Recent studies still use racial classifications when referring to hair curvature[73].

1.4 BIOCHEMICAL CHARACTERISTICS OF HUMAN HAIR SHAFT COMPONENTS

The human hair shaft is comprised of 3 components; the outer cuticle layers, the cortex and the medulla.

1.4.1 The Hair Cuticle

The cuticle component of the hair shaft is a chemically resistant[22,74] imbricated[75] multi-layer (6 to 8 layers) of flattened keratinized cells that are attached at the root end of the hair fibre[76]. The keratins present in cuticle cells are mainly arranged in β-sheet conformation[53]. These flattened cells have a thickness of 0.5 – 1.0μm and an average length of 45μm[39]. Each cuticle cell is made up of A-layer, exocuticle, endocuticle and cell membrane complex (CMC)[77]. On its own, the hair cuticle is higher in cystine content[78] and in other non α-helical amino acids than the whole hair fibre[22]. The cuticle is reported to have lower tryptophan and histidine content[79]. Cuticle cells contribute negligibly to the mechanical properties of whole hair fibres[76,80] but play an important role in the diffusion of water and other substances onto the hair cortex [39].

1.4.2 The Hair Cortex

The hair cortex accounts for the bulk of the hair fibre. The thickness and length of cortical cells are usually 1-6μm and 100μm, respectively[22]. The main components of the cortex are the intermediate filaments (macrofibrils) and the matrix[39]. Intermediate filaments (IFs) are rich in the amino acids that are usually found in α –helical proteins and in leucine and glutamic acid. Cystine (~ 6%), lysine and tyrosine are present in smaller quantities[81]. The hair matrix has high cystine content (~21%), proline and is

rich in amino acids that do not form α-helices [81]. Pigment granules are incorporated into cortical cells via phagocytosis at the zone of differentiation[39].

There are 3 different cortical cell types (ortho, para and meso-cortex) that are usually distributed across the cortex of hair or wool fibres[22,82]. Orthocortical cells have lower sulphur content (~3%) and less matrix between intermediate filaments; while paracortical cells have higher sulphur content (~5%) and tend to be smaller, with smooth rounded borders[83]. Mesocortical cells have an intermediate sulphur content[84]. The ultrastructure of cortical cells is usually visualised using transmission electron microscopy[31,85,86].

The differences in the cell types are associated with the arrangement of keratin intermediate filaments or macrofibrils and matrix within these cells for wool[50,87]. The macrofibrils within the inter-macrofibrilar material (IMM) of orthocortical cells are cylindrical and are arranged as double twists[88,89], while those of paracortical cells are packed in a parallel arrangement and that of mesocortical cells is intermediate between these two[89]. The double-twisted macrofibrils are observed as whorls in transverse sections[50] and are usually used to locate orthocortical cells in the hair cross section.

In the human hair cortex, there are variations in the arrangement of macrofibrils within single cells[90]. This variation was elucidated in straight hair by Harland *et al*. using electron tomography[91]. Harland *et al.* observed similar IF arrangement and spacing in the cortical cells of straight hair but found that there were variations in the staining intensities of hair sections prepared for transmission electron microscopy (TEM).The researchers concluded that for hair sections, orthocortical cells had a high intensity while para-cortex has low intensity staining macrofibrils[91].

Variations in the distribution of cortical cell types has been associated with hair morphology[62,85,90]. The cortex of straight hair is composed of predominantly paracortical cells[90] while that of curly hair has an asymmetric distribution of orthocortical and paracortical cells[60,62,90]. Figure 1-9 shows an illustration of how the cortical cells types would typically be distributed on a fibre with curvature.

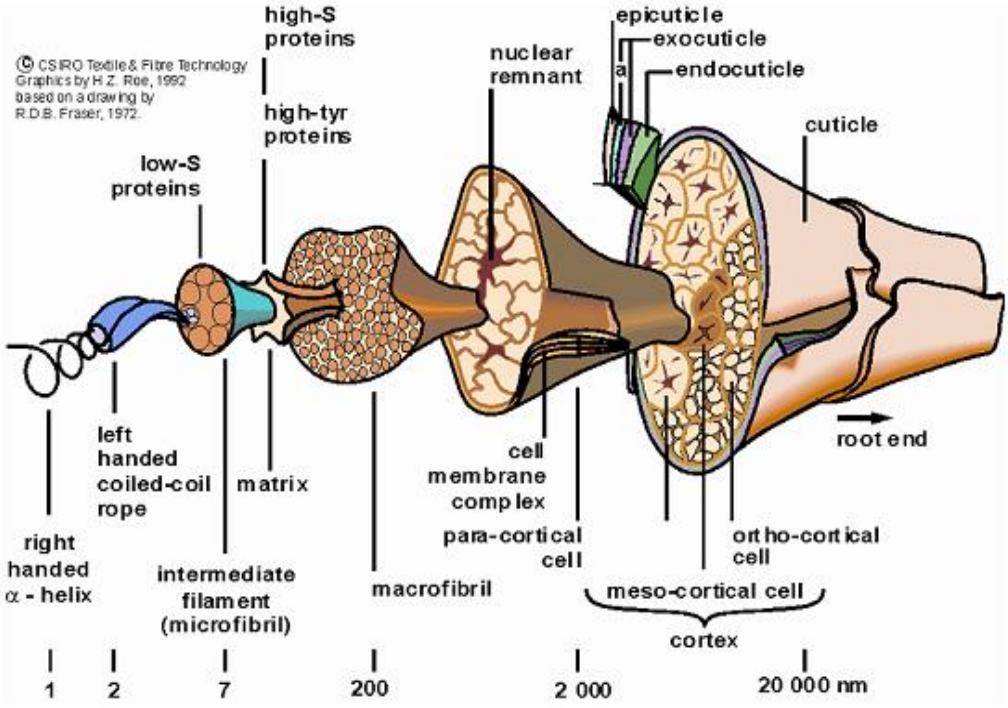

Figure 1-9 Hierarchical structure of the hair shaft showing the composition and distribution of cortical cell types[81].

The cortex is the component of the hair structure that is responsible for mechanical properties of the hair fibre[39,92,93]. Hair with high curvature is reported to be the least resistant to mechanical extension and to exhibit profiles of premature failure[92]. The mechanical characteristics of curly hair are unlikely to be related to hair biochemistry. Using silver-staining and TEM, Khumalo *et al.*(2005) showed there was similar staining in different race groups and suggested that the fragility of African hair is not related to the distribution of cystine-rich protein[94] and likely to be due to other mechanical influences, such as grooming.

1.4.3 The Medulla

The medulla, the innermost component structural component of the hair shaft is not present in fine hair but is usually seen in coarse or thicker scalp and beard hair fibres[32,95,96]. When present, the medulla is observed as a series of vacuoles along the hair fibre and does not contribute significantly to the mechanical properties of the hair fibre[39].

1.4.4 Biochemical Characteristics of Whole Hair Fibres

Whole hair fibres are composed of 65 to 95% proteins that are condensation polymers of amino acids. The remaining composition is water, lipids, hair pigment (melanin) and trace elements[39]. There is significant overlap in the amino acids quantities of hairs of volunteers from different races (Tables 1-1)[93], although some amino acids vary depending gender and hair colour; the cystine content of male scalp hair is higher than that of female hair, while highly pigmented or dark hair also has higher cystine content than lighter hair[97]. The lipids found of the hair shaft are usually categorised according to their origin, with external hair lipids being those secreted by the sebaceous and internal lipids being those present within hair matrix cells[98–101]. Hair lipids account for 1-9% weight of the total hair fibre[39,73]. These lipids are cholesterol esters (ChE), cholesterol (Ch), cholesterol sulphate (ChS), ceramides (Cer)[102] and free fatty acids (FFA). Of these lipids, the ChE and some FFAs are attributed to the sebaceous gland[99]. The major external lipid is 18 Methyleicasonoic acid (18-MEA), which is covalently bound to the cuticle surface via thio-ester linkages[93,103]. Disruption or depletion of this lipid renders the hair hydrophilic[104]. Both internal and external lipids have been reported to contribute to the physical properties of hair fibres[99,105].

Duvel *et al*. reported that the decrease in mechanical properties of distal hair fibres might be due to progressive loss of free and covalently bound lipids[105]. The researchers showed gradual decreases of ceramides, cholesterol sulphate and bound fatty acid (18-MEA) as one moves from hair root to tip[105].

Table 1-1 Amino acid content across 3 major racial groups. Table taken from Wolfram 2003[55].

	Hair type		
Amino acid	African	Brown/Caucasian	Asian
Alanine	370-509	345-475	370-415
Arginine	482-540	466-534	492-510
Aspartic acid	436-452	407-455	456-500
Cysteic acid	10-30	22-58	35-41
1/2 Cystine	1310-1420	1268-1608	1175-1357
Glutamic acid	915-1017	868-1053	1026-1082
Glycine	467-542	450-544	454-498
Histidine	60-85	56-70	57-63
Isoleucine	224-282	188-255	205-244
Leucine	484-573	442-558	515-546
Lysine	198-236	178-220	182-196
Methionine	6-42	8-54	21-37
Phenylalanine	139-181	124-150	129-143
Proline	642-697	588-753	615-683
Serine	672-1130	851-1076	986-1101
Threonine	580-618	542-654	568-593
Tyrosine	179-202	126-194	131-170
Valine	442-573	405-542	421-493

Recent work has showed that internal lipids are variably distributed all over the hair cortex and contribute to the structural arrangement of keratins within cortical cells[73]. These lipids may influence hair texture or be associated with hair morphology of hairs from the 3 major racial groups. Cruz *et al.* observed that African hair has the highest internal lipid content (3.48%), with Asian and Caucasian hair having similar amounts (2.07% and 2.05% respectively)[73]. The study showed that the arrangement of internal lipids in the hair matrix influences the secondary structure of keratins and keratin associated proteins.

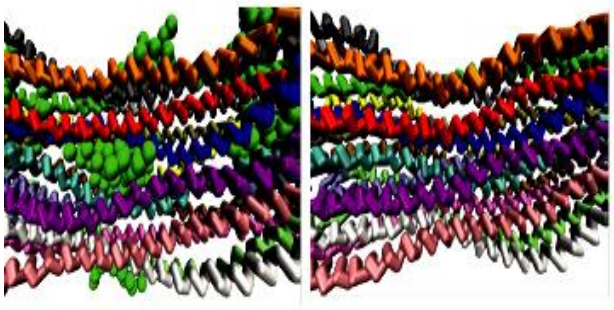

Figure 1-10 Martini Force Field model showing the arrangement of keratins with and without internal lipids[73]

The presence of these lipids caused an intercalation of keratin dimers, changing the architectural arrangement of hair filaments[73] (Figure 1-10). Integral hair lipid levels and other intermolecular components of hair are reported to be significantly affected by adverse biological changes such as the presence of cancerous cells[18,106–108]. These will be discussed further under section 1.6.

1.5 THE USE OF HUMAN SCALP HAIR IN MEDICINE

There are two approaches that can be employed to gain information from hair; the changes in the biochemical composition can be indicative of disease presence/progression [15,18,19,108,109] and exposure to (or incorporation of) various substances (including drugs and toxins)[5,7,8,110] which can be investigated and even detectable years post-mortem[3]. Levels of exposure can be quantified from scalp, pubic or auxiliary hair long after exposure[6].

Substances are incorporated into the hair shaft via various mechanism; passive diffusion through blood into the hair matrix during keratinization, transfer into the hair follicle from surrounding tissue, absorption onto the formed hair shaft from sebum, sweat and from the environment[3]. Figure 1-11 shows the routes of incorporation for ethyl glucuronide, a metabolite of ethanol which can be used as an objective marker of chronic alcohol intake[110].

The incorporation of substances into the hair shaft may depend on their chemical nature; neutral and lipophilic substance enter the hair shaft[17,53] and get diffused into matrix cells, while basic compounds are reported to bind to melanin[111,112]. These substances are usually extracted from hair shafts and analysed using various analytical tools including liquid and gas chromatography mass spectrometry [9,17,110].

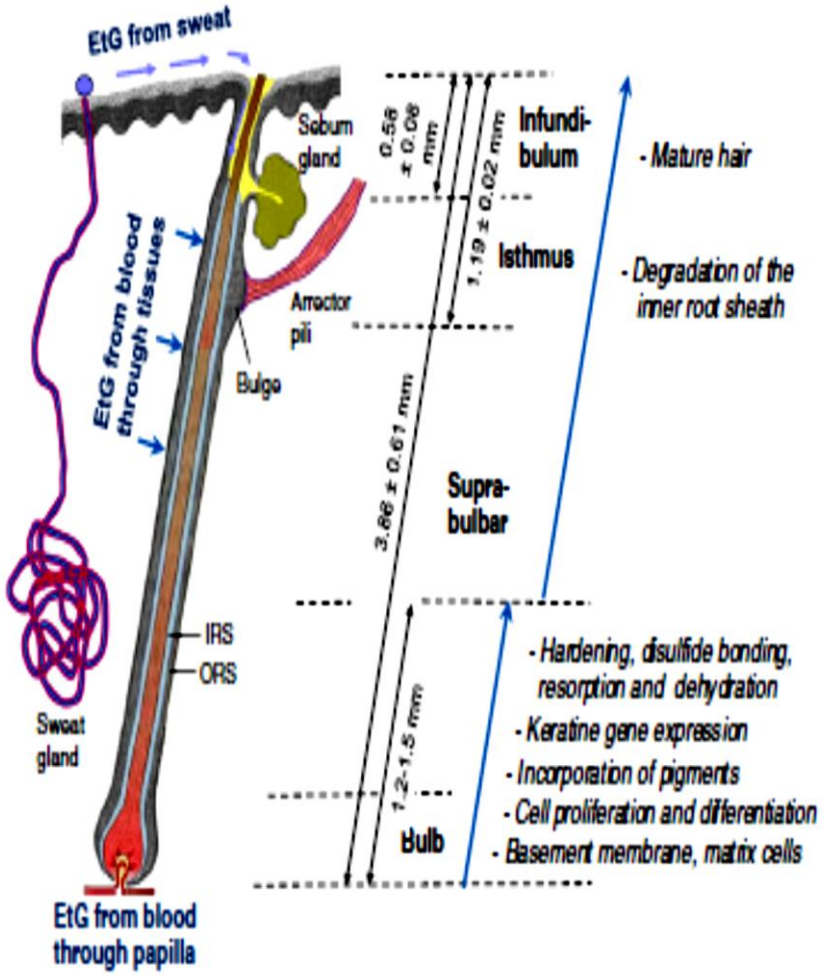

Figure 1-11 Schematic diagram showing the incorporation of ethyl glucuronide (EtG), a metabolite of ethanol, into the hair shaft[110].

Changes in hair biochemistry arising from disease progression can be investigated using synchrotron radiation[113], Fourier Transform Infrared (or Raman) spectroscopy[107,114]. Hair sampled from breast and colon cancer patients reportedly has different X-ray diffraction patterns than that from healthy volunteers[108,115], while FT-IR may be able to differentiate breast cancer patients from non-breast cancer patients and even separate those that did or did not have the cancer resection[107]. This makes FT-IR a promising non-invasive diagnostic tool for the early detection of breast and other cancers[116,117].

The regions of the IR spectra that are reported to be altered in breast cancer patients are the C-H bending absorptions at 1400 -1500 cm^{-1}, 1739 -1740 cm^{-1} resulting from

lipid esters, 1240 cm^{-1} from C-H lipid, 1163 cm^{-1} from C-O stretching in lipid, 1161 cm^{-1} C-O-C stretching in lipids and at 1055 cm^{-1} from cholesterol. These changes in lipid content are thought to result from an increase in the lipid material in the delta layer of the cuticle – cortex cell membrane complex (CMC)[106,107,118] as well as from fatty acid synthases that are expressed in cancer[107,119].

Hair analyses and interpretation of results have mainly focused on differences between race, however racial categorizations is limited and subjective and could be biased[120]. The growing use of hair in medicine and forensic medicine therefore requires that the baseline characteristics of human scalp be holistically elucidated in order to interpret results. The most recent increasing use of hair for testing incorporated substances includes testing for antiretroviral drug levels to monitor treatment compliance[9–13].

Race continues to be used as a surrogate for hair curvature in the interpretations of hair analyses results, however racial categorizations is limited, subjective and could give biased results[120]. Further, if curly hair indeed has the highest internal lipid content as previously suggested[73] both hair curl and its potential influence (e.g. on incorporation of lipid soluble drugs) have to be objectively quantified. Objective measures of hair curl and its influence on biochemistry would allow appropriate interpretation of results and improve the validity of the growing use of hair as a testing substrate in Medicine and Forensic Sciences[6–19].

1.6 STUDY AIMS

The current study aimed to;

1. Evaluate the reliability of the geometric classification of hair curl and explore whether its reliability could be improved.
2. To explore the relationships that may exist between the hair curl and biochemical characteristics (internal lipid content and FTIR of whole hair fibres).
3. To investigate relationships between physical characteristics (mechanical properties, hair growth rate and hair density) and the degree of hair curl.

CHAPTER TWO

GEOMETRIC CLASSIFICATION OF HUMAN SCALP HAIR CURL: REDUCING GROUPS FROM 8 TO 6 IMPROVES RELIABILITY

ABSTRACT

Background: The use of race to describe human hair variation (Asian, Caucasian and African) is unscientific. This study aimed to test the reliability of a classification that is based on 3 geometric measurements (curve diameter, curl index and number of waves).

Methods: After ethical approval and informed consent, proximal virgin (6cm) hair sampled from the vertex of 128 healthy volunteers was evaluated. Three raters each scored hairs from 48 volunteers at two occasions each for the 8 and 6-group classifications. One rater also classified hair from all 128 volunteers using the 6-group method. Kappa statistics were used to assess inter and intra-rater agreement.

Results: Each rater classified 480 hairs on each occasion. No rater classified any volunteer's 10 hairs into the same group; the most frequently occurring group was used for analysis. The inter-rater agreement was poor for the 8-groups (k = 0.418) but improved for the 6-groups (k = 0.671). The intra-rater agreement was also poor for 8 (k = 0.444 to 0.648) and improved for 6-groups (0.599 to 0.836). The intra-rater agreement for the one evaluator for all volunteers was good (k = 0.754). The 6-group method reduced the classification time of curly hair from 30 to 10 minutes.

Limitations: Although the current study had a small sample size, it is the first to test the reliability of a geometric classification.

Conclusions: The 6-group method was quicker and more reliable. However, a digital hair curl classification that correlates with biochemistry is warranted and likely to reduce operator error.

2 INTRODUCTION

The variation in hair curvature is the most distinct characteristic of human scalp hair morphology. Studies have indicated that differences in hair curl arise from the bulb[40,58,59].Using computer-aided reconstruction of scalp biopsy samples, Lindelof demonstrated that hair emerged from follicles at a right angle to the surface of the scalp for Asian hair and at an acute angle for African hair resulting in straight and curly hair respectively[59]. Recent studies using mouse models show that the size and shape of the dermal papilla dictates hair shaft morphology and thickness[26]. Natural hair curl varies widely across the world possibly due to diversity arising from heredity and environmental factors[61]. However, the use of race (African, European, Asian) as a descriptor of hair form has limitations because it is subjective[68] and presents with overlaps[1,121].

The accurate identification of hair curl is crucial for forensic investigators wanting to link trace evidence found at crime scenes to suspects[116,122,123]. Further, certain hair disorders such as folliculitis keloidalis nuchea are predominantly associated with high curvature hair[124]. Objective characterization of hair would also be useful for hair-curl-specific hair product development. This would better address the needs of different hair curl phenotypes; for example, sebum is not evenly distributed along curly hair shafts resulting in dryer hair[125]. The proposal to abandon the use of race in describing human hair phenotypes[67,68] is even more relevant for the exploding interest in the use of hair as a testing substrate in medicine[9,15–17,19,126]. There is evidence to suggest that curly hair has a higher lipid content;[73] this may influence the incorporation of lipid soluble drugs, requiring adjustments for hair morphology when interpreting results.

A few objective hair classification systems have been attempted[64,70,71]. The first was introduced by anthropologist Hrdy[71] who assessed hair form variation in seven populations (Bougainville, East Africa, Northwest European, Malaita, Sioux, Japan and Ifugao). He measured the average diameter, medullation, scale count, kinking, average curvature, ratio of maximum to minimum curvature, crimp and ratio of natural to straight hair length then compared within and between population variations using F-tests. The average curvature and ratio of curvature were the two most important variables in describing hair form. Correlation matrices showed a strong correlation

between curling variables (kinking, average curvature, ratio of maximum to minimum curvature, crimp and ratio of natural to straight length) while a weak correlation was observed between scale count and the curling variables. Principal component analysis (PCA) showed that 3 components (curling, size and regularity of curl) accounted for 80% of the variance in the data.[71]. Hrdy also observed that the average curvature varied between groups and suggested it would have the greatest contribution in differentiating groups[71]. The precision of the contribution of average curvature to variation was later investigated by Bailey and Schliebe[70] who measured hair curvature of 30 strands (6cm long) from the same individual three times on a template of circles of known radii (Figure 2-1) (and compared means) in one experiment. They described average curvature as an inverse of the radius as did Hrdy[71]. In a second experiment, they compared the curvature of hair form recorded for five family members and found overlaps in recorded means[70]. They did not investigate the reliability by calculating intra and inter rater agreement.

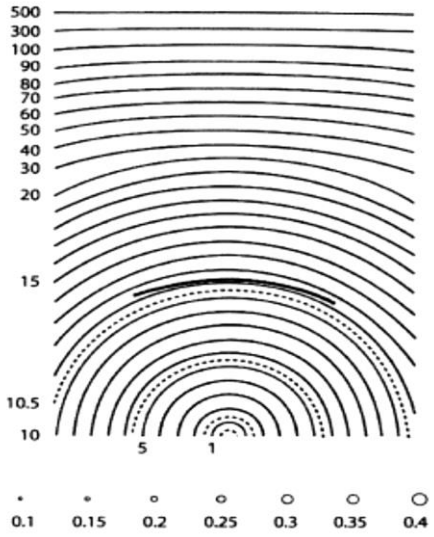

Figure 2-1 Curve diameter template derived by De La Mettrie *et al.*[63] from Bailey and Schliebe[70].

Most recently, De La Mettri*et al.* expanded on the Bailey & Schliebe system by introducing 3 additional variables (for curly hair), also measured on a 6cm length of proximal hair. They classified hair collected from 1442 volunteers, originating from 18 countries[63], by measuring the curve diameter (CD), the ratio between relaxed and extended hair length (termed the curl index or *i*), the number of twists (*t*) and waves

(*w*). The number of waves was counted by constricting a 5cm segment of the hair to 4cm, while the number of twists is the number of natural constrictions along the hair axis[63]. They reported a direct correlation between the number of twists and number of waves which supported the exclusion of the number of twists measurement for future analyses. Using the remaining three variables (Figure 2-2), PCA and hierarchical ascendant clustering (HAC), they reported that hair could objectively be classified into 8 groups and provided a set of rules for the classification[63] (Figure 2-3).

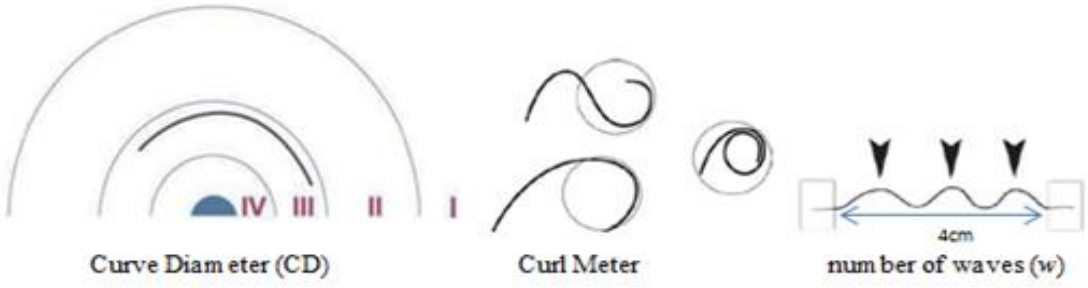

Figure2-2 Geometric templates used for the 8-group hair classification[69].

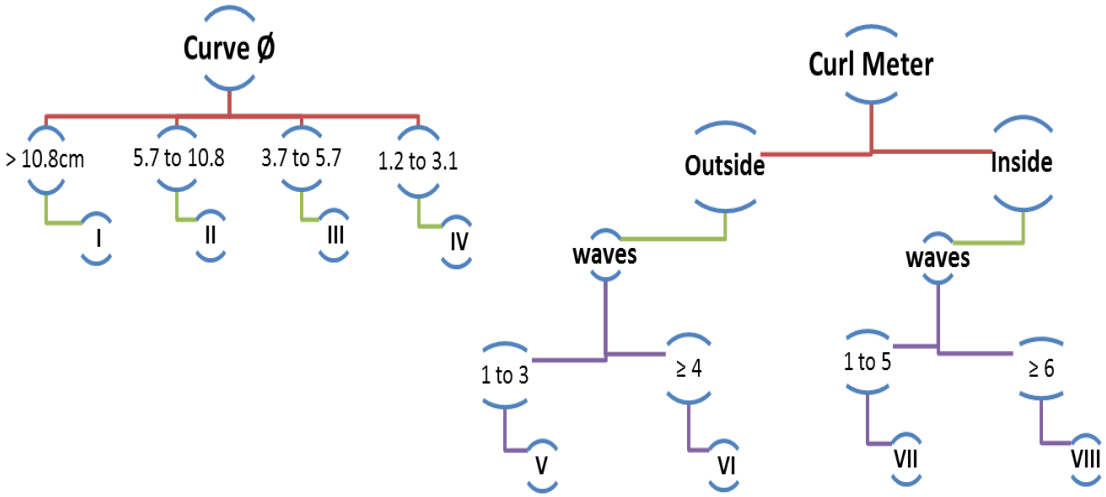

Figure 2-3 Hair classification rules described by De La Mettrie *et al*[63] and Loussouarn *et al*[69].

The curve diameter was used to distinguish four groups in the straight hair spectrum based on cut-off values obtained from the PCA and HAC analysis. Curly hair was differentiated based on combinations of curl index (*i*) scores and maximum number of waves. A follow-up study led by Loussouarn*et al.*[69] included an additional 1007 volunteers and aimed to demonstrate the reproducibility of the geometric classification.

They proposed a simplified approach to the classification, where instead of measuring the curl index (*i*), a curl meter which is a circle with a diameter of 0.98cm was used first to see if the 6cm of hair fits completely (hair curl group VII and VIII) or not (hair V and VI) within the circle. Thereafter the 6cm hair is taped down ,0.5cm on each side , giving rise to a 5cm segment which is then constricted to 4cm and the number of waves counted. Thus, classification of the curlier hair groups depended on the combination of the curl meter and number of waves[69].

Although the authors had large sample sizes, they only measured 3 hair fibres sampled from different parts of the head for each volunteer. Further, although the classifications in both[63,69] studies were conducted by different scientists, the inter-rater agreement was not calculated. Both studies also did not report comparisons of repeat measurements (intra-rater reliability).

The aim in this study was to evaluate the reliability of the geometric classification and explored whether reliability could be improved.

2.1 MATERIALS AND METHODS

2.1.1 Participants and Sample Preparation

Permission to conduct the study was granted by the Faculty of Health Sciences, Research Ethics Committee (HREC REF: 328 2012). Participants with at least 6cm of virgin hair (and had not used any chemical straightener or dyes for > 7 months) were invited to participate in the study via notices, fliers and University online research notices. After participants gave informed consent, an area of 0.56cm^2 (using the same sterilized electric shaver) was shaved from the vertex of the scalp and kept in a dry sealed evenlope. Prior to geometric measurements, the hair was washed in a petri dish using 10 ml of 1% sodium dodecyl sulphate solution (30 seconds of soaking,60 secods of lathering by shaking hair petri dish, 60 seconds of rinsing under warm (37℃) running water, followed by 2 rinses with 100 ml of cold distilled water). Hair was then air-dried for a minimum of 4 hours and stored in sealed packets at room temperature, away from direct sunlight, until geometrically classified.

2.1.2 Geometric Characterizatin

Three scientists classified 6cm of proximal virgin hair from the same pool of 48

volunteers using published classification templates and rules (Figures 2-2 and 2-3)[69]. Each rater classified 10 hairs at 2 different occasions; therefore, each volunteer's hair was classified 60 times.

Single strands of natural hair (Figure 2-4) were classified using the curve diameter (CD) meter which identified hair groups I to IV. Six centimetre long strands of hair were place on top of the curve diameter template and a glass slide placed on the hair without shifting or altering its natural curl. The hair was then classified as hair curl group I, II, III or IV by superimposing it to the best fit half-circle. For hair with curls too tight to fit in the curve diameter template, both the curl meter [i.e. hair fits completely (VII and VIII) or does not (V and VI) fit within within the circle] and the number of waves calculated [up to 3 for V; ≥ 4 for VI; up to 5 for VII and ≥ 6 for VIII] were used for classification.

The most frequently occurring hair curl group for each set of 10 strands was reported as the representative hair curl group for the volunteer for each rater at occasion 1 and 2.

2.2 Statistics

The inter and intrarater agreement, reflecting the reliability of the geometric classification systems was assessed using Cohen's kappa coefficient (StataCorp. 2013. Stata: Release 13. Statistical Software. College Station, TX: StataCorp LP). The Kappa coefficient measures chance corrected agreement between two or more raters and can range between +1 and -1[127].A coefficient of 1 denotes perfect agreement, 0 reflects agreement obtained by chance and a negative value shows worse than expected agreement[128]. Kappa values 0.41-0.60 reflect moderate, 0.00–0.20 slight 0.61-0.81 substantial and > 0.81 reflects almost perfect agreement between raters[127,129,130].

2.3 RESULTS

A total 128 volunteers (83% female and 18% male) aged 18 -55 years from 4 self-identified racial groups (Asian, Caucasian, Mixed and African) were included. Single strands of natural hair (Figure 2-4)were classified using published geometric

templates.Sixty hair strands were classified for each volunteer for the 8 and again for 6-group classification. It took approximately 15 to 30 minutes to classify 10 strands for curly hair groups (V – VIII) and approximately 10 minutes for straighter hair. In all, 2880 hair strands (48 volunteers X 10 strands X 3 raters X 2 occasions) were initially classified. No rater classified any volunteer's 10 hairs into the same group; hair was classified into at least 2 (and occasionally 3) groups. The most frequently occurring hair curl group of the 10 strands at each assessment time point was chosen as the representative hair group for the volunteer.

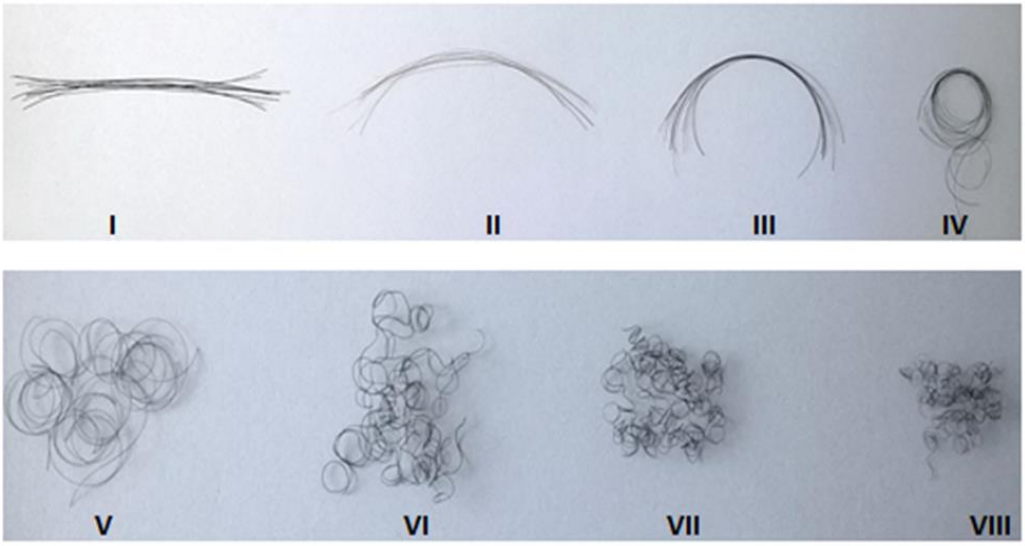

Figure 2-4 Variations in the degree of air curvature across 8 hair curl groups (I – VIII).

The inter-rater agreement for the 8-groups, was fair to moderate[129,130], and higher at occasion 2 (k = 0.455, CI; 0.389– 0.521) than occasion 1 (k = 0.380, 95% CI; 0.313 – 0.447). The intra-rater agreement [ranged from k = 0.444 (95% CI; 0.334 – 0.553) to k = 0.648 (95% CI; 0.525 – 0.771)] showed the lowest agreement between the three raters for the most extreme groups (I and VIII, k = 0.170 and k = 0.074 respectively) at occasion 1 (Table 2-1).

Table 2-1 Inter-rater agreement for the 8-group classification: 3 evaluators at occasion 1 and occasion 2.

	Occasion 1		Occasion 2	
Hair Curl Group	Kappa	95% CI	Kappa	95% CI
I	0.170	0.007 - 0.334	0.603	0.440 - 0.766
II	0.419	0.256 - 0.583	0.443	0.279 - 0.606
III	0.379	0.216 - 0.543	0.439	0.275 - 0.602
IV	0.515	0.352 - 0678	0.554	0.391 - 0.717
V	0.604	0.441 - 0.768	0.364	0.200 - 0.527
VI	0.182	0.018 - 0.345	0.407	0.244 - 0.571
VII	0.396	0.232 - 0.559	0.453	0.290 – 0616
VIII	0.074	0.000 - 0.237	0.399	0.236 - 0.562
Combined	0.380	0.313 - 0.447	0.455	0.389 - 0.521

Table 2-2 Intra-rater agreement for the 8-group classification. Rater 1 to rater 3.

	Agreement	Expected Agreement	Kappa	95% CI
Rater 1	58.33%	13.02%	0.521	0.413 – 0.629
Rater 2	52.08%	13.89%	0.443	0.334 – 0.553
Rater 3	70.8%	17.19%	0.648	0.525 – 0.771

The third step of the classification for curly hair i.e. counting the number of waves (taping the ends down to count the number of waves) was reported by all 3 raters as laborious, the tiny hair as difficult to handle and at risk of breakage. As a result this, repeat measurements were again performed at two time points by the 3 raters where the third step [the number of waves count (*w*)] was excluded. This resulted in a 6-group classification where the first step categorized hair curl groups 1 to 4 similarly to I to IV[69] but ended at the second step where the curl meter classified hair as falling outside of the circle (Group 5 equivalent to V and VI) [69] or completely inside (Group 6 equivalent to VII and VIII). The inter-rater (k = 0.613 at occasion 1 and k = 0.729 at occasion 2) and intra-rater agreements [range: k = 0.599 (95% CI: 0.422 – 0.776) to k = 0.836 (95% CI; 0.691 – 0.981)] for the 6-group classification were higher than those of the 8-group classification (Table 1-2).

Table 2-3Inter-rater agreement for the 6-group classification: 3 evaluators at occasion 1 and occasion 2.

Hair Curl Group	Occasion 1		Occasion 2	
	Kappa	95% CI	Kappa	95% CI
1	0.171	0.008 – 0.335	0.000	0.000 – 0.149
2	0.534	0.371 – 0.698	0.610	0.447 – 0.773
3	0.578	0.414 – 0.741	0.645	0.482 – 0.809
4	0.531	0.367 – 0.694	0.806	0.643 – 0.970
5	0.206	0.045 – 0.369	0.463	0.299 – 0.626
6	0.883	0.720 – 1.000	0.913	0.750 – 1.000
Combined	0.613	0.527 – 0.699	0.729	0.641 – 0.817

Table 2-4 Intra-rater agreement for the 6-group classification: rater 1 to rater 3.

	Agreement	Exp. Agreement	Kappa	95% CI
Rater 1	87.50%	23.87%	0.836	0.691 – 0.981
Rater 2	70.83%	27.13%	0.599	0.422 – 0.776
Rater 3	81.25%	24. 70%	0.751	0.601 – 0.901

One evaluator who also assessed (at a different time point) 10 hairs each for all volunteers using the 6-group classification was found to have similar intra-rater agreement [k = 0.754 (95% CI; 0.669 – 0.839)] to that reported for the 48 volunteer sample. The overall distribution of classified hair curl groups somewhat correlated with subjective racial classification, where Asian hair is usually straight, Caucasian hair is straight to curly and African hair was the curliest (Figures 2-1 and 2-2).

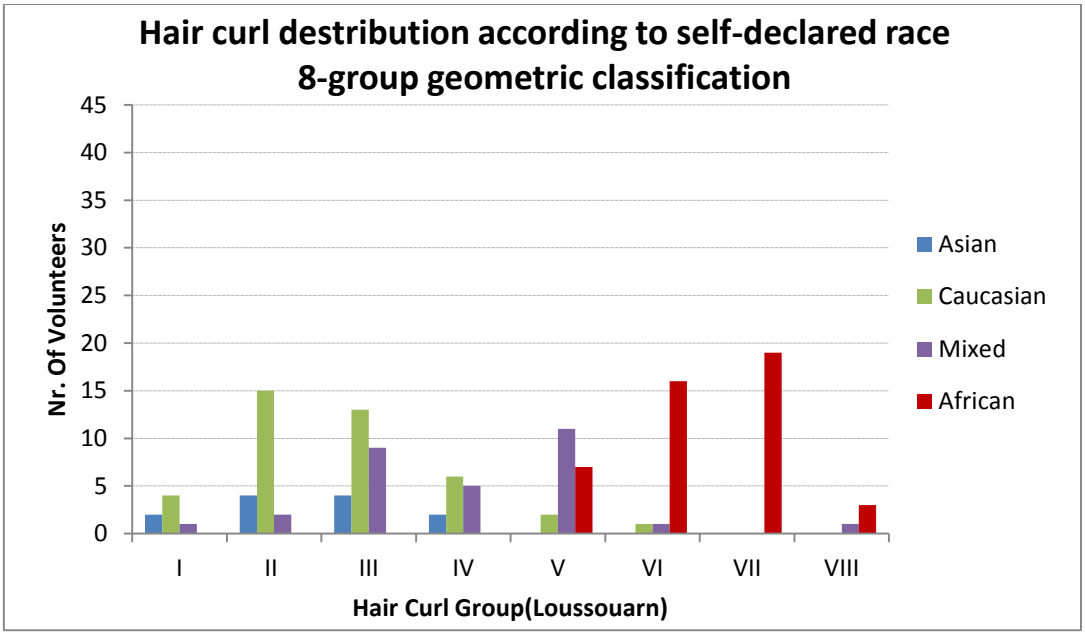

Figure 2-5Distribution of hair curvature (8 groups) according to self-declared racial group

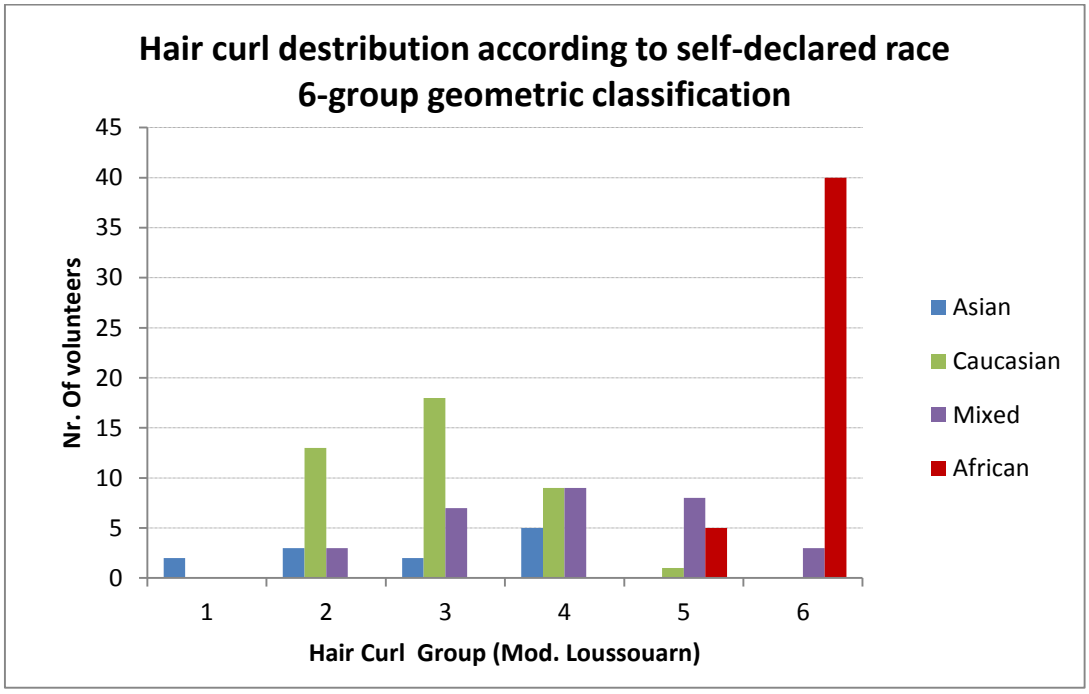

Figure 2-6 Distribution of hair curvature (6 groups) according to self-declared racial group

.

2.4 DISCUSSION

Self-declared racial groups showed significant overlap with each “race” falling into 4 of the 8-group and at least 2 of the 6-group classifications; thus confirming “race” as an unreliable descriptor of hair curl. Although representative hair samples (10 strands, one volunteer) from each geometric group, demonstrate a gradual increase in hair curvature from group I to VIII (Figure 2-4); statistical analysis suggests that including the third step (‘counting the waves’) does not reliably distinguish curly hair phenotypes into 4 four groups (Group V versus VI and VII versus VIII) as previously suggested[69]. For all raters, classification of hair from the same volunteer fell into at least 2 (and occasionally 3) groups which may suggest observer error or heterogeneity of hair morphology even within a small area (0.562cm^2) as previously reported[70,71]. The straight hair phenotype of Asian (Chinese and Indian) volunteers in our sample was grouped into group I to IV; the Indian participants likely contributed to the presence of hair curlier phenotypes. Participants who identified their race as Caucasian were classified in all hair curl groups except VII and VIII. The absence of participants who identified as mixed race in hair group VII was thought to be by chance. African hair ranged from curl group V to VIII. This was consistent with observations by Loussouarn *et al*.[69] and other workers [62,69,131].

Inter-rater agreement for the 8-group classification system was moderate [occasion 1 (k = 0.380) even though slightly improved (k = 0.455) at occasion 2]. This may reflect improved rater proficiency with the geometric classification.

The major challenge encountered with the 8-group classification system was the difficulty in handling the hair to count the number of waves for hair groups V to VIII. Further, the distinction of hair group V from VI and hair group VII from VIII was somewhat subjective. For instance, a strand could be a V or VI based on one extra or less wave. Eliminating this step (counting waves) from the classification resulted in improved inter and intra-rater agreement as seen in the kappa values of the 6-group classification (Table 2-3).

The worst inter-rater agreement values were obtained for Hair curl groups I, VI and VIII (Tables 2-1 and 2-2) for the 8-group and hair curl group 1 and 5 for the 6-group classification; these could reflect ambiguity and lack of uniqueness of the groups. The existence of the two extreme hair curl groups (I and VIII) is likely to reduce in future,[76]

while groups III – V are predicted to increase because of increasing human migration and admixture. The distribution of hair curl groups according to race varied slightly when comparing the 8 and 6-group classifications (Figures 2-5 and 2-6) with more group 1 hair in the 8 than the 6-group classification of the same volunteers. The most frequently occurring hair curl for each set of 10 strands was used as representative for the volunteer. This was done for all raters at occasion 1 and occasion 2. In instances where no one hair curl was the most frequent in a set of 10 strands, the curliest hair was used (i.e. considered more likely to be representative for the volunteer than straighter hair that could have straightened due to mechanical damage or extension). Temporary hair curl change as a result heat and/or cosmetic physical curling would not have survived the sample preparation steps. Chemically altered hair (straightened or curled) was excluded from the study. Further, hair samples were washed in between evaluators in order for the hair to regain its natural non-extended hair form. Lastly, the overall hair curl for each of the 48 volunteers was based on the most frequently occurring hair group of the 6 evaluations (i.e. from 60 hairs) made by the 3 raters each for the 8 and 6-group classifications.

There is an exponential increase in the number of studies that report the use hair as a testing substrate, including investigations of drug hair levels as objective measures of treatment compliance[10,12,13,132,133]. Unlike blood and urine that have a high turnover, human hair is a medical repository that can be used to extrapolate exposure to drugs, toxins and poisons dating back many months (depending on hair length) . However, lipid content may vary with hair curl[73].

The geometric classification system presented by De La Mettri *et al.* and Loussouarn *et al*. is a significant contribution to the scientific use of hair for various applications.

2.5 CONCLUSION

The 6-group geometric hair classification is quicker and more reliable than the one has 8-groups. However, there is a need to investigate the potential contribution of hair biochemistry, mechanical and ultra-structural characteristics. The investigations of the biochemical characteristics are presented in Chapter Three.

CHAPTER THREE

DOES FOURIER TRANSFORM INFRARED ANALYSIS CORRELATE WITH GEOMETRIC CLASSIFICATION OF HUMAN SCALP HAIR?

ABSTRACT

Background: Recent studies report the use of various spectroscopy techniques to identify biomarkers for screening and early diagnosis of disease e.g. breast and colon cancer. The reliability of such diagnostic approaches is likely to be influenced by the "natural" baseline state of the hair samples under investigation. It is thus crucial to elucidate the basic science of hair in order to understand the potential influence of morphology on test results. The aim of the current section was to investigate whether the biochemical characteristics of hair vary with curvature.

Method: Natural scalp hair of varying morphology was collected from 128 healthy volunteers and grouped according to geometrically measured hair curl; for practical reasons 53 samples were used for this component of the study. The biochemical profile of unprocessed whole hair fibres was non-destructively assessed using Attenuated Total Reflectance-Fourier Transform Infrared Micro-spectroscopy. Relative total lipid content of pulverized hair samples was assessed using the Sulfo-Phospho-Vanillin assay.

Results: The total internal lipids of geometrically grouped hair samples were highest in the curly hair compared to straight hair. When the biochemical analysis of unprocessed geometrically classified whole hair fibres was investigated, there was a trend toward higher absorbance of lipid associated bands for curly hair groups (V to VIII or 5 and 6).A supervised statistical approach applied to 4 hair groups using the FTIR data improved classification success to 79% (range: 69% – 88%).

Conclusion: Based on FTIR analysis a geometric classification with 4 groups may be more reliable than an 8 or 6-group system. Confirmation of such a system is however needed for the reliable use of hair as testing substrate in Medicine.

3 INTRODUCTION

The biochemical composition of the hair shaft has long been reported to be uniform across different racial groups [55,93,134–137]. However, recent studies are increasingly reporting that chemical composition may actually vary with hair morphology[62,73]. Using differential scanning calorimetry (DSC) and 2-D gel electrophoresis experiments, Porter *et al.* showed variations in the thermal characteristics and staining intensities of intermediate filaments of hair samples from different ethnic groups[62]. Cruz *et al*.[73] reported that African hair had the highest total lipid content, followed Caucasian and Asian hair. The authors used confocal microscopy and computational simulation techniques to demonstrate that the arrangement of internal lipids in the hair matrix influence the secondary structure of keratins and keratin associated proteins[73].

Internal lipid material is present in the cell membrane complex (CMC) that binds cuticle and cortical cells[99,138].The CMC is composed of a δ-layer and β-layer. The δ-layer is made up proteins and glycoproteins and it makes up the intercellular cement[99,139,140], while the β-layer is a thin layer of lipids[100,141]. There are two classes of lipids that have been identified in the CMC; internal, free lipids and integral, bound lipids[39,99], also referred to as integral hair lipids (IHL)[101]. Free fatty acids, sterols and polar components make up the internal lipids and are extractable with organic solvents[102]. Integral lipids are composed of stearic, palmitic and 18-methyleicasonoic acid and are covalently bound onto hair fibres via ester linkages[105,140]. The latter group is only extractable by hydrolysis with a strong alkali[100,142].

The biochemistry of whole hair fibres can be assessed non-invasively using techniques such as synchrotron radiation, Fourier Transform Infrared (or Raman) spectroscopy. These techniques are also used to investigate changes in hair biochemistry arising from changes in health status[107,113,114]; hair sampled from breast and colon cancer patients reportedly has different X-ray diffraction patterns than that of healthy volunteers[108,115], while FTIR may be able to differentiate breast cancer from non-breast cancer patients and even separate those that did (and not) have the cancer resected[107]. This makes FTIR a promising non-invasive diagnostic tool for the early detection of cancers[116,117,143].

FTIR is an ambient temperature analytical method that can directly monitor the vibrations of functional groups that characterize molecular structure by irradiating samples in the mid-infrared region (4000 to 400 cm^{-1})[144].The sample absorbs the electromagnetic radiation and converts it to vibrational energy of the chemical bonds that join the atoms of the molecule. Different molecules absorb at different wavelengths and this depends on the masses of the atoms, the force constants of the bonds as well as the geometries of the masses of the atoms. In order for a molecules to be IR active, there must be a change in its electric dipole moment during vibration[145].

The vibrational modes that are usually observed in keratin polypeptides are the Amide I – VIII bands, C-H stretching bands from lipids and bands from nucleic acids. The Amide I band are arises from carbonyl stretching, amide II is due mostly from NH bending vibrations[146].The bands of interest as assigned in the current study are indicated in figure 3.2 below.

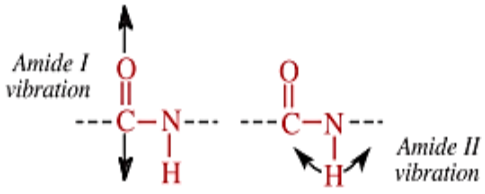

Figure 3-1 Vibrations responsible for Amide I and Amide II bands. Illustration taken from Gallagher 1997[146].

The equation for absorption wavenumbers and related parameters is as described below:

$$\boldsymbol{v} = \frac{\mathbf{1}}{\mathbf{2\pi C}} \sqrt{\frac{\boldsymbol{k}}{\boldsymbol{\mu}}} \qquad \text{Equation 4-1}$$

Where

ν is the IR absorption wavenumber

C is the propagation velocity of electromagnetic waves;

k is the force constant of a chemical bond, and

μ is the reduced mass, with $\mu = \frac{\boldsymbol{m_1 m_2}}{\boldsymbol{m_1 + m_2}}$ Equation 4-2

IR absorption follows Beer-Lamberts law and thus the peak absorption intensity is directly proportional to molecular concentration of a said material.

The FTIR absorption peaks observed in the study were assigned as laid out in the band assignment in Table 3-2.

In the chemical or pharmaceutical industries, FTIR is commonly used routinely in process control[144], to identify unknown compounds or to assess the purity of materials. In biochemical applications, FTIR can provide information about the content of the secondary structure of proteins and lipids[146] .In hair research ,FTIR instruments can be used on ATR (attenuated total reflectance) mode which allows the analysis of hair fibres with very little or no sample preparation[116,143,147].

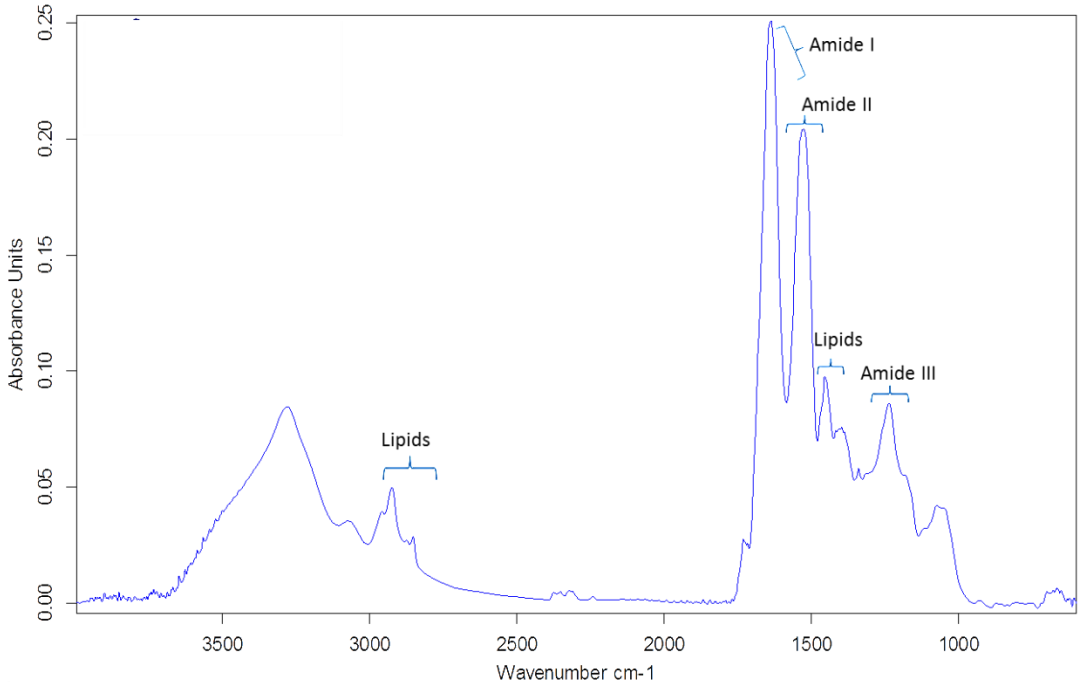

Figure 3-2 Typical FTIR spectrum of intact human hair fibre.

The regions of the IR spectra that are reportedly altered in breast cancer patients are the C-H bending absorptions at 1500 – 1400 cm^{-1}, 1739 -1740 cm^{-1} resulting from lipid esters, 1240 cm^{-1} from C-H lipid, 1161 cm^{-1} C-O-C stretching in lipids and at 1055 cm^{-1} from cholesterol[107]. These changes in lipid content are thought to result from an increase in the lipid material in the δ- layer of the cuticle – cortex cell membrane complex (CMC)[106,107,118] as well as from fatty acid synthases that are expressed in cancerous cells[107,119]. Baseline understanding of hair lipids is however crucial for

accurate interpretation of test results that depend on lipid variation as a biomarker of disease.

The aim in the current chapter was thus to investigate the relationships that may exist between hair curl and biochemistry, specifically lipid characteristics.

3.1 MATERIALS AND METHODS

3.1.1 Sample Collection and Preparation

Hair from 53 volunteers, out of the 128 that had been classified using geometric templates (chapter two) was used for this exploratory study. Representative samples were included from each of the 8 hair curl group for quantification of total internal lipids and FTIR micro-spectroscopy. Care was taken to use the first 6cm of hair fibers for analysis in order to minimize introducing confounding variability arising from environment damage and other external features.

3.1.2 Total Internal Lipid Quantification

3.1.2.1 *Lipid extraction*

External lipids were removed from the hair surface by placing whole hair fibres in glass tubes with 1ml of hexane[93] (S303 K02/0415, Kimix South Africa) for 5 minutes at room temperature. Hair samples were then dried and placed into suitable sample tubes for pulverisation. Samples were pulverised with an Omni Bead Ruptor (Omni International Inc.) using two cycles of pulverization (60 seconds long at speed setting 5 with a 2 second pause in between cycles. One milligram (1mg) of pulverised hair was then used for total internal lipid extraction. Endogenous hair lipids were extracted in glass vials using a serial extraction with 2:1, 1:1 and 1:2 v/v mixtures of $CHCl_3$:CH_3OH (Chlorofrom: Methanol) (S327 K15/05/15, TAP10042965 K02/0415, Kimix, South Africa) for two hours each at room temperature followed by an overnight extraction at 4℃ with 100% methanol [73,100]. Extracts from each mixture were pooled and concentrated using a miVac Quattro concentrator (United Scientific, South Africa) at 30℃ for 45 minutes.

Care was taken not to heat extracted lipids beyond 35℃ to minimise degradation of extracted lipids[98] during drying. One millilitre (1ml) of HPLC grade methanol was used to reconstitute the dried lipids for analysis. When not analysed immediately, extracted lipids were stored in methanol at 4℃ until total lipid content quantification using the Sulfo-phospho Vanillin (SPV) Assay[148].

3.1.2.2 *Sulfo-Phospho-Vanillin Assessment Assay of Total Lipids*

The Sulfo-phospho Vanillin Assay method is a colorimetric assay for the quantification of total lipids. The assay is a two-step reaction, the first of which is the reaction of unsaturated lipids at 100℃ with concentrated sulphuric acid (H_2SO_4) to yield carbonium ions. The vanillin reagent is made by reacting vanillin (4-methoxy-3-hydroxy-benzaldehdye, $C_8H_8O_3$) with phosphoric acid, yielding vanillin phosphate. Phosphate esters from the vanillin reagent then react with the carbonium ions formed in the first step of the assay, yielding a pink complex that can be measured spectrophotometrically[149,150].The intensity of the complex depends on the composition of unsaturated fatty acids present. Oleic acid yields more intense colour than linoleic acid which in turn has a more intense colour than cholesterol[151]. Table 3.1 below shows the composition of standard used (sunflower oil) for the assay[152].

Table 3-1 The main unsaturated fatty acids found in sunflower oil.

Unsaturated fatty acids in Sunflower Oil	**Content (%)**
Palmitic Acid (C16:0)	6.07
Stearic acid (C18:0)	3.57
Oleic Acid (C18:1)	28.7
Linoleic Acid (C18:2)	60.0
Linolenic Acid (C18:3)	0.22
Arachic Acid (C20:0)	0.25
Behenic Acid (C22:0)	0.71

The vanillin reagent was prepared by dissolving 2mg of vanillin (Sigma Aldrich, BCBN9635V) in 10ml of 1:5 mixture of 85% phosphoric acid (Sigma Aldrich, STBF0263V)) in distilled water. The vanillin assay was first developed and used for the quantification of total lipids in serum[150] and has been adapted for use in multi-well plates for higher lipid analysis throughput[148,153]. For the assay, 50µl of extracted lipids

in 100% methanol and prepared standards were transferred into glass test tubes and the solvent was evaporated by placing onto a heating block at 90℃ – 100 ℃ for 5 minutes. A standard curve was made with sunflower oil at a concentration range of 0 – 3mg/ml. Ideally, the choice of standard used should be adapted to the sample or materials being analysed, however for convenience, sunflower oil can be used[151] because it is rich in unsaturated fatty acids[152].

One hundred microliters (100 µl) of concentrated sulphuric acid were added to glass test tubes, mixed gently and incubated on the heating block at 90℃ – 100℃ for 10 minutes. Samples were then removed from the heating block and cooled at 4℃ for 5 minutes before being transferred into a 96-well plate. Background absorbance of samples was read at 540nm using a Modulus Microplate reader (Promega Biosystems, Sunnyvale, CA, USA). Fifty microliters of freshly prepared Vanillin reagent was added into each well, mixed by gently pipetting and incubated at 37℃ for 15 minutes. Absorbance was read again at 540nm. Total lipid content was calculated from the sunflower oil derived standard curve.

3.1.3 Fourier Transform Infrared Microscopy of Whole Hair Fibres

The biochemical profile of whole hair fibres was investigated using Attenuated Total Reflectance Fourier Transform Infrared (ATR-FTIR) Microspectroscopy according manufacturer instructions (Bruker LUMOS, Bruker Optik GmbH 2014). Samples were collected and cleaned as described in chapter two. Three 2 cm strands of hair were taken from a minimum of 5 randomly selected volunteers from each of the 8 hair curl groups. Each strand was measured at three different positions 1cm apart to assess variation across different areas of the shaft. ATR-FTIR absorption spectra were obtained from 4000 to 400 cm^{-1} using 64 scans at a resolution of 4 cm^{-1} with a midband mercury cadmium telluride (MCT) detector. The detector was cooled with liquid nitrogen for at least 30 minutes prior to sample analysis. The ATR germanium (Ge) crystal with a diameter of 100µm was set at medium pressure for the acquisition of spectra.

3.2 RESULTS AND DISCUSSION

3.2.1 Total Lipid Content

The total lipid content of different hair groups was assessed using the Vanillin Assay. The method is a quantitative technique for unsaturated fatty acids[149,153]. The efficiency of the SPV approach is consistent with standard gas chromatography analysis, as demonstrated in a lipid assay for microalgae [154].

Although attempts were made to collect similar numbers of samples from each group, the 8-group method that was used initially was later shown to be unreliable (chapter two) – thus resulting in unequal numbers in the hair groups. Internal free lipids were extracted from a minimum of two volunteers per hair group. The data did not follow a Gaussian distribution and there was a lot of variation within groups. To gain insight in the observed variation between hair groups and reduce their influence on overall results, outliers (Interquartile range *1.5) in the box and whiskers plot (Figure 3-3) were excluded and results reanalysed. The median total internal lipid of the curliest hair groups (VII and VIII) was significantly higher than that of the straightest hair groups (I and II).The same trend was observed in the 6-group geometric classification. Interestingly, the median total internal lipid content of group V was also significantly lower than that of groups VII and VIII, while hair group 5 was significantly lower than group 6.

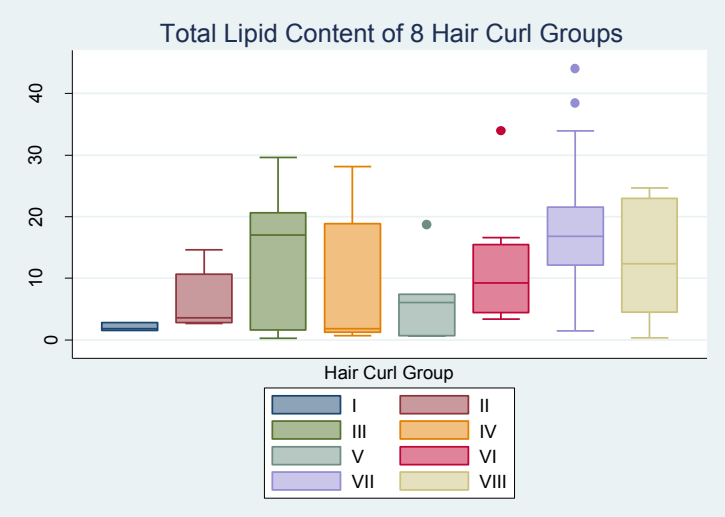

Figure 3-3 Box and whiskers plot (median and IQR) showing the distribution of total internal lipids across 8 hair curl groups. (Group I (n = 2), II (n = 7), III (n = 5), IV (n = 3), V (n = 3), VI (n = 5), VII (n = 11) & VIII (n = 3)).

The total lipid content results obtained from the volunteers across the 8 hair curl groups were then arranged according to self-assigned racial group in order to assess the relationship between race and total lipid content. The median total lipid content (Figure 3.4) of hair volunteers who self-declared as 'African" and "Mixed race" were significantly higher than the Caucasian group [($p<0.05$) and ($p<0.01$) respectively]

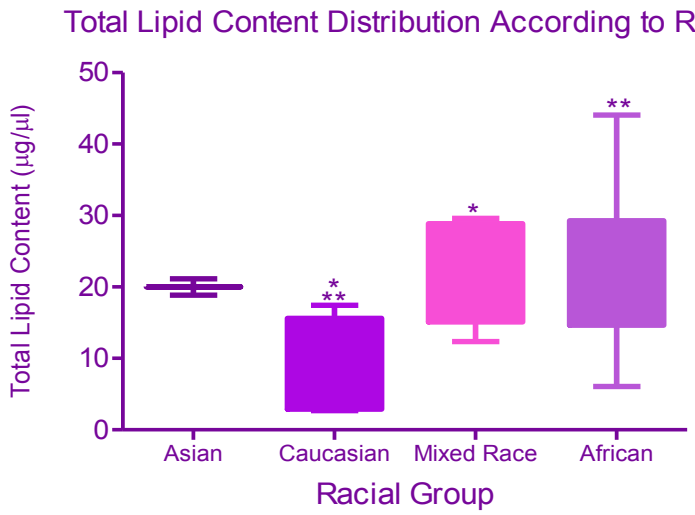

Figure 3-4 Box and whiskers plot (median and interquartile range) showing the distribution of total internal lipids in 4 racial groups.

These observations were similar to those made by Cruz *et al* who reported that the total lipid content of African hair was higher than that of Asian and Caucasian volunteers[73]. The total internal lipids quantified in this study are thought to be the unsaturated fatty acids (FFAs) such as oleic (C18:1) and linoleic acid (C18:2n-6) and polysaturated Fatty Acids (PUFA) (C18:2, C18:3) present in the hair[155].

Internal hair lipid levels were investigated in the current study in order to establish the baseline quantities of internal hair lipid across of hair with varying degrees of curvature. This was done in order understand the possible role of lipids in how lipid soluble substances are incorporated into the growing hair shaft. It is acknowledged that factors such as diet could have a confounding effect on these lipids. Is it also possible that exogenous lipids were incorporated from hair maintenance products although all surface lipids should have been removed when the hair was cleaned and flushed hexane wash[99,100].

3.2.2 Fourier Transform Infrared Micro-spectroscopy

The biochemical profile of whole hair fibres, from the cuticle inwards, was measured in the medium IR region, which spanned the fingerprint and functional group regions of the IR spectrum. The fingerprint region is the region below 1300 cm^{-1} while the region beyond that is the functional group region[156]. A representative ATR-FTIR spectrum acquired from the hair is shown in Figure 3-2. Variations in functional group region of hair spectra from different hair groups were first investigated by comparing the absorbance of selected IR bands. The selected bands were some of the characteristic bands observed in the spectra of proteins and amino acids. C-H stretching (usually assigned to lipids) at 2957cm^{-1}, Amide I band at 1637 cm^{-1} and Amide II at 1531cm^{-1}. These bands were also selected because they could be discerned without the requirement of spectral processing. Correlations between these bands and hair morphology would thus allow for rapid classification of hair for practical applications.

The peak absorbance of 0-H stretching band from H_2O was excluded. The peak area was measured relative to the local baseline. Other peaks that were observed in the spectra of whole hair fibres but were excluded for the current comparisons are listed in Table 3-2. An illustration of peak position and integration can be found in Appendix 3-1.

Two representative volunteers were randomly selected from each the 8 hair groups to explore the variations in adsorption of bands of interest. Three strands were assessed for each volunteer and each strand was measured in 3 positions along the length of the hair shaft. Sixty-four spectra were captured in each position and one representative spectrum was generated for each position.

Table 3-2 Band assignment chart for FTIR absorbance[147]

Wavenumbers (cm-1)		Assignment
Left edge	**Right Edge**	
3669.1000	3119.4000	OH (H2O)
3113.5600	3025.8400	Unknown
2996.6000	2949.8200	C-H
2949.8200	2903.0400	C-H
2897.1900	2832.8600	C-H
1721.7000	1575.5000	Amide I
1587.2000	1482.0000	Amide II
1481.9800	1429.3400	$-CH_3$
1429.3400	1359.1700	CH3 deforms

3.2.2.1 *Biochemical Variation between Racial Groups*

The FT-IR data was not normally distributed, no spectral processing was applied to the data and median and interquartile ranges were therefore used for all comparisons. The Kruskal Wallis with Dunn's post-hoc test was used for all statistical analysis, except where otherwise indicated. Figure 3-5 shows the variation observed in the band absorbance of C-H, Amide I and Amide II bands across the three racial groups. The results for the statistical analyses are reflected in Figures 3-6 and 3-8.

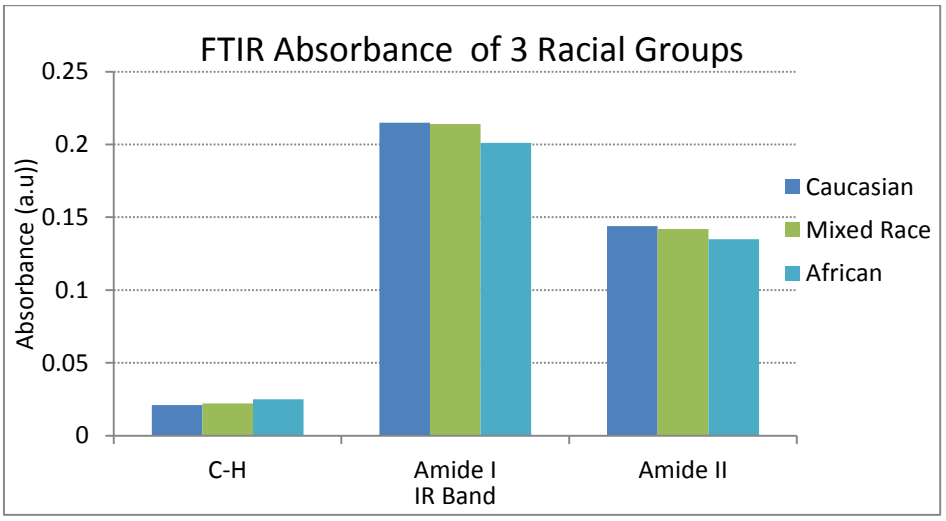

Figure 3-5 FTIR absorbance of different racial groups

Statistically significant differences were observed for the median total lipid across racial groups. The absorbance of C-H stretching vibrations of African hair significantly higher than that of Caucasian ($p < 0.01$) and Mixed race ($p < 0.05$) hair. This confirmed the elevated total lipid content obtained with the Vanillin Assay.

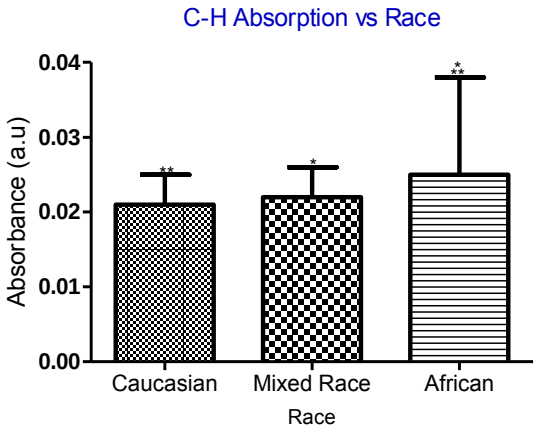

Figure 3-6 Absorbance of C-H band across racial groups

No statistically significant differences were observed between the absorbance of Caucasian and Mixed race racial groups. Asian hair samples were not included in the current analysis as a consequence of random sampling. The absorption of Amide I and II bands was significantly lower for African hair ($p < 0.01$ and $p < 0.001$). No significant differences were observed between Caucasian and Mixed race groups. The absorbance of the Amide II band was lower than that of Amide I, as expected and observed in the spectra in Figure 3-5.

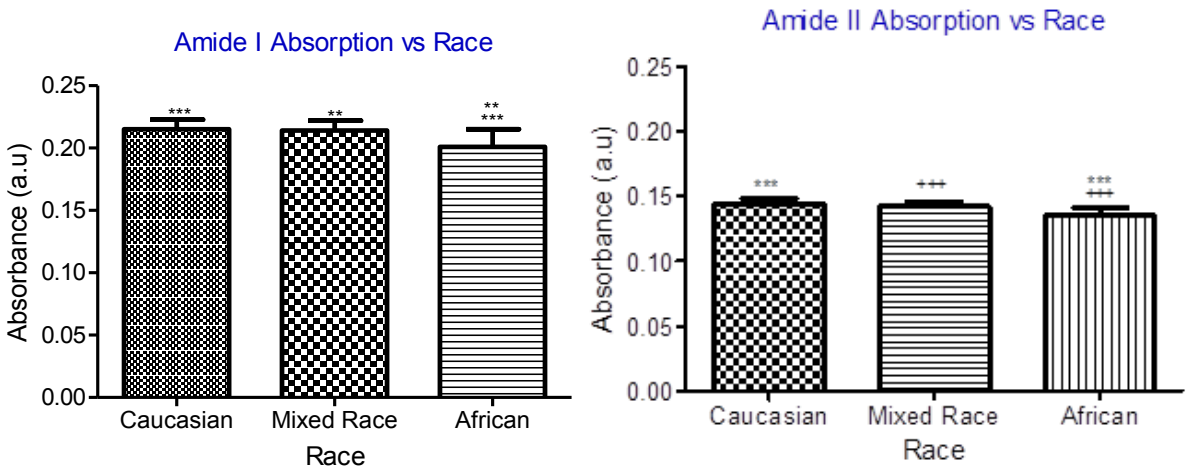

Figure 3-7 Absorbance of Amide I and Amide II bands across different racial groups.

The position of the Amide I and Amide II band are related to the structural conformations in the biological sample; Amide I at approximately 1652 cm $^{-1}$ and Amide II at approximately 1548 cm^{-1} are indicative of α-helical conformation of tertiary proteins[114,146]. An Amide I band at 1630 cm $^{-1}$ with an Amide II band between 1515 – 1525 cm^{-1} indicate proteins that have a β-sheet conformation[146,157]. The keratin conformation observed in the current study was closer to the ranges of the β-sheet form, indicating the IR radiation did not did not reach the hair cortex.

3.2.2.2 *Biochemical Variation across Hair Curl Groups*

The variation observed in the biochemical profile of different hair curl groups was assessed using the Kruskal Wallis test with Dunn's post-hoc test (GraphPad Prism Version 5). The hair groups with high curvature (V – VIII) were generally observed to have greater peak area for the lipid region (C-H). Some of these observed differences were statistically significant ($p < 0.001$ to $p < 0.05$) (Figure 3-8).The groups that have statistically significant variations are denoted by identical symbols, the level of statistical significance is illustrated by the weight of these symbols, for example + denotes a statistically significant variation with a $p < 0.05$, ++ denotes $p < 0.01$ and +++ denote $p < 0.001$. The band absorbance of hair group V was significantly higher than that of hair groups I, III and IV, while hair group VII was lower than hair groups II and IV ($p < 0.001$). The tendency of curly hair groups to have greater peak absorbance in the lipid was more consistent in the 6-group classification system (that was shown to be more reliable in Chapter 2), where hair groups 5 and 6 had the highest median peak absorbance. These were significantly higher than groups 1, 2 and 3 (Figure 3-8). The absorbance of the lipid band did not differ between groups 5 and 6.
A comparison of another lipid peak at 1481 cm^{-1} is shown in Addendum 1 in this report. Variations for this cancer associated peak were uniform across hair all groups for the 6-group classification, reflecting that this band could be a good region to focus on to monitor changes in lipid content in cancer patients across different hair types.

For the absorption of Amide I and II, curly hair groups were observed to have lower peak areas in both regions, and this was more consistent when hair morphology was categorised into 6 groups instead of 8.

Hair group V absorbed less amide I than groups II to IV, while the absorbance in group VII was lower than that of groups I, III, IV and interestingly VIII. (Figure 3-8, bottom panel). The same was observed for the 6-group classification; hair group 5 was significantly lower than hair groups 1, 3 and 4. The median amide II absorbance of hair group V was lower than that of hair groups I to IV ($p < 0.001$) (Figure 3-9), while hair group III was statistical higher than the highest curvature hair groups (V to VIII) ($p < 0.05$), for the 8-group classification. For the 6 group classification, there was significant variation between low (1 to 3) and high curvature hair groups (5 and 6). The absorption of Amide II by hair groups 5 and 6 was significantly lower than 2, 3 and 4 ($p < 0.001$ to $p < 0.05$). Hair group 1 could not be shown to be statistically different from any of the other hair groups. In most instances, no statistically significant differences were observed between straight hair groups (I to IV), reflecting a level of possible biochemical homogeneity in these hair types.

There were no clear correlations between biochemistry and geometry for the 8 group classification. There were however some discernible trends between the biochemical characteristics and different hair groups for the 6-group geometric classification where high curvature hair groups tended to have higher lipid content and lower amide I and amide II absorption. It is thus likely that biochemical variations are easier to detect when hair curl groups are fewer because in the 6 group classification, the high curvature are reduced from 4 to 2 groups. It is however still likely that the 3 racial groups are not only subjective but are too few.

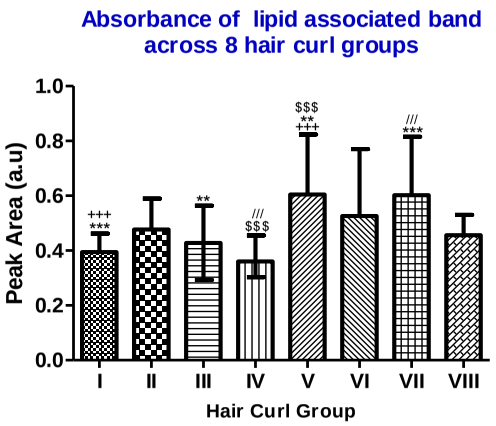

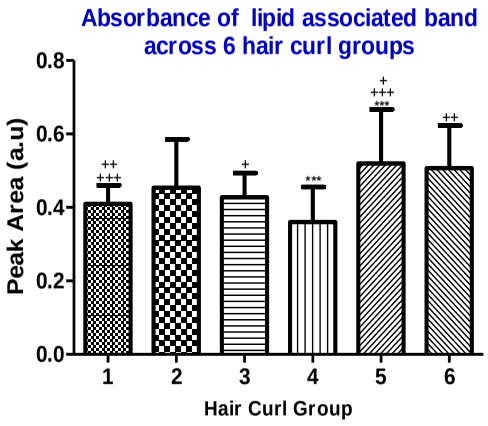

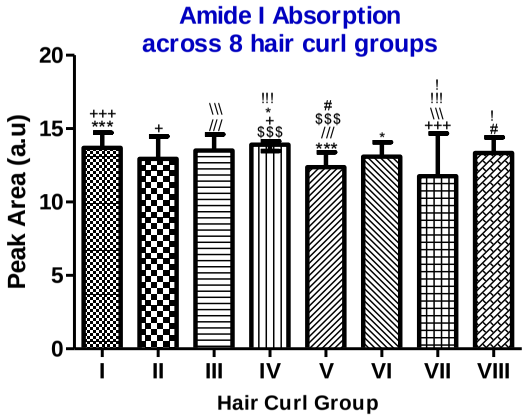

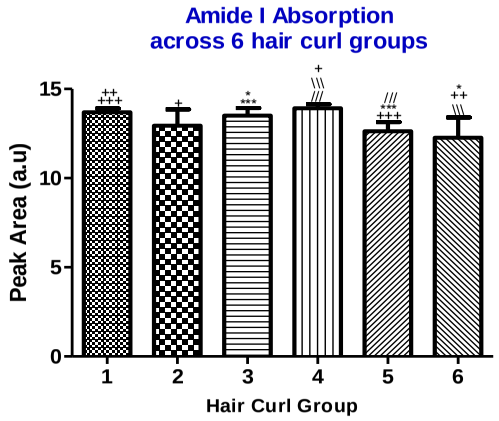

Figure 3-8 statistically significant differences observed in the selected FTIR bands for the 8 and 6-group classifications. Median and IQR.

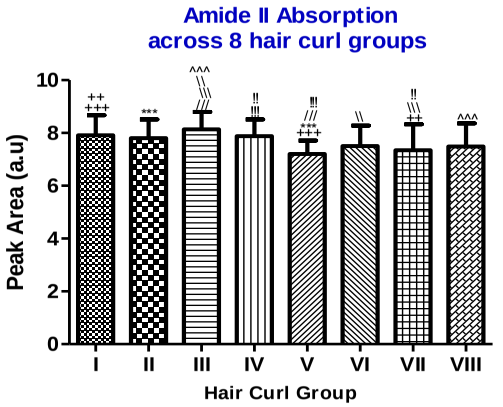

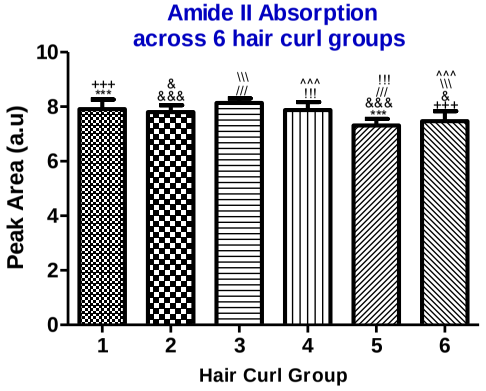

Figure 3-9 Amide II band absorption by different hair curl groups. Median and IQR.

3.2.2.3 *Discriminative analysis of hair groups by ATR-FTIR*

The capability of ATR-FTIR to discern the variation observed between the different hair groups and correctly identify which hair group the spectra originated from was explored. Principal component analysis (PCA) applied to the full FTIR data obtained from 53 volunteers. Each volunteer had multiple spectra as described in the methods section. Spectra that were clearly outliers, possibly reflecting poor contact between the ATR crystal and the test sample were excluded. This was indicated by spectra whose absorbance was lower than the majority of the spectra for a particular individual.

3.2.2.3.1 Variations in ATR-FTIR Spectra of Different Hair Curl Groups

Figure 3-10 is a scatter plot from a PCA showing the variations between and within the different hairs. Up to four components were retained and the PCA did not reflect any distinct hair groups. The first four components explained more than 80% of the observed variation between the hair groups. Variation was also observed within some of the hair curl groups.

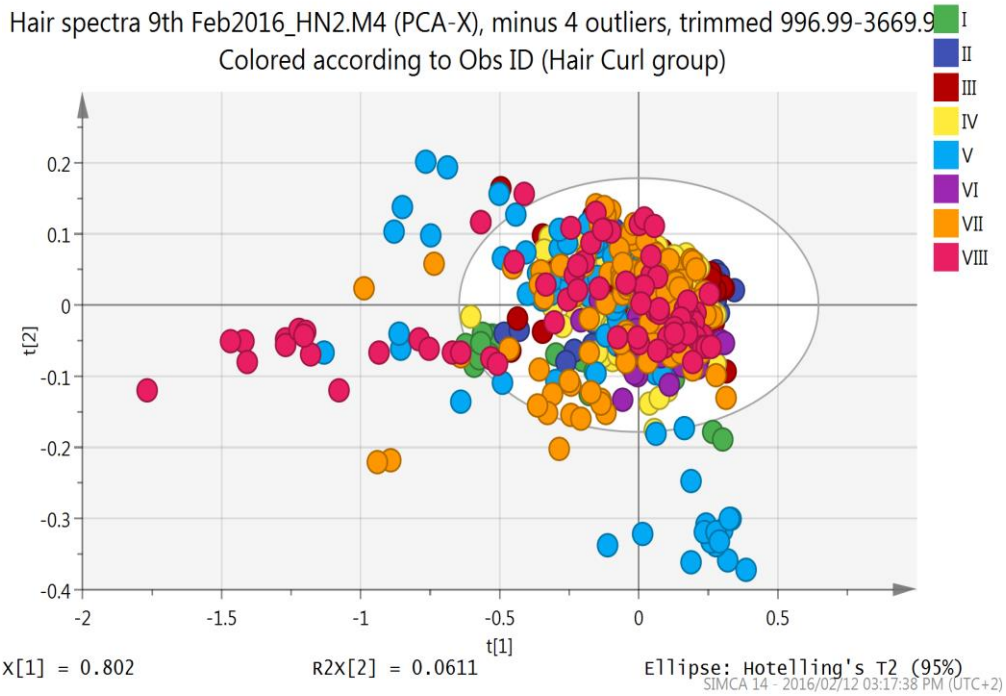

Figure 3-10 PCA-X scatter plot of FTIR spectra from 8 hair curl groups

Orthogonal partial least squares discriminative analysis (OPLS-DA) (SIMCA, Version 14.1 MKS Umetrics) was used to investigate the validity and uniqueness of the 8 hair curl groups. OPLS-DA fits an OPLS model using dummy variables and interprets variation in X. The X variable is orthogonal to Y (SIMCA, Version 14.1 MKS Umetrics).

Figure 3-11 is an example of the scatter plot post pairwise OPLS-DA applied to hair curl groups I and II. The scatter plot shows that the majority of the spectra from hair group I could be discriminated from that of hair group II. The variation between the groups is observed along the x-axis, while the variation with the groups is observed the y-axis.

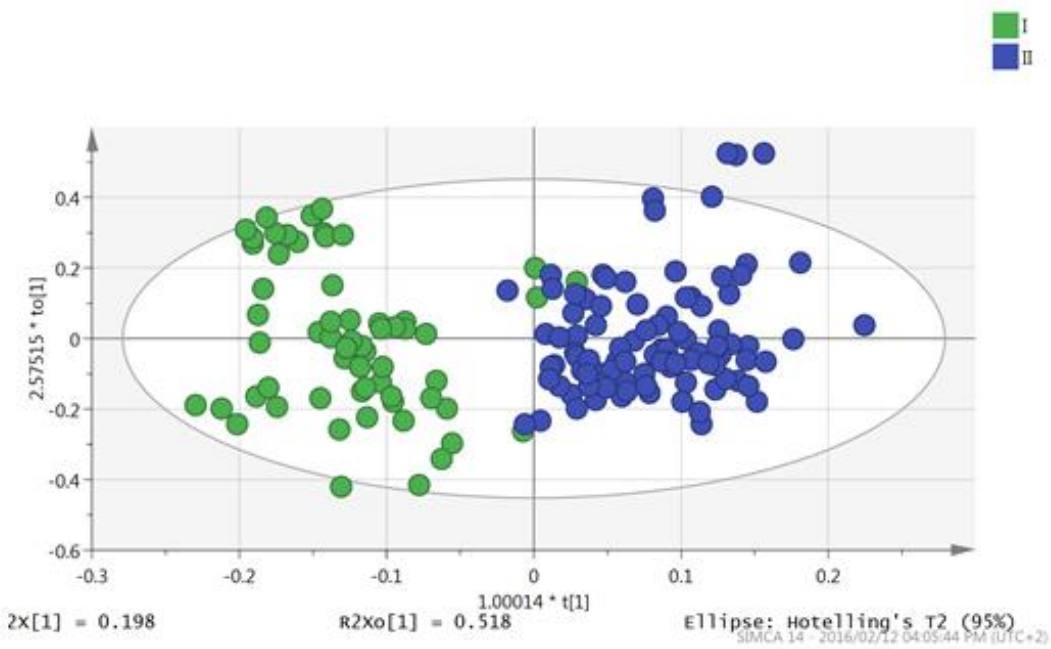

Figure 3-11 Pairwise Orthogonal Partial Least Squares Discriminative Analysis of hair groups I and II.

Pair-wise OPLS-DA was applied to all pairwise combinations found in the 8-group classification. Most of the groups could correctly predict the group membership of most of its spectra. Table 3-3 is a misclassification table showing the results of the pairwise OPLS-DA between major groups. The first column shows the chosen pairs, the second column shows the number of spectra in each group and the third column is the % of spectra that were correctly assigned to their original group by each prediction model.

Table 3-3 Summary of Orthogonal Partial Least Squares Discriminative Analysis

Summarized Misclassification Table			
Class Pairs	Members	Correct (%)	Fisher's prob.
I	47	91.49	
II	99	98.99	3.8 e-031
II	99	58.59	
III	133	77.44	2.1e-008
III	133	96.99	
IV	56	98.21	1.2e-041
IV	63	100	
V	43	88.37	1.1e-023
V	43	100	
VI	35	97.14	2.4e-021
VI	43	97.14	
VII	49	100	9.5e-023
VII	54	100	
VIII	26	100	1.3e-021

The groups could be discriminated for more than 50% of the spectra for each pairwise OPLS-DA, the worst discrimination was observed between hair groups II and III, as reflected by a correctly classified score of 58.59. In the comparison between these two groups, 41 out of the 99 spectra from group II were incorrectly classified as belonging hair group III and 30 spectra belonging to hair group III were given class membership of group II. The misclassification table for the OPLS-DA of all 8 hair groups is shown Table 3-4 .

Table 3-4 Misclassification table of 8 hair groups

	Members	Correct (%)	I	II	III	IV	V	VI	VII	VIII
I	47	23.4	11	4	29	0	0	3	0	0
II	99	43.4	0	43	29	13	6	1	7	0
III	133	87.2	1	9	116	5	0	0	2	0
IV	63	33.3	1	9	21	21	0	6	5	0
V	45	80.0	0	0	6	0	36	0	2	1
VI	37	89.2	1	0	0	1	1	33	1	0
VII	54	40.7	0	3	17	2	9	1	22	0
VIII	30	26.7	0	12	4	1	1	3	1	8
No class	0		0	0	0	0	0	0	0	0
Total	508	57.1%	14	80	222	43	53	47	40	9

When the FTIR data was arranged into the 6-group system, there was no significant improvement in the overall classification ability of the 6-group model. Improvements were however observed in its ability to correctly classify high curvature but not low curvature hair groups. Some spectra from hair groups 5 and 6 were classified as belonging to hair groups 2 and 3, but the majority of their spectra (78.1% and 71.4%) were correctly classified.

Table 3-5 Misclassification table for 6 hair groups

Hair Group	Members	Correct (%)	1	2	3	4	5	6
1	47	12.8	6	8	29	0	3	1
2	99	32.3	1	32	47	5	10	4
3	133	83.5	0	8	111	2	0	12
4	63	25.4	1	6	27	16	5	8
5	82	78.1	0	6	6	0	64	6
6	84	71.4	0	7	9	1	7	60
No class	0	0	0	0	0	0	0	0
Total	508	56.9%	8	67	229	24	89	91

To minimize the effect of the variation observed within individuals, the spectra of each individual was averaged, resulting in 53 spectra. The misclassification results of the averaged spectra are shown in Tables 3-6 and 3.7. The worst classification was

observed for hair groups II, IV and VI where none of their group members were correctly classified. All the members belonging to hair group II & VI were classified as hair group III, while 6 out the 7 members of group IV were classified as group III. Hair groups III and V had the best classification, with 100% of their members being correctly classified. The total classification score for the averaged spectra was 35.85%.

Table 3-6 misclassification table of averaged spectra (8 hair groups)

	Members	Correct	I	II	III	IV	V	VI	VII	VIII	No
I	5	20%	1	0	4	0	0	0	0	0	0
II	8	0%	0	0	8	0	0	0	0	0	0
III	11	100%	0	0	11	0	0	0	0	0	0
IV	7	0%	0	0	6	0	1	0	0	0	0
V	5	100%	0	0	0	0	5	0	0	0	0
VI	4	0%	0	0	4	0	0	0	0	0	0
VII	8	12.5%	0	0	4	0	3	0	1	0	0
VIII	5	20%	0	0	3	0	1	0	0	1	0
No	0		0	0	0	0	0	0	0	0	0
Total	53	35.85%	1	0	40	0	10	0	1	1	0
Fisher's	3.1e-005										

Table 3-7 OPLS-DA Misclassification table of averaged spectra (6 hair groups)

	Members	**Correct**	**1**	**2**	**3**	**4**	**5**	**6**	**No**
1	5	0%	0	0	3	0	1	1	0
2	8	0%	0	0	6	0	2	0	0
3	11	100%	0	0	11	0	0	0	0
4	7	0%	0	0	3	0	3	1	0
5	8	37.5%	0	0	2	0	3	3	0
6	11	36.36	0	0	5	0	2	4	0
No class	3		0	0	0	0	0	0	0
Total	53	36.0%	0	0	30	0	14	19	0
Fisher's	0.023								

3.2.2.4 *Predictive models for FTIR hair classification*

The variation observed in the average d spectra was also investigated by multiple linear regression (Statistica). For this, hair morphology was treated as a continuous variable, with the straightest and curliest hairs being 1 and 8 respectively. The full FTIR spectrum (500 to 4000cm^{-1}) was condensed by taking every 10th wavenumber and discriminative analysis was conducted on every 10th scan. A linear regression model consisting of 8 variables (obtained by variable selection) showed that 78% of the variance in hair curl is explained by the proposed model (Figure 3-12). These observations were validated using leave-one out cross validation method and the calculated R^2 was 0.6713 and the mean squared error (MSE) was 1.625.

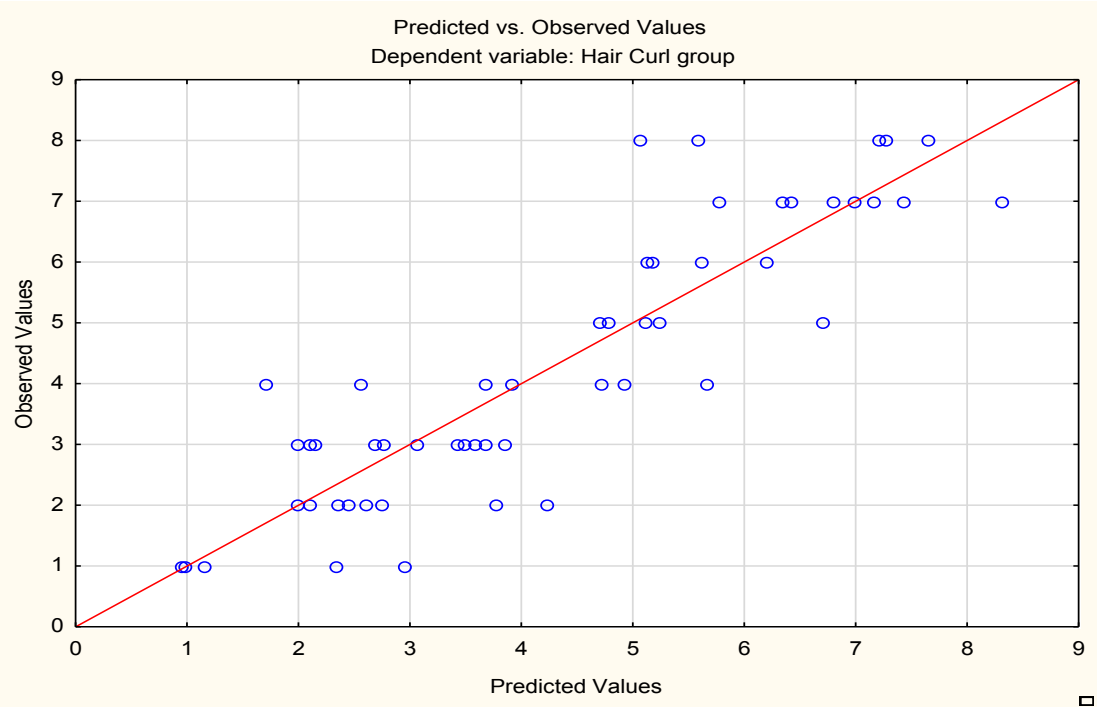

Figure 3-12 Multiple linear regression model of the relationship between hair morphology and spectroscopy.

The multiple linear regression model when hair curl is treated as a continuous variable from 1 to 8 is shown below in Equation 3-3:

$$\hat{Y}=W2038.84+W1814.57+W2446.61+W1304.86+W1284.47+W1406.80+W2181.56+W2120.39+W2507.77 \quad \text{Equation 3-3}$$

Where Ŷ is the predicted hair curl. The W are the different wavenumbers that contributed to the model. The regression summary for the model is show below in Table 3-8.

Table 3-8 Regression for hair curl (8 hair groups)

Regression Summary for Hair Curl R = 0.8844 R^2 = 0.7821 Adjusted R^2 = 0.7303 Std. Error of estimate: 1.154		
Wavenumber (cm^{-1})	Coefficient (b*)	p-value
Intercept		0.000910
2038.84	-4.476	0.01014
1818.57	0.523	<0.0001
2446.61	25.697	<0.0001
1304.86	3.780	<0.0001
1284.47	-3.052	<0.0001
1406.80	-0.809	<0.0001
2181.56	-30.148	<0.0001
2120.39	19.563	<0.0001
2507.77	-10.745	<0.0001

When a multiple linear regression model with a hair curl scale of 1 to 6 was fitted (Figure 3-13), better correlation was noted between the observed and predicted values (R^2 = 0.8137).

The linear regression model for this scale (1 to 6) was:

$$\hat{Y}=W1814.57+W2038.84+W1733.01+W2711.65+W2752.43+W2344.66+W1610.68+W3139.81+W3078.65+W2222.33 \quad \text{Equation 3-4}$$

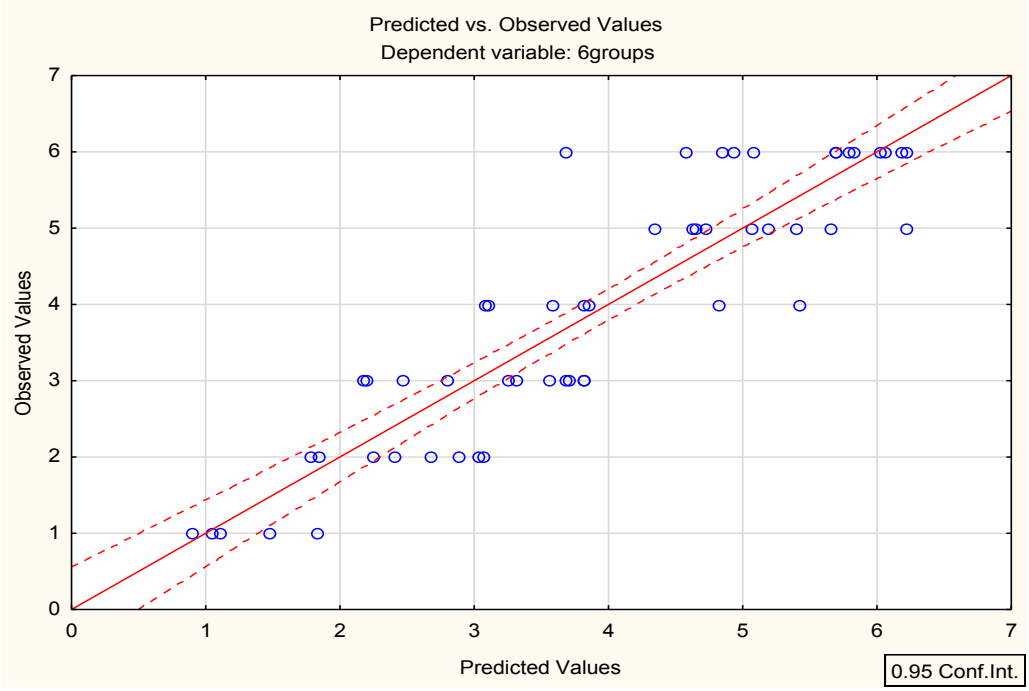

Figure 3-13 Multiple linear regression model of the relationship between hair morphology and spectroscopy of 6 hair curl groups.

When the model was validated with leave-one out cross-validation, the observed R^2 was 0.7497 and MSE was 0.705. The model for a 6-group hair classification was thus better than that of a classification with 8 groups; R^2 =.0.8167 vs R^2 = 0.7821. The regression summary for the 6 groups is shown below in Table 3-9.

Table 3-9 Regression summary for hair curl (6 groups)

Regression Summary for Hair Curl R = 0.9020 R^2 = 0.8137 Adjusted R^2 = 0.7629 Std. Error of estimate: 0.811		
Wavenumber (cm^{-1})	Coefficient (b*)	p-value
Intercept		0.4399
1814.57	0.821	<0.0001
2038.84	-3.489	<0.0001
1733.01	-0.736	<0.0001
2711.65	41.004	<0.0001
2752.43	-32.189	<0.0001
2344.66	-0.236	0.0114
1610.68	1.999	<0.0001
3139.81	4.135	<0.0001
3078.65	-5.089	<0.0001
2222.33	-4.735	<0.0001

A supervised approach was then applied to the data set; the original 8 hair groups were merged into 4 groups (I & II (A), III & V (B), V & VI (C) and VII & VIII (D)) and the variation between these groups was investigated with partial least squares discriminative analysis. Three principal components were retained. The resubstitution classification matrix is shown in Table 3-10, the overall classification success was higher than 79% across the 4 hair groups. Figure 3-14 is a scatterplot of the first 2 canonical scores from 4 hair groups. Four clusters of partially heterogeneous groups can be observed. The kappa statistics investigation of a 4-group classification at attached in this report as Addendum 2.

Table 3-10 Resubstitution classification matrix of 4 hair groups

Hair Group	Percent Correct (%)	1	2	3	4
A	69.23	9	3	1	0
B	83.33	2	15	0	1
C	88.89	1	0	8	0
D	79.92	0	3	0	10
Total	79.25	12	21	9	11

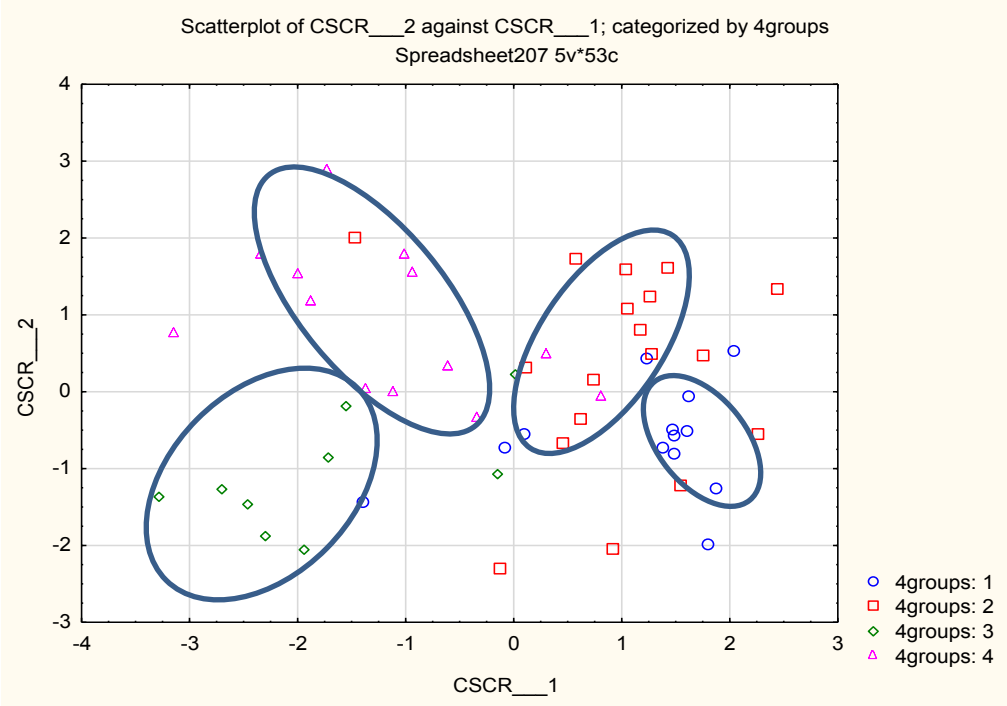

Figure 3-14 Scatter plot of canonical scores from 4 hair curl groups.

3.3 CONCLUSIONS AND FUTURE WORK

The total internal lipid content was highest in curly hair in both the 8 and 6 group classification. This was consistent with findings of other workers that had racially classified their hair samples[73]. The unique aspect of the current investigation was the objective geometric classification that is geared towards minimizing variation that arises from the heterogeneity of (i.e. more objective than) race based classification. For the FTIR analysis, the peak areas of the C-H band were higher for curly compared to straight hair groups, also indicating higher lipid content. Lipid variations of a cancer

associated peak were uniform across hair groups (shown in addendum 1). This confirms that this band could be a suitable region to monitor changes in lipid content in cancer patients.

Although there were no identifiable groups on PCA, more than 50% of spectra from geometrically classified hair groups could be discriminated using pairwise OPLS-DA. However, when average spectra per group were used, the 8-groups had a poor averaged classification score (35.85%) which was similar to that for the 6-group classification (36.0%). Further, predictive models were also similar for the 6 and the 8-group classification (R^2 =.0.8167 vs R^2 = 0.7821).

The analysis of FTIR spectra suggested a correlation with biochemistry (internal lipid content) for the extremes (i.e. straight versus curly) both the 8 and 6-group hair classification. The wavenumbers that were statistically significant for the relationship between FTIR and hair morphology are shown in Tables 3-7 and 3-8. Although pairwise OPLS-DA comparisons do not provide evidence to merge groups, except hair groups II and III, the 6 group classification is simpler because it excludes the hair count requirement (as described in chapter two) without loss of information.

The FTIR investigation in this study was explorative, only participants with natural (not chemically altered hair were investigated). It is suggested that future work should also include investigations of the factors (e.g. age, gender, hair preparation) that may contribute to the variability in hair spectra of healthy volunteers. Such influence on FTIR should be taken into consideration when interpretation changes in hair chemistry that arises from certain disease.

Overall, the relationship between hair geometry and biochemistry was more consistent in the 6 group classification than in the 8. Therefore it is likely that biochemical variations are easier to detect when hair curl groups are fewer. Compared to the 8 group, in the 6-group classification the curly hair is effectively reduced from 4 to 2 groups. Consistent with improved reliability for fewer groups, when a supervised statistical approach was applied to 4 groups using the FTIR data classification success improves from 36.85% (8 groups) and 36.0%(6 groups) to 79% (range: 69% – 88%).

Such a 4-group classification needs validation but seems more objective than using racial groups to describe hair testing samples in clinical or research studies.

Appendix 3-1 : Integration of FTIR bands for peak area comparions

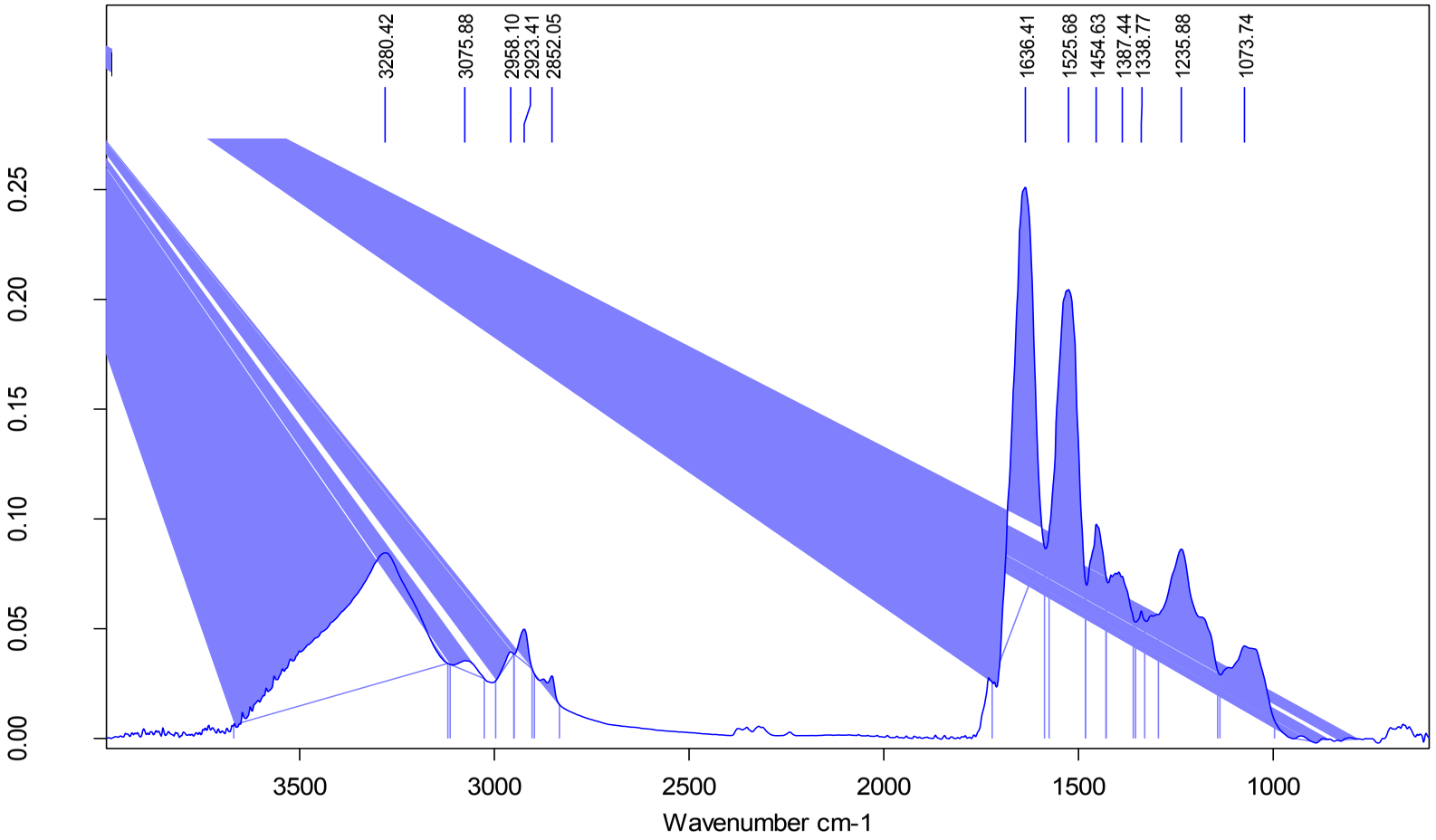

CHAPTER FOUR

MECHANICAL CHARACTERISTICS, HAIR GROWTH PARAMETERS AND ULTRASTRUCTURE OF HUMAN SCALP HAIR

ABSTRACT

Background: Human hair characteristics are commonly described using race; however racial classification (Asian, Caucasian and African) is limited and unscientific. A recently published geometric classification allows for less subjective investigation of hair features. The aim of this study was to investigate relationships between hair curvature using 2 classifications (I–VIII and 1-6; for straight to tightly curly hair) and other physical characteristics [mechanical properties (elasticity, tensile strength, yield extension and break extension), growth parameters (growth rate and hair density) and ultra and micro structure].

Methods: Virgin hair from 128 volunteers was classified using published templates. Mechanical characteristics were measured using a Miniature Tensile Tester and growth parameters using a computerized trichogram as well as a formula based on interscale distance (ISD) and diameter; samples were also imaged using Electron and Fluorescent Light Microscopy (FLM) to elucidate ultra-structural difference.

Results: The yield strength of all hair groups was higher (> 100MPa) than published data from racially assigned groups (58 MPa – 100 MPa). The straightest hair (group 1) had the highest average diameter and although this was not statistically significant from that of high curvature hair groups. Hair groups 2 and 3 surprisingly had the thinnest diameters even compared to curly hair groups. Overall the tensile strength was lowest for the curliest hair groups, although there was no consistent correlation (in elastic modulus, yield strength, Break strength and strain failure) with fibre geometry.

The growth rate based on the TrichoScan® was fastest for the straightest hair (group1, 0.72 ± 0.3 cm/month) and slowest for the curliest hairs (0.39 ± 0.2 cm/month). Growth rates based on ISD were haphazard and did not correlate with hair curl. This study is

the first to confirm that FLM gives similar results to TEM for visualization of cortical cell in curly African hair (as previously reported for straight hair). There was also no consistent correlation between density and fibre geometry.

Conclusion: This study suggests that the common assumption of 1.0cm growth rate for all hair phenotypes may be incorrect. This may lead to incorrect estimation of drug exposures for curly hair.

4 INTRODUCTION

Human scalp hair characteristics vary beyond morphology[1,61,62,76]. Straight hair is reported to have a higher break stress and faster hair growth than hair with curvature[76,158]. The hair cortex is the hair component that is largely responsible for the mechanical properties of the hair fibre[32,39]. Hair cuticles cells form multiple layers over the hair cortex[22],protecting it from physical and chemical insult[76]. The contribution of hair cuticles to the mechanical properties of the hair[39]. The distance between cuticle cells is reported to be related to the rate of hair growth[159]; Baque *et al*. measured interscale distance (ISD) and observed that straight hair from Japanese volunteers was thicker, had shorter ISD and faster rates of hair growth, while curly hair the inverse was observed for Caucasian volunteers with slightly curly hair[159]. Table 4-1 shows the differences observed in the cross-sectional properties[92] and surface properties[92,159] of African, Asian and Caucasian hair .

Table 4-1 Hair characteristics of hair 3 racial groups[92,159]

Race	Shape	No. of scales	Cuticle Scale Thickness(μm)	Interscale Distance	ISD Hair Growth Rate (mm/day)
African	Oval-flat	6 - 7	0.3 - 0.5	-	-
Asian	Nearly oval	5 - 6	0.3 - 0.5	7.99	0.4335
Caucasian	Nearly round	6 - 7	0.3 - 0.5	8.06	0.376

Recent advances in hair classification now allow for the investigation of correlation with other hair features such as mechanical and physical properties beyond racial categorization. Natural scalp hair can now be classified using 3 geometric parameters; curve diameter, curl meter and the number of waves present [63,69] resulting in 8 hair curl groups[69]. However, our investigation, using Kappa statistics, showed that that a 6-group classification is more reliable (chapter two).

4.1 Mechanical and Growth Parameters of Human Scalp Hair

4.1.1 Mechanical Properties of Scalp Hair

The tensile properties of human scalp hair are an important metric of its strength[160].Scalp hair with a high degree of curvature is reported to be least resistant to mechanical extension and to exhibit profiles of premature failure[92]. African hair is

reported to have average yield strength of 58 MPa, while that of Asian and Caucasian hair is 100 MPa and 67 MPa respectively and shown in Figure 4-2 and Table 4-2. Furthermore, the tensile strength of African hair has been reported to be lower than that of Caucasian or Asian hair[137].

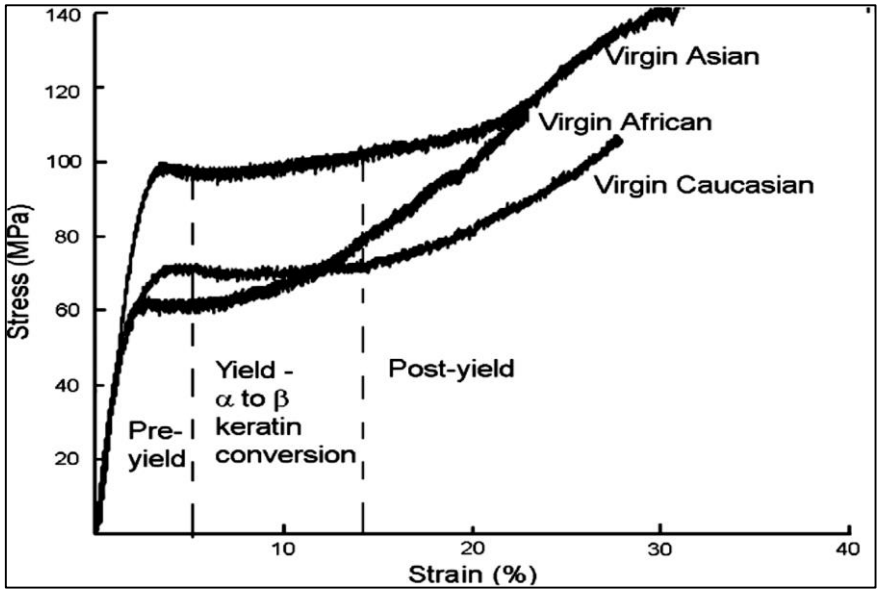

Figure 4-1 Stress and strain profiles of African , Asian and Caucasian hair[160].

Table 4-2 Mechanical properties of hair from different races[160]

Mechanical Property	African	Asian	Caucasian
Elastic modulus (GPa)	2.5	4.7	3.3
Yield strength (MPa)	58	100	67
Breaking strength (MPa)	101	139	117
Strain at failure (%)	20	32	35

4.1.2 Hair Growth Parameters (growth rate and density)

African hair is reported to have the slowest hair growth rate and to have the second lowest hair density, after Caucasian hair[158,161]. African hair is reported to have a growth rate of 256 ± 44 μm/day (0.6 - 0.9cm/month), Caucasian hair: 396 ± 55 μm/day (1.0 -

1.35cm/month)[158,162]. Hair analysis interpretations usually cite a blanket growth of 1.0cm per month for all racial groups[3,6,17,126] and sampling 3cm as indicating a 3 month exposure[126]. The rate of hair growth could influence levels of incorporation onto the growing hair shaft and variations across hair groups elucidated and taken into for all hair groups in order to correctly interpret results obtained for various hair analyses[120,126].

4.1.3 Structural Properties of Scalp Hair Cross-sections

The hair cortex, like wool, made up of 3 different three cortical cells types; ortho, para and mesocortical cell types[22,60,77,90,163]. The differences between these cell types are their biochemical composition[22] .Orthocortical cells are reported to contain less matrix between their intermediate filaments than paracortical cells and they have been shown to have a lower sulphur content (~3%) than Paracortical cells (~5%) while that of mesocortical cells is intermediate[22].Correlations have between drawn between hair morphology and arrangement of various cortical cells within the hair cortex[90]. Straight hair groups are reported to be composed of predominantly paracortical cells, with a layer of orthocortical and mesocortical usually observed adjacent to the hair cuticles [22,60,90]. African hair has been reported to have higher proportions of orthocortical cells than Caucasian[77] and the cell types usually have an asymmetrically distribution on the hair cortex cross-section[60].

The aim of this chapter was to investigate relationships between hair curvature and mechanical characteristics, hair growth parameters and ultrastructure. The mechanical characteristics investigated were elastic modulus (elasticity), break stress (tensile strength), yield extension and break extension. The hair growth parameters of interest were hair growth rate and hair density. The ultrastructural details that the study sought to elucidate were the arrangement of the cortical cells across different hair groups.

4.2 MATERIALS AND METHODS

4.2.1 Participants and Samples

Permission to conduct the study was granted by the Faculty of Health Sciences, Research Ethics Committee of UCT (HREC REF: 328 2012). Participants with at least

6cm of virgin hair (had not used any chemical straightener or dyes for > 7 months) were invited to participate in the study via notices, fliers and university's online research invitations. After participants gave informed consent, an area of 0.56cm^2 was shaved from the vertex of the scalp. To prepare the hair samples for geometric measurements, they were washed using a 1% sodium dodecyl sulphate (SDS) solution, rinsed with warm water (37℃) and air-dried for a minimum of 4 hours. Samples were then stored at room temperature until used for various assessments.

4.2.2 Geometric Characterization

Hair samples were classified were first classified into 8 geometric groups following published templates and the rules[69] as shown in Figure 4-2. Inter and intra-observer data showed better reliability of a 6-group classification (chapter two). This was used in the current study to investigate the relationships between hair geometry and characteristics discussed below.

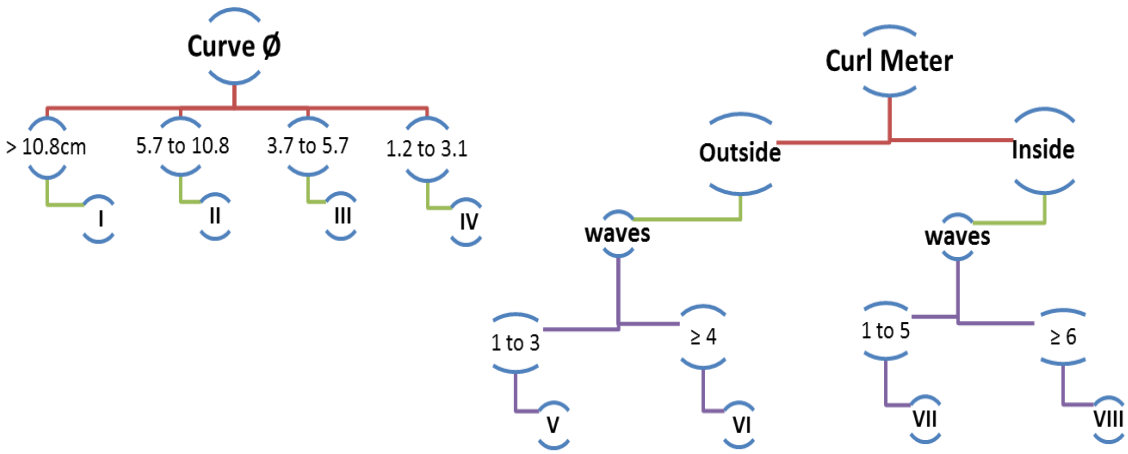

Figure 4-2 Hair classification rules for the 8-group geometric classification[69].

4.2.3 Measurement of Mechanical Properties of Single Hair Fibres

The tensile properties of dry natural hair were measured using a Miniature Tensile Test (MTT686, Dia-stron Ltd, Hampshire). The mechanical properties of single hair fibres were measured using a 20 Newton (N) load cell and a strain of 12.5 mm/min. The gauge force was set to 0.5g. All measurements were carried out in an

environmentally controlled chamber (Electro-tech systems, Inc) that was set at a temperature and a relative humidity of 22 ± 5℃ and 45 ± 5 %, respectively. All hair samples were equilibrated in the environment chamber for 12 hours before mechanical assessments. The elastic modulus, break stress, yield extension and break extension were recorded for all hair groups.

4.2.4 Hair Growth Rate and Hair Density Assessments

4.2.4.1 *Automated Hair Growth Assessment: TrichoScan®*

Hair growth parameters (hair growth rate and hair density) were quantified using the TrichoScan® platform. Hair density is reported as the number of hairs in an area of 0.562cm^2 immediately after shaving (day 0). Our current license version of the TrichoScan® software did not automatically calculate of hair growth. Instead, an output of hair length frequencies (hair length versus count) was obtained. Image processing platforms (MATLAB 6.1 and GRABIT (MATLAB and Statistics Toolbox Release 2012b, The MathWorks, Inc., Natick, Massachusetts, United States)) were used to quantify TrichoScan® outputs at each time point (day 0 and day 2). The combination of these two image processing platforms allowed for the collection of "raw data" points. An illustration of this is included as appendix 4-1. The collected raw data was used for assessments of hair growth rate and hair density. Hair growth rate, in micrometres (μm) per day, was calculated using equation 4.1.

$$\textbf{Hair growth rate} = \frac{(D2-D0)}{2} \qquad \text{(Equation 4.1)}$$

Where day 0 (D0) is the average hair length, measured immediately after shaving and Day 2 (D2) is the hair length in the same area, measured at the second visit ,two days later.

4.2.4.2 *Manual Hair Growth Assessment Using SEM Micrographs*

Hair growth rate was also calculated from interscale distance (ISD) and the hair diameter as described by Baque *et al*. [159]. Representative hair samples from each of

the 8 hair groups were imaged using SEM (FEI Nova nanoSEM 230). SEM images were captured at 600 and 1000-fold magnification and at a working distance of 6mm. ImageJ processing software (ImageJ 1.47v, National Institutes of Health, USA http://imajeJ.nih.gov//ij)[164] was used to measure the distance between successive cuticle scales and hair shaft diameter[159]. Care was taken to image within 1 to 6cm of hair fibres in order to exclude damaged hair. Equations 4.2 taken from Baque *et al*. were then used to calculate hair growth.

$$\boldsymbol{ISD = -9.4337X\ Growt\ rate + 11.831} \qquad \text{(Equation 4.2)}$$

4.2.5 Structural Characteristics of Human Scalp Hair Cross-sections

4.2.5.1 *Transmission Electron Microscopy*

Representative hair samples were selected from the geometric 8-groups and prepared for transmission electron microscopy (TEM) viewing as outlined in Appendix 4-1. Once processed, ultra-thin sections (95nm) were sections using a diamond knife on a Leica ultra-microtome (*Leica Wild M3Z Reichert Utracuts and Diatome Static line II made by HAUG)*. Sections were then stained with uranyl acetate and lead citrate and then imaged with TEM.

4.2.5.2 *Fluorescence Light Microscopy*

Structural characteristics of cross-sectional properties of different hair groups were also imaged using Fluorescent Light Microscopy. For this protocol, clean hair samples, taken from the first 6cm length of a volunteer's hair were fixed with glutaraldehyde and osmium tetroxide before being embedded in LR White resin overnight at 70^0C. Thick hair sections (1.5µm) were cut using an ultra-microtome. Sections were lifted onto positively charged glass slides (SuperFrost Plus®, Menzel-Glaser, Thermo Scientific), dried and stained with 0.002% phosphate buffered Fluorescein sodium (FS) (Sigma Aldrich, USA) in a dark room for 18 hours. After 18 hours, the slides were rinsed with water, dried and then stained with 0.0005% phosphate buffered Sulforhodamine 101 (SR) (Sigma Aldrich,USA) for 2 - 15 minutes. Slides were then washed with water, dried and mounted with mowiol 4-88 containing N-propyl galate anti-fade (Sigma

Aldrich, USA) before being incubated overnight at room temperature in the dark and viewed with a fluorescent light microscope (Carl Zeiss, Axiovert 200M) the following day. Fluorescent light microscopy (FLM) images were captured with an Axiocam high resolution microscope camera (Carl Zeiss, Germany) and analysis was performed with the associated Axiovision software (Release 4.8).

4.3 STATISTICS

The normality of all data sets was assessed using the D'Agostino-Pearson normality test recommended on GraphPad (GraphPad Prism version 5.00 for Windows, GraphPad Software, San Diego California USA, www.graphpad.com). One-way ANOVA with Tukey's post-test was performed for normally distributed data sets. The levels of significance for Tukey's column pair-wise comparison were as follows; $p < 0.05$ (*), $p < 0.001$ (**) and $p < 0.001$(***). Statistically significance in non-parametric data sets was assessed using the Kruskal-Wallis test with Dunn's post-test for pair-wise comparisons (GraphPad).

4.4 RESULTS

4.4.1 Mechanical Properties if Single Hair Fibres

Hair samples from 5 volunteers were chosen from each of the 8 hair group. Ten strands of hair were used for each volunteer and only data from hair fibres that showed normal hair fibre failure profiles were used. The normal hair fibre profiles of 8 hair groups, illustrated with stress & strain curves, are shown in Figure 4-4. Representative data from 2 volunteers per group was used for stress & strain curves illustrations.

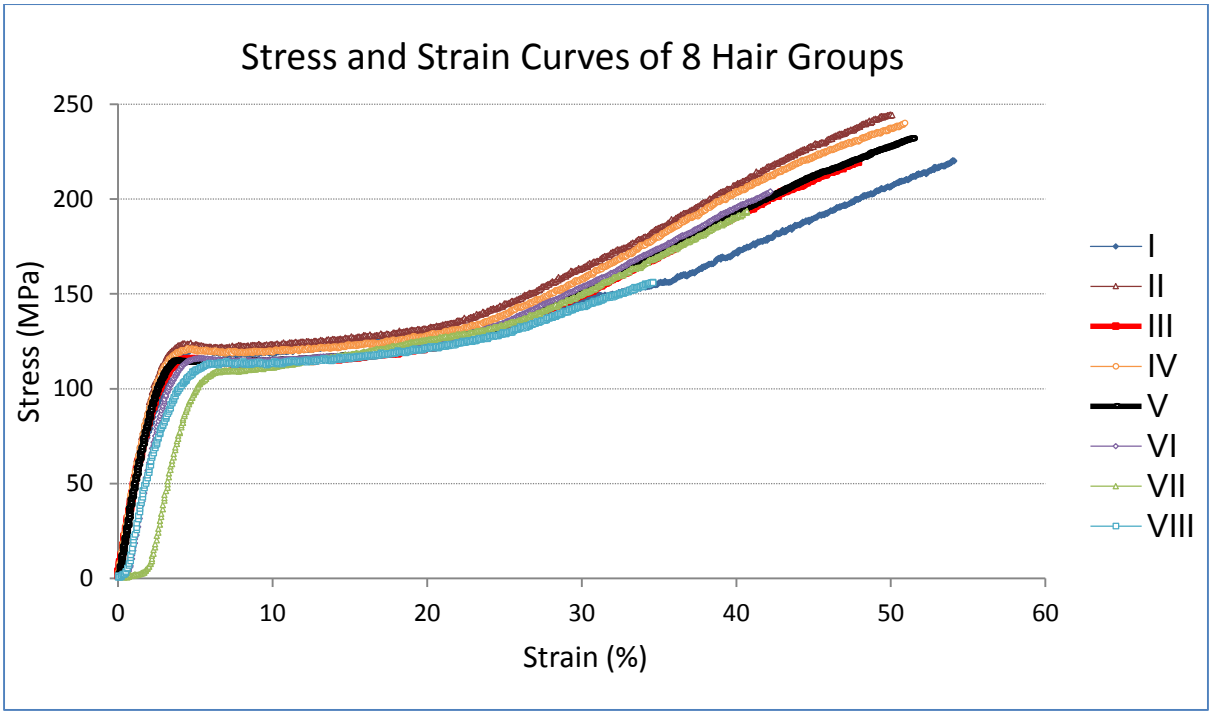

Figure 4-3 Stress & strain curves illustrating the mechanical behaviour of 8 hair curl groups

The lag typically observed for high curvature hair groups can be seen here for hair groups VII and VIII. The yield strengths of the different hair groups were above 100MPa for all hair groups. Hair groups I, II and IV had similar yield strengths (highest) while groups III and V were lower. Hair groups VI to VIII were even lower, with group VII exhibiting the lowest yield strength.

Hair thickness (diameter) was measured using a laser scan micrometre (LSM500, Mitutoyo). The data was normally distributed. The average hair diameter of 8 hair groups was uniform across most of the hair groups. Statistically significant differences in hair diameter were observed for hair groups II and III (Figure 4-5). The average hair diameter of hair group III was significantly lower than that of group I ($p < 0.001$) and groups IV to VIII ($p < 0.001$ to $p < 0.05$), while that of hair group II was significantly lower than that groups I , V and VI ($p < 0.001$). The hair diameters of hair groups II and III were not statistically different ($p > 0.05$). The straightest hair group, I, had the highest average diameter but this was not statistically significant from that of groups IV to VIII ($p > 0.05$). The straightest was observed to be thickest for the 6-group classification as shown in Figure 4-5.

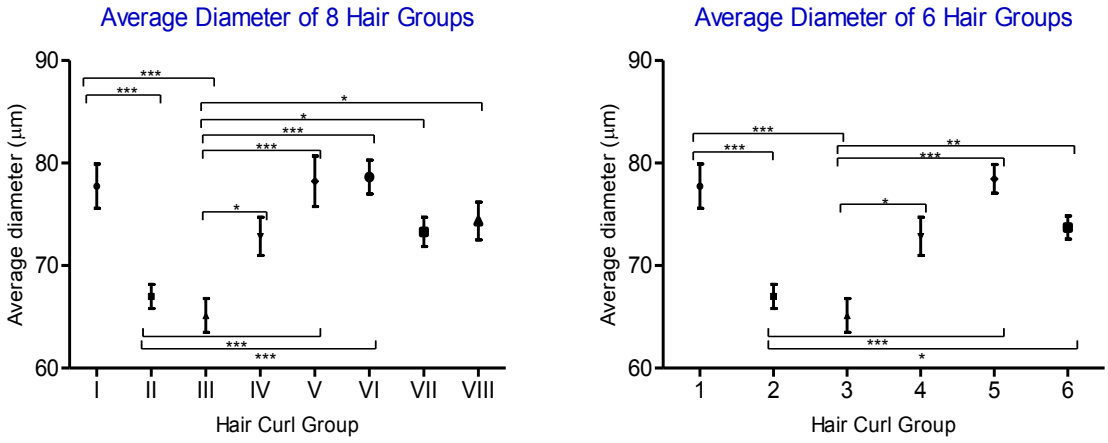

Figure 4-4 Average hair thickness of geometrically classified hair groups.

The data for mechanical properties (excluding tensile strength) was not normally distributed. The Kruskal-Wallis and Dunn's multiple comparison tests were used assess variation between the groups.

When the elastic modulus, referred to here as the elasticity, of the original 8 groups was compared, hair group III had the highest median elasticity (3319 MPa, range 2159 - 4331) (Table 4-3). Statistically significant differences were observed between hair group III and VI ($p < 0.001$) and VII ($p < 0.05$). Hair group IV was also statistically significant higher from groups VI and VII ($p < 0.001$ and $p < 0.05$ respectively).The elasticity of the hair group with the highest curvature (VIII) was only statistically significant from that of group VI ($p < 0.05$). The statistical outputs for the multiple comparisons are attached as appendix 4-2.

For the 6 group classification, there were significant differences between hair group 2 and 5 ($p < 0.05$), 3 and 5 ($p < 0.001$) and between 4 and 5 ($p < 0.001$) (Table 4-4). The statistical outputs of the multiple comparisons for the 6-group classification are attached as appendix 4-3.

Table 4-3 Mechanical characteristics of 8 hair groups. Median and range (minimum to maximum).

HAIR GROUP	CROSS-SECTIONAL AREA (μm²)		ELASTIC MODULUS (MPa)		YIELD EXT. (% Strain)		BREAK EXT. (% Strain)	
	Median	Range	Median	Range	Median	Range	Median	Range
I	4641	2506 - 8264	3080	2288 - 3909	26,46	21,12 - 31,89	50,41	39,28 - 60,99
II	3352	2302 -6054	3227	1996 - 3869	25,53	19,71 - 29,73	48,94	37,30 - 55,52
III	3236	1290 - 6489	3319	2159 - 4331	25,33	19,24 - 29,86	48,39	35,97 - 57,37
IV	4137	1629 - 7144	3275	2346 - 8099	25,65	18,25 - 29,22	48,49	34,24 - 55,79
V	4248	2263 - 7865	3085	2188 - 3625	25,31	18,17 - 32,03	47,65	32,88 - 61,06
VI	4142	1911 -7007	2824	1023 - 3723	24,10	14,01 - 31,22	43,85	24,29 - 59,89
VII	3490	2324 - 4919	2967	1802 - 4222	22,29	17,43 - 35,03	40,75	31,34 - 56,72
VIII	3704	2518 - 5471	3137	2295 - 4117	23,13	18,53 - 26,96	41,79	33,31 - 48,47

Table 4-4 Mechanical characteristics of 6 hair groups. Median and range (minimum to maximum).

HAIR GROUP	CROSS-SECTIONAL AREA (μm²)		ELASTIC MODULUS (MPa)		YIELD EXT. (% Strain)		BREAK EXT. (% Strain)	
	Median	Range	Median	Range	Median	Range	Median	Range
1	4641	2506 - 8264	3080	2288 - 3909	26,46	21,12 - 31,89	50,41	39,28 - 60,99
2	3352	2302 -6054	3227	1996 - 3869	25,53	19,71 - 29,73	48,94	37,30 - 55,52
3	3236	1290 - 6489	3319	2159 - 4331	25,33	19,24 - 29,86	48,39	35,97 - 57,37
4	4137	1629 - 7144	3275	2346 - 8099	25,65	18,25 - 29,22	48,49	34,24 - 55,79
5	4248	1911 - 7865	2965	1023 - 3723	24,66	14,01 - 32,03	46,01	24,29 - 61,06
6	3543	2324 - 5471	3029	1802 - 4222	22,63	17,43 - 35,03	41,42	31,34 - 56,72

More variation was observed in the yield extension of the 8 groups (Table 4-3) when compared to the 6 groups (Table 4-4). For the 8 group classification, significant differences were observed between the medians of hair groups VII and VIII when compared to most hair groups (I – V). The yield strength of hair groups VII and VIII was statistically lower than that of hair groups I to V ($p < 0.001$ to $p < 0.05$). Similar trends were observed for the 6 groups. The median yield extension of hair group 6 was significantly from all other hair groups ($p<0.05$) (Appendix 4-3).

A decrease in median break extension with increasing hair curl was observed for the 8 hair groups; the hair group with the least curvature had the highest median break extension (Table 4-3). The median break extensions of hair groups VI to VIII was statistically lower than that of the first 4 groups [$p < 0.001$ to $p < 0.05$ (appendix 4-3)].The break extension of hair group V was statistically lower than that of hair groups VII and VIII ($p < 0.001$ and $p < 0.05$). Similarly, significant differences for the 6-group classification were observed between hair groups 5 and 6 versus all hair groups (Figure 4-5) .These groups had significantly lower break extensions ($p < 0.001$ to $p < 0.05$).

For the ultimate measure of each group's mechanical properties, the break stress, referred to here as the tensile strength, was measured. The average tensile strength of the hair curl group with the second highest curvature had the lowest tensile strength. This was statistically significant from the average tensile strength of hair groups II to V ($p < 0.001$ to $p < 0.05$) (Figure 4-5). The tensile strength of hair group IV was significantly higher than that of hair groups VI ($p < 0.01$) and VII ($p < 0.01$). For the 6-group classification (Figure 4-5), the average tensile strength of hair group 6 was significantly different lower ($p < 0.05$ to $p < 0.001$) than that of hair groups 2 to 4. A table of means and 95% confidence intervals for the 8 & 6-group classifications is included in appendix 4-4.

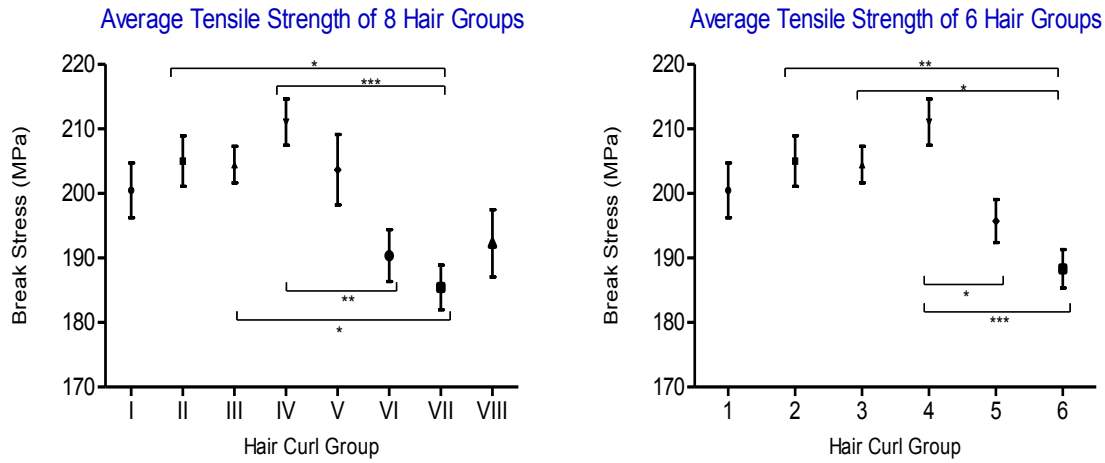

Figure 4-5 The average tensile stress of geometrically classified hair groups

Overall there was a n indication of (3 and 2) groups on the curliest hair spectrum having the lowest break stress (for the 8 and 6-group classification respectively)

4.4.2 Hair Growth Parameters

4.4.2.1 *Hair Growth Rate (TrichoScan®)*

The Trichoscan® platform uses epiluminiscence microscopy and automatic digital image analysis to compare and analyse images taken at days 0, 2 or 3, resulting in an output of various hair parameters such as hair density, anagen to Telogen ratios. Hair growth parameters were assessed in a 0.56cm^2 newly shaved area on the scalps of volunteers as shown in Figure 4-6.

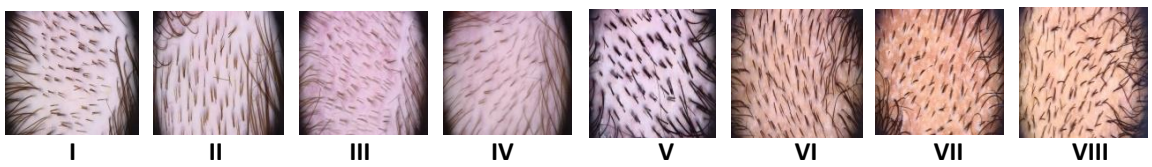

Figure 4-6 Shaved scalp areas of volunteers for the assessments of hair growth rate and hair density. Images were captured using a TrichoScan® Fotofinder.

Almost all groups were unique with regards to their hair growth rate for the 8-group classification (Figure 4-7).

For the 8-group classification, the average hair growth rate (μm/day) of hair group I was statistically significant higher than that of hair groups VI ($p < 0.01$) and VIII ($p < 0.05$). The growth rate for hair group II was statistically higher than that of hair groups

III ($p < 0.001$), V ($p < 0.05$), VI ($p < 0.001$), VII ($p < 0.001$) and VIII ($p < 0.001$). The growth rate of hair group VI was statically slower than that of hair group IV ($p < 0.001$).

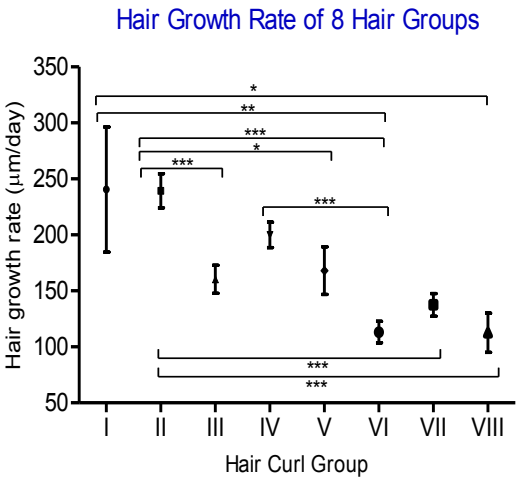

Figure 4-7 The average hair growth rate of 8 hair groups. (Mean ± SEM). Hair growth was assessed from TrichoScan® outputs.

For the 6-group classification the average hair growth rate of hair group 1 was statistically faster hair groups 5 and 6 ($p < 0.05$), while hair group 2 was statistically faster ($p<0.001$) than that of hair groups 3 to 6 ($p < 0.001$ to $p < 0.05$) (Figure 4-8). The hair of volunteers in hair group 4 hair grew at a statistically faster rate than those in hair groups 5 ($p < 0.01$) and 6 ($p < 0.05$), however the curliest 2 groups (5 and 6) has the lowest growth rates.

Overall the growth rate calculations based on TrichoScan® data for hair group 1 was significantly faster (0.72 ± 0.3 cm/month) than that of the hair group with the greatest curvature (6) (0.39 ± 0.1 cm/month).Hair group 2 was also observed to be significantly faster than all hair groups with greater curvature (3 to 6) (0.48 ± 0.1 to 0.39 ± 0.1 cm/month).The average hair growth for each of the 8 groups is shown in Table 4-5).Distributions of growth rate across self-declared race groups were ;Asian (0.64 ± 0.1 cm/month, Mixed (0.59 ± 0.1 cm/month, Caucasian (0.58 ± 0.2 cm/month and African (0.36 ± 0.1 cm/month) (Table 4-7).Calculations of monthly growth rate used were based on 30-day long months.

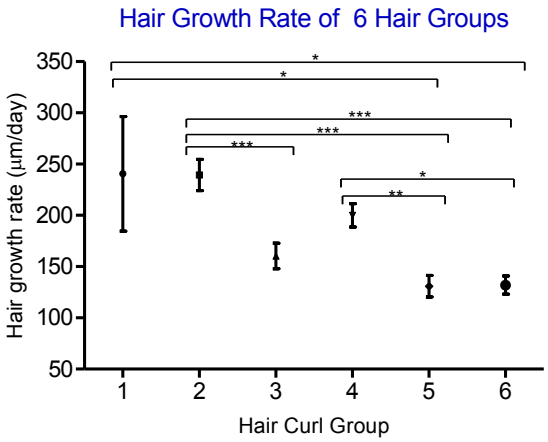

Figure 4-8 Average hair growth rate of 6 hair groups .Mean ± SEM

4.4.2.2 *Hair Growth Rate from SEM Micrographs*

For the preliminary investigation of the Baque *et al.* hair growth rate approach[159], one volunteer was selected to represent each of the 8 hair groups. Three hair fibres were taken from each volunteer. Each hair fibre was imaged in triplicate at 3 different positions along the hair shaft and hair shaft diameter measurements were carried out 3 time times for each position. Therefore, each volunteer's hair diameter was measured 27 times (3 strands X 3 images X 3 positions).For interscale distance (ISD) measurements, multiple lines, starting and ending on a cuticle edge, were drawn for each hair fibre as illustrated in Figure 4-9.

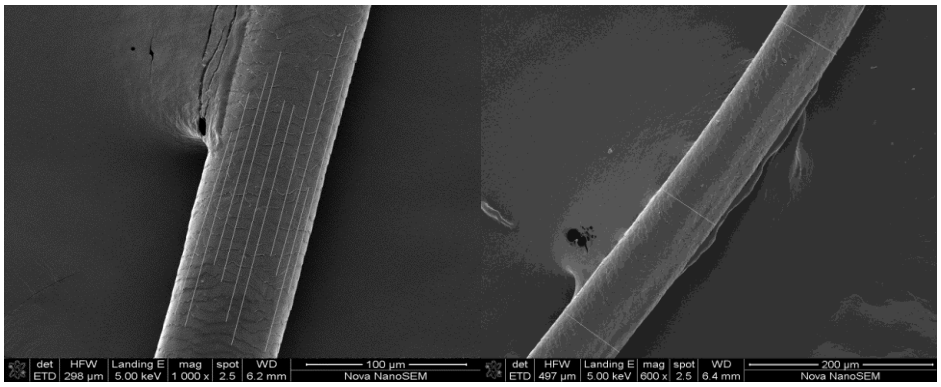

Figure 4-9 SEM images captured at 600 and 1000 fold for the assessment of ISD (a) and hair diameter (b).

The ISD was then calculated by dividing the length of each line with the number of scales it spanned over. The average ISD was observed to be uniform between most of the 8 hair group. However, the average ISD for hair group III was longer than that of hair groups II to VIII (Figure 4-10) ($p < 0.001$ to $p < 0.05$) and that of hair group VI was statistically shorter than that of hair groups I and IV ($p < 0.01$ and $p < 0.05$).

For the 6-group classification, the longest ISD was observed for hair group 3. This observation was found to be statistically significant ($p < 0.001$ to $p < 0.05$). Hair group 1 had a statistically longer ISD than hair group 5 ($p < 0.05$).

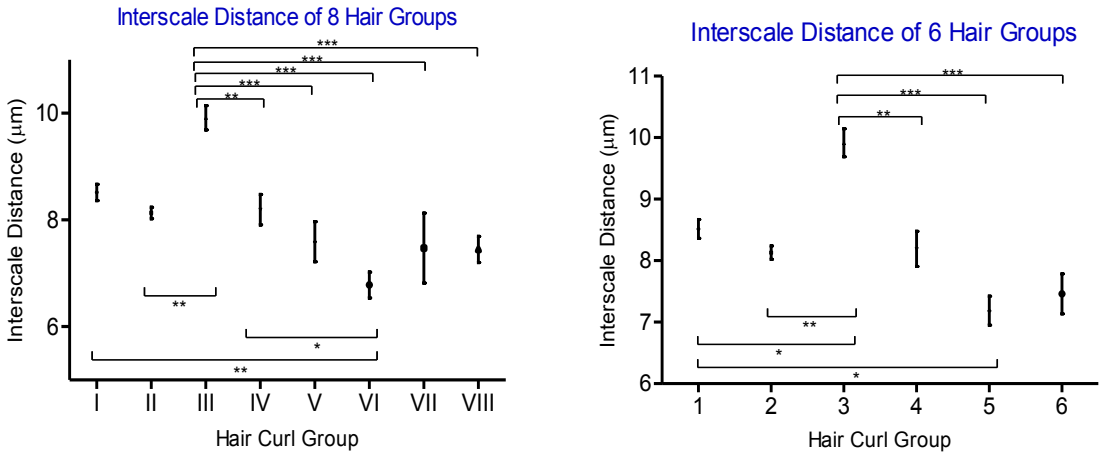

Figure 4-10 Interscale distances of different hair groups

Hair growth rate was then calculated from ISD using equation 4-2. The calculated average hair growth rate was observed to be generally uniform across most hair groups (Figures 4-11 and 4-12),however the hair growth rate of hair group III or 3 was significantly lower than most hair groups ($p < 0.001$ to $p < 0.05$) for the 8 and 6-group classifications (Figures 4-11 and 4-12).

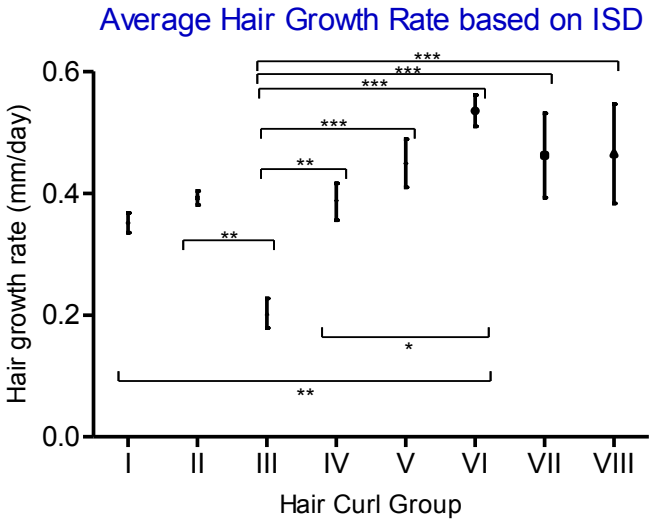

Figure 4-11 Average ISD calculated hair growth rate of 8 hair groups (Mean ± SEM).

The hair growth rate of hair group VI was unexpectedly higher than that of groups I and IV ($p < 0.01$ and $p < 0.05$).Finally, there was no overall trend of lower growth rate as calculated by inter-scale distance for either the 8 or 6-group classification for high curvature hair groups, instead, one of the high curvature hair groups (5) was observed to have be significantly faster hair group 1 ($p < 0.05$).

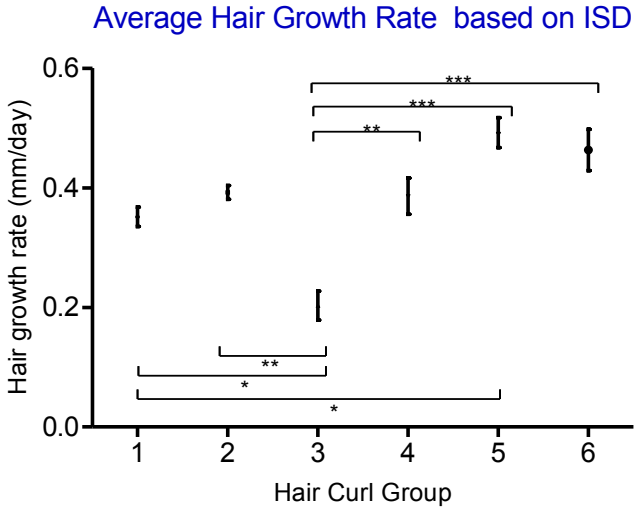

Figure 4-12 Average ISD calculated hair growth of 6 hair groups (Mean ± SEM).

The average monthly hair growth rates based on ISD for the 6-group classification were; 1.1 ± 0.2cm/month (group 1), 1.2 ± 0.1cm/month (group 2), 0.6 ± 0.2 cm/month (group 3), 1.2 ± 0.3 cm/month (group 4), 1.4 ± 0.3 (group 5) and 1.4 ± 0.5 cm/month (group 6). A summary of the hair growth rates based on the TrichoScan® and ISD

approaches is shown below in Tables 4-5 and 4-6 for the 8 and 6-group classifications respectively. Table 4-7 shows the variations of TrichoScan based growth rates observed in the current study.

Table 4-5 Hair growth rate (HGR) of 8 hair groups

Hair Curl Group	TrichoScan® HGR (cm/month)	ISD based HGR (cm/month)
I	0.72 ± 0.2	1.1 ± 0.2
II	0.72 ± 0.3	1.2 ± 0.1
III	0.48 ± 0.1	0.6 ± 0.2
IV	0.60 ± 0.1	1.2 ± 0.3
V	0.50 ± 0.2	1.3 ± 0.4
VI	0.34 ± 0.1	1.6 ± 0.2
VII	0.41 ± 0.1	1.4 ± 0.6
VIII	0.34 ± 0.1	1.4 ± 0.2

Table 4-6 Hair growth rate (HGR) of 6 hair groups

Hair Curl Group	TrichoScan® HGR (cm/month)	ISD based HGR (cm/month)
1	0.72 ± 0.2	1.1 ± 0.2
2	0.72 ± 0.3	1.2 ± 0.1
3	0.48 ± 0.1	0.6 ± 0.2
4	0.60 ± 0.1	1.2 ± 0.3
5	0.39 ± 0.2	1.4 ± 0.3
6	0.39 ± 0.1	1.4 ± 0.5

Table 4-7 Hair growth across racial groups, based on the TrichoScan

Racial Group	TrichoScan® HGR (cm/month)
Asian	0.64 ± 0.1
African	0.36 ± 0.2
Caucasian	0.58 ± 0.2
Mixed	0.59 ± 0.1

4.4.3 Hair Density

Hair density was assessed in a newly shaved area of 0.562cm^2 (Figure 4-6).The average hair densities for the 8 groups ranged between 223 - 266 hairs/cm^2 when taken recorded from the TrischoScan® output. Manually calculated hair densities using Matlab and GRABIT gave a range of 257 - 292 hairs/cm^2. No significant differences in average hair density were observed between the different hair groups for any of the groups (8 or 6) ($p > 0.05$) (Figure 4-13).

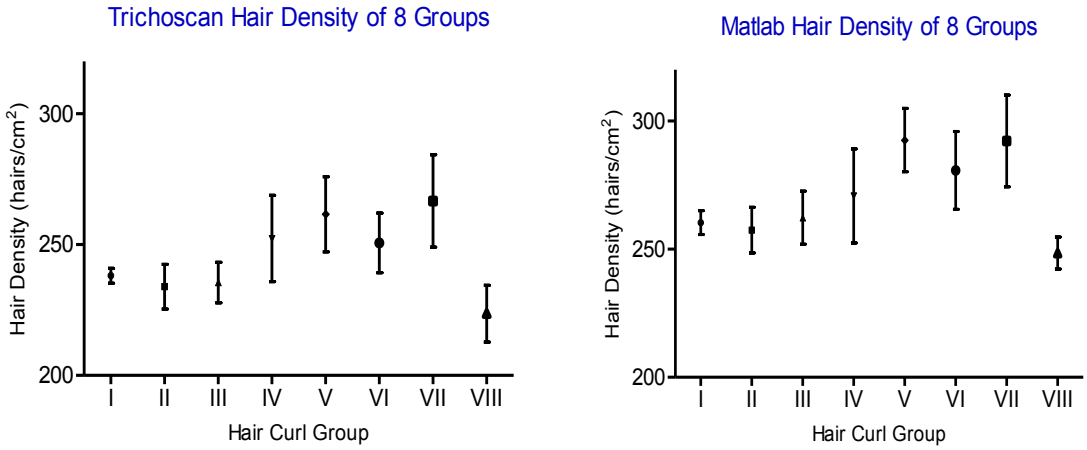

Figure 4-12 The assessment of hair density using an automatic and manual approach.

4.4.4 Ultrastructural Characteristics of Different Hair Curl Groups

4.4.4.1 *Transmission Electron Microscopy*

The ultrastructural characteristics of geometrically classified hair samples were investigated using TEM. Two representative samples were used for each of the 8 hair groups. Sample preparation for curly hair groups was extremely challenging because ultra-thin (95nm) sections of these hair groups were tended to lift off the resin as shown in Figure 4-14. Sections were stained with a 1% Toluidine blue in 1% sodium borate for 30 seconds in order to visualize samples orientation. Toluidine blue stained sections were imaged with light microscopy. Successful TEM imaging was achieved for hair groups I, III and IV. The TEM micrographs are shown in Figures 4-15 to 4-17.

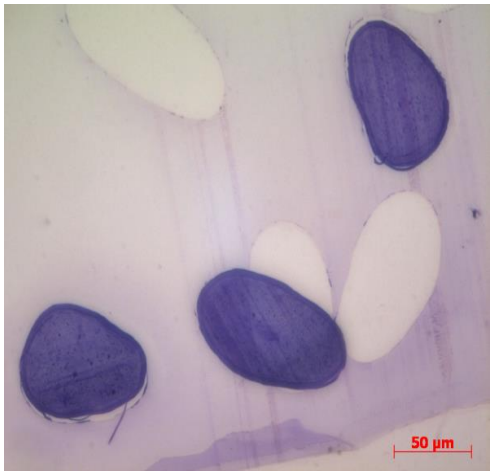

4-13 Toluidine blue staining of ultrathin hair sections (hair group VIII).

In the TEM micrographs of hair group I, 2 – 5 layers of orthocortical cells were observed at the periphery of the hair cortex (Figure 4-15a and b). Paracortical cells were accounted for the bulk of cortex. Randomly distributed melanin granules (M) can also be observed on the hair cortex and sometimes amongst cuticle cells. Six – seven layers of cuticle cells were observed for hair groups I (Figure 4-15) and III (Figure 4-16).

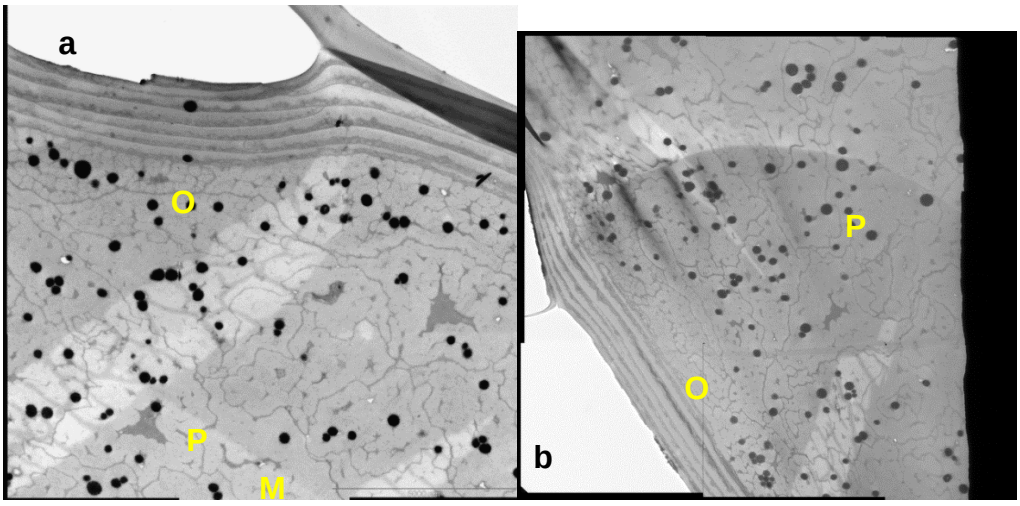

Figure 4-14 TEM micrographs hair group I. Orthocortical cells (O) were observed on the periphery of the hair cross section, while paracortical (p) cells made up the bulk of the hair cortex.

A slightly thicker arrangement (8 layers) of orthocortical cells was observed for hair group III (Figure 4-15).These were also observed on the periphery of the cortex as in

hair group I. Paracortical cells still appeared to account for the greater portion of the hair cortex.

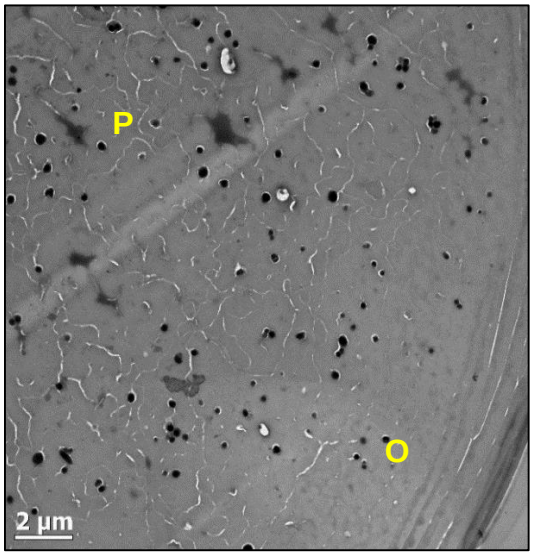

Figure 4-15 A TEM micrograph of hair group III, showing a thicker layer of orthocortical cells.

Of the 3 hair groups visualised with TEM, the hair group with the highest degree of curvature (hair group IV) had the thickest layer of orthocortical cells. Ten layers of orthocortical cells were observed on the representative samples imaged for this hair group (Figure 4-17). Fewer cuticle layers were also observed for this group.

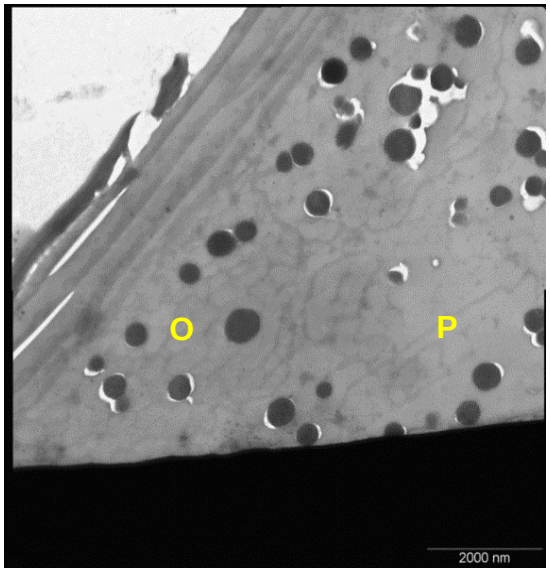

Figure 4-16 A TEM micrograph of stained hair section from hair group IV. A thicker layer of orthocortical cells is observed for this group than group I and III.

To overcome the challenges encountered with obtaining ultrathin sections for high curvature hair groups, another imaging method was used. Fluorescent light microscopy (FLM) can be used to visualise thicker sample sections (1.5µm).

4.4.4.2 *Fluorescence Light Microscopy*

Representative samples that had been prepared for TEM were used for FLM. Embedded sample sections were dual stained with Fluorescein Sodium (FS) and Sulforhodamine (SR). FS (green) preferentially stained paracortical cells while SR (red) stained orthocortical cells. FLM micrographs were captured for hair groups I, III, IV, V, VII and VIII.

Orthocortical cells were observed at the periphery of the hair cortex for hair groups I (Figure 4-18) and III (Figure 4-19) while an approximately 1:1 distribution of the two cortical cell types was observed for hair groups IV (Figure 4-20) and V (Figure 4-21).

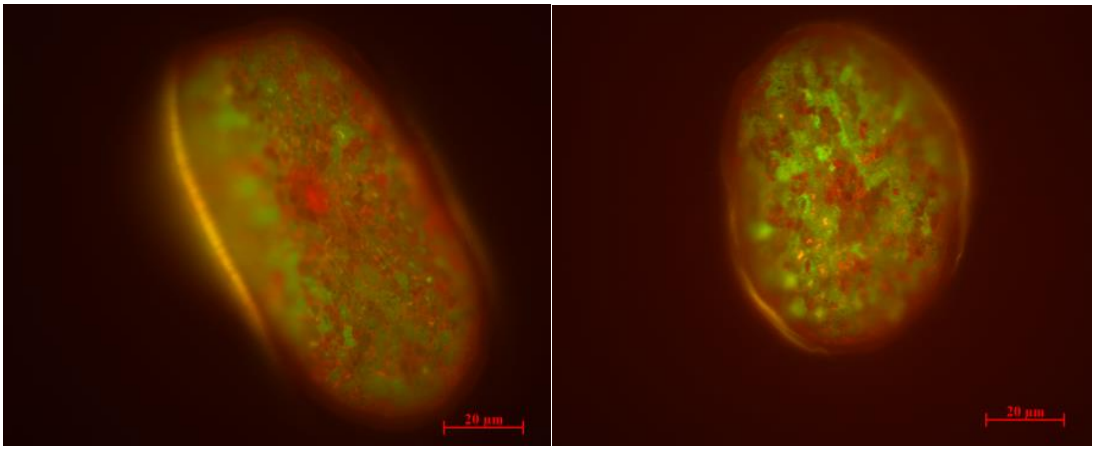

Figure 4-17 FLM images of hair group I showing a layer of Flourescein Sodium (FS) stained orthocortical cells (red) at the periphery of the hair cortex. Paracortical cells are stained green with Sulforhodamine (SR).

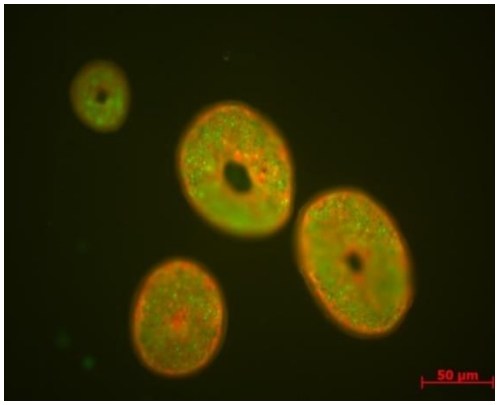

Figure 4-18 FLM image of hair group III hair cross section. A single layer of orthocortical cells can be observed at the edges of the hair cortex, adjacent to cuticle cells.

Half the cross-section of hair groups IV, V and VII hair were comprised of orthocortical cells while the other half had paracortical cells. Similar observations were made for hair group VII (Figure 4-22). Stained sections of hair group VIII had a lower ratio of orthocortical cells than type VII (Figure 4-23).

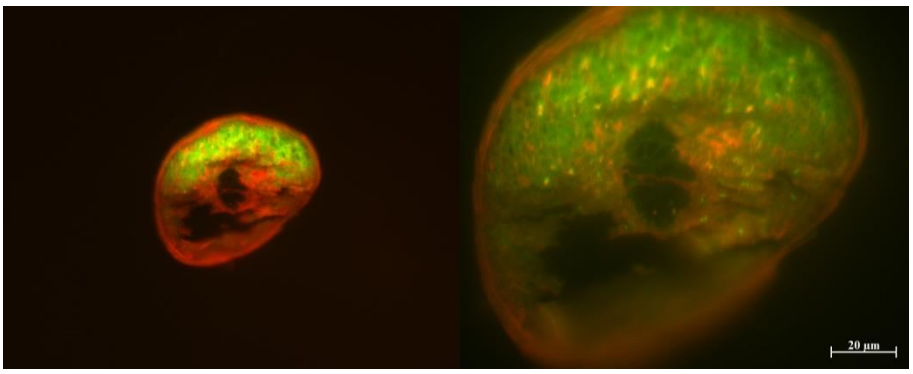

Figure 4-19 FLM images of hair group IV showing an asymmetric distribution of ortho and paracortical cells.

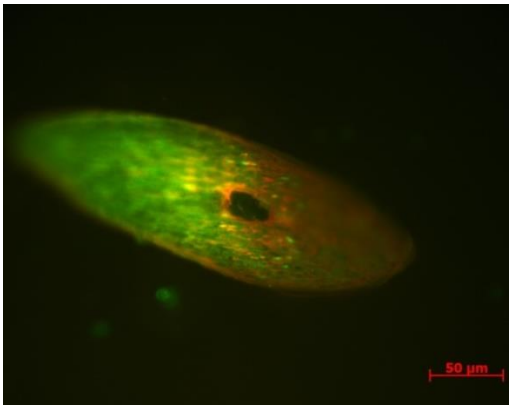

Figure 4-20 FLM image of hair group V. Orthocortical cells (red) on the RHS of the image and paracortical cells (green) are observed on the LHS.

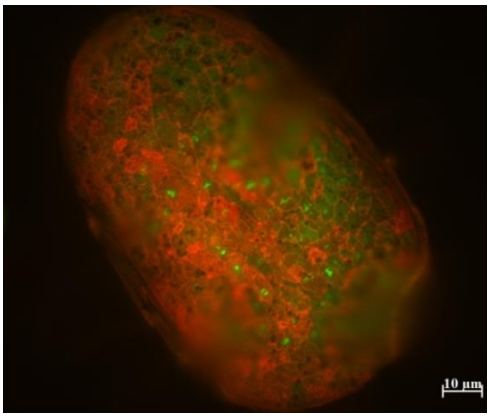

Figure 4-21 FLM image of hair group VII hair. Although the image is out of focus in some areas, the asymmetric distribution of the two cell types can be observed.

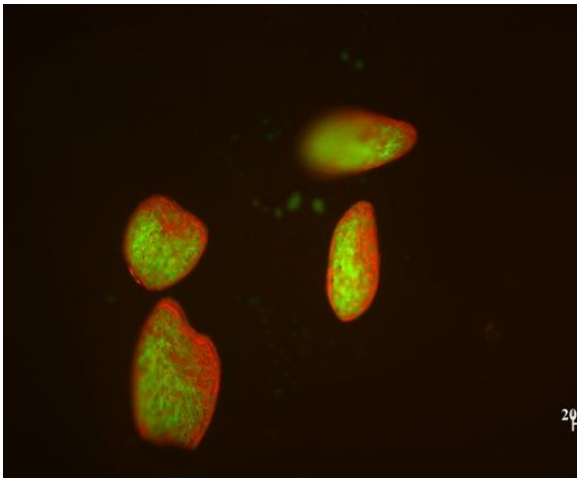

Figure 4-22 FLM image of hair group VIII with less orthocortical cells than hair group VII.

4.5 DISCUSSION

Mechanical Properties

The average hair thickness of 8 hair groups was generally uniform except for significantly smaller diameters for hair groups II and III. The hair group with the straightest hair (group I), comprising of Asian volunteers, had the greatest average diameter; however this variation was not statistically significant from that observed for hair groups IV to VIII. Hair groups hair shafts were II and III were significantly thinner than that of all other groups. This was expected because Caucasian hair samples are usually reported to be fine or thinner than Asian or African hair samples[22,93,122].

The mechanical properties of hairs with varying degrees with curvature were of interest in the current study because African hair is usually reported as being mechanically weaker [55] than other hair groups, although the biochemical composition of all hair groups has been said to be quite uniform [93,94,135–137]. The lower tensile properties of hair groups with high curvature have been attributed to the kinks present along the hair shafts of such hair groups. These kinks become areas where the applied stress gets concentrated, leading to premature breakage or failure[62].

One of the contributors to the widely reported intrinsic weakness of highly curly hair has been said to be its yield extension. African hair is said to reach their yield extension at a faster rate than other hair groups [55,160]. The median yield extensions of the 8 different hair groups are shown in Tables 4-3 and 4-4. Hair group I statistically had the highest yield extension. No significant differences were observed between the yield extensions of all the straight hair groups (I – IV). For the curlier hair groups (V – VIII), significant differences were only observed between hair group V and VIII. Hair groups VII and VIII, which have been assigned to African hair, had the lowest yield extension. This lower yield extension was shown to be statistically significant from that of hair types I, II, III, IV and VI.

A low yield extension reflects an earlier transition of the keratin structure from alpha-helical to being β-sheets [32]. The yield region arises from the uncoiling of α-helical chains into β-sheet [22,160], a process that happens without much resistance and is reflected by very small changes in the % strain with increasing stress in the pre-yield (Hookean) region[160].

All hair groups had a yield extension below 30% strain, which is in line with literature that reports that hair is perfectly elastic up to 30% extension [165], after which point it will not regain its original shape even if the exerted mechanical energy is lifted. The yield strengths observed in the current study were higher than those reported in literature. All yield strengths were above 100MPa (Figure 4-4). The reported average yield strength for Asian , Caucasian and African hair is 100 MPa, 67 MPa and 58 MPa respectively[160].

In the pre-yield region, stress and strain are proportional and the gradient this linear relationship, termed the elastic modulus, can be found. The elastic modulus of the hair group III was statistically higher than that of all hair groups with a higher degree of curvature. No significant differences were observed between hair groups I to III and V to VIII. These observations give indications of two major groups; those with low curvature and those with high curvature, masking variations that could be observed for intermediate hair groups.

Beyond the yield region, the β-sheet configuration of the keratin resists stretching and stress increases with strain until the fibre reaches the highest stress it can withstand and breaks[39,160].Hair groups with lower yield extensions were subsequently observed to reach their breaking point at a lower extension (break extension in % strain). Hair groups VII and VIII had the lowest break extensions (Table 4-3). An inversely proportional relationship was observed between hair curvature and break extension. There was a decrease in break extension with increasing curvature (Tables 4-3 and 4-4).

The tensile strength is the maximum stress that each single fiber was able to withstand.

The average tensile strength of the different groups was observed to be statically significant from the hair group with the second highest degree of curvature (VII) (185.4 ± 18.97 MPa) when compared to hair groups I to V [200.5 ± 22.86 to 211.1 ± 22.71 MPa] for the 8 group classification. No significant differences were observed between groups nearest to each other (I vs II, II vs III, etc.) for the 8 group classification. This provides evidence that supports merging some the groups as done the last 4 groups of the 8-group classification, resulting in the 6-group classification.

Variations between hair groups 4 (211.1 ± 22.71 MPa) and 5 (188.3 ± 21.50 MPa) were statistically significant for the 6 group classification (Figure 4-8). The trends observed for average tensile strength for the 8 group classification were similar to those reported by other workers[62,131], where the break stress decreased with increasing hair curvature, Asian hair (straightest) is reported to have highest tensile strength[160]. For the 6-group classification, the average tensile strength of the group

with the highest curvature (hair group 6) was statistically lower than all hair groups 2 to 4.

Interestingly, higher break stress results were observed in the current study for hair groups, the lowest break stress was 153 MPa for hair group VIII, Break stress results usually reported in are 101, 139 and 117 MPa for African, Caucasian and Asian hair respectively[160].

Hair Growth Parameters

Hair growth rate

Hair growth parameters were measured using the TrichoScan® platform, a quantitative method that combines epiluminiscence microscopy and automatic digital image analysis [166,167]. As already outlined in the methods section, the hair growth rate of different hair forms was assessed using two approaches; using data extracted from the TrichoScan® platform and using an approach that correlates the Interscale distance with hair growth rate. The hair growth rates calculated from the TrichoScan® platform were consistent with data available where type I and II is usually termed as Asian hair, type II – IV as Caucasian and hair group V – VIII as African hair.

If hair groups I, III and VIII are used to represent Asian, Caucasian and African hair respectively, their average hair growth rates would be 240.6, 160.4 and 131.9 µm / day as shown in Figure 4-7. This is similar to observations by Loussouarn *et al.* that showed that Asian hair had the fastest hair growth (244 - 611 µm/day) compared to African and Caucasian that grew at 165 -201 and 165 - 506 µm/day [158]. Variations exist in the reported hair growth of different racial groups. Loussouarn had earlier reported earlier (2001) that African hair has a growth rate of 256 ± 44 µm/day while Caucasian was seen to grow at 396 ± 55 µm/day [161].

Although the relationship between hair morphology and hair growth is not directly proportional, the growth rate of the curliest hair group was the slowest, as previously reported by other workers [161]. In the current study, significant differences in hair growth rate were observed between the straightest hair groups (I and II) and the curly hair groups (IV – VIII).No significant differences were observed between hair group I and II while variations observed in hair groups II and III were statistically significant. No statistically differences were observed for the hair group with the highest hair curvature

hair (VIII) when compared to other high curvature groups (VI and VII). Variations in the intermediate hair groups (IV and V) could also not be shown be to statistically significant. These observations cluster the 8 group classification into 4 groups (I & II, III, IV & V and VI to VIII).

Hair growth rate has been shown to be related to the distance between cuticle layers for straight hair [159]. Using ISD and hair shaft diameter, Baque *et al*. showed that for straight hair from Asian and Caucasian volunteers, a thick hair fibre and short ISD corresponded with a high growth rate[159]. A fibre with a dimeter of 100 µm and growth rate of 20 µm per hour is reported to produce 5 -10 µg of protein per 24 hours[28].
ISD therefore reflects the rate of cell turn over in the hair bulb; hairs with slower growth have lower cell over and would thus have longer distances between successive cuticle cells.

The authors corroborated hair growth rate calculations from their new approach to those observed with conventional hair growth rate measurements. This new hair growth rate calculation method was explored in the current study in order to assess its suitability for curlier hair groups. The results observed in the current study were similar to those obtained by Baque *et al*. for the ISD of straight hair.

Overall, the anticipated trend that the curliest hair ought to have the longest ISD was not observed. The curliest hair groups (VII and VIII) were observed to have shorter inter scale distances than straight hair groups (I and II) .Similar results were observed for the 6-group classification (Figure 4-11).

ISD had no association with hair curl. Hair group VI had an average hair growth rate that was statistically higher than that of hair groups I and IV, while that of hair group III was statistically lower than most groups. These deviations from the expected trend that curlier hair groups would have lower growth rates could be explained by the wide variations usually reported for hair growth rates (Asian: 0.73 – 1.8 cm/month, Caucasian: 0.50 – 1.2cm/month, African: 0.5 – 0.6 cm/month)[158] , making the assignment of average hair growth rate to geometric groups challenging. The variation in the ISD calculated hair growth rate could also be due to limited sample size in the

current preliminary investigation. Including more volunteers for each group could improve results.

The magnitude of hair growth rate was however similar to that reported from conventional methods: the average hair growth of hair group 1 was 1.1 cm/month (± 0.2) when calculated using ISD and 0.72 cm/month (± 0.3) when measured with the TrichoScan® (Figure 4-8 and 4-12).

This approach is similar to the older hair classification method of counting the number of scales and using that as a descriptor of hair form[71]. Measurements of this parameter are reported to vary widely from researcher to research and it is recommended that comparisons should be limited to one's own data[71].

The rate of hair growth could influence levels of incorporation onto the growing hair shaft, although hair analysis interpretations usually cite a blanket growth of 1.0 cm per month for all racial groups[3,6,17,126]. Variations across hair groups should be taken into consideration for all hair groups in order to correctly interpret results obtained for various hair analyses[120,126].

Overall, the growth rates based ISD had no association with hair curl and were higher than those observed for the conventional TrichoScan® method; 1.1 ± 0.2cm/month (group 1) to 1.4 ± 0.5 cm/month (group 6) .

The distributions of TrichoScan® based growth rate across self-declared race groups (Asian (0.64 ± 0.1 cm/month, Mixed (0.59 ± 0.1 cm/month, Caucasian (0.58 ± 0.2 cm/month and African (0.36 ± 0.1 cm/month)) were similar to published data for Caucasian (0.50 – 1.5cm/month), African (0.5 – 0.6 cm/month)[158], but lower for Asian(0.73 – 1.8 cm/month). This study is the first to report on the growth rate of a mixed racial group. Variations of ISD based hair growth rate across racial groups were not calculated due limited sample size.

Hair Density

No significant differences were observed in hair density across hair groups when comparing data obtained from the automatic TrichoScan® output and data obtained

using MATLAB and GRABIT software. This reflected consistency between the two approaches, although the Matlab approach showed greater variability within groups.

The hair density results observed in this study were consistent with results obtained for racially classified hair where the reported ranges in hair density usually overlap for the three major racial groups; African: 194 ± 44 hairs/cm^2, Asian: 224 ± 38 hairs/cm^2 and Caucasian hair: 285 ± 66 hairs/cm^2 [2, 158].

Ultrastructure

Orthocortical cells are reported to contain lower sulphur content (~3%) than paracortical cells (~5%) and it would be expected that hair shafts with greater composition of paracortical cells would have the highest tensile strength, while those with 1:1 proportions would have intermediate tensile properties. However ,disulphide bonding is reported to not affect the tensile properties of dry hair[39] and the fragility of African hair to be unrelated to the distribution of cystine-rich proteins[94] .

The distribution of cortical cells within the hair cortex has also been related with hair morphology[60,90]. This relationship was investigated using transmission electron microscopy and fluorescence light microscopy. Several researchers have visualized the variation in the ratios and distributions of cortical cells within the cortex of different hairs using TEM[77,168]. However, to our knowledge, the current work is the first to show the distribution cortical cells of more than 2 hair groups using the FLM dual staining protocol; Baque *et al.* investigated cortical cell distributions in Caucasian and Asian (Japanese) hair.

Straight hair from Japanese volunteers was found to be predominantly composed of paracortical cells[90], similarly, in the current work, the straight hair cortex of samples from hair groups I to III was predominantly stained with Sulforhodamine, reflecting abundance of paracortical cells. For curlier hair groups, there were variations in the distributions of orthocortical and paracortical as expected. Samples from hair groups IV, V and VII were stained with Sulforhodamine and fluorescein sodium in almost equal proportions, reflecting 1:1 distribution of these cells types. Hair group VIII was mostly stained with Sulforhodamine, reflecting paracortical cells. Interestingly, the

asymmetric distribution of these cell types[40] was only observed in the curliest hair group (VIII).

4.6 CONCLUSIONS

The current chapter presented investigations on the relationships between morphology and other physical characteristics of hair.

The yield strength and break stress results observed were higher than those previously reported for racial groups, although this could be due to the measurement technique used. The overall trends in mechanical properties were similar to published results (i.e. the curliest hair had the lowest tensile strength, whilst the straightest had the highest). The intermediate hair group (4) had the highest median hair elasticity.

Although there was a statistically significant difference in hair diameter between some of the groups, this did correlate with hair curl.

The growth rates observed with the TrichoScan® were similar to those previously published (i.e. the straightest hair group had the fastest growth rate (0.72 ± 0.3 cm/month) compared to the curliest hair (0.39 ± 0.2 cm/month). However growth rates based on ISD were haphazard and did not correlate with hair curl.

New dual staining techniques by FLM have been used for visualizing cortical cell in straight hair and were found to give similar results to TEM. This study is the first (that we are aware of) to confirm that this is also the case for African hair; FLM techniques are cheaper and more efficient than TEM.

Understanding the relationships that exist between hair morphology and other previously characterised hair features is important. Hair morphology and hair growth rate are two characteristics that could have an influence on how substances are incorporated into the hair follicle and emerging hair shaft. These substances could include illicit drugs, chronic medication or alcohol. The rate of hair growth could influence levels of incorporation into the growing hair shaft. Variations across hair groups should be taken into consideration for all hair groups in order to correctly interpret results obtained for various hair analyses[120,126].

Appendix 4-1. A screen shot illustrating how data points extracted from TrichoScan® output using MATLAB and GRABIT image processing software.The ranges for the x (0.25 – 2.15) and y (0 – 24) axis had to be defined first in order to pick data points accurately, the set ranges on the axis are shown by blue or red cross hairs. The preview box, top right, shows the trend of picked data points, which matches that of the histogram and the panel on the bottom right is a summary of picked data points. This summary was then exported onto excel for data analysis.

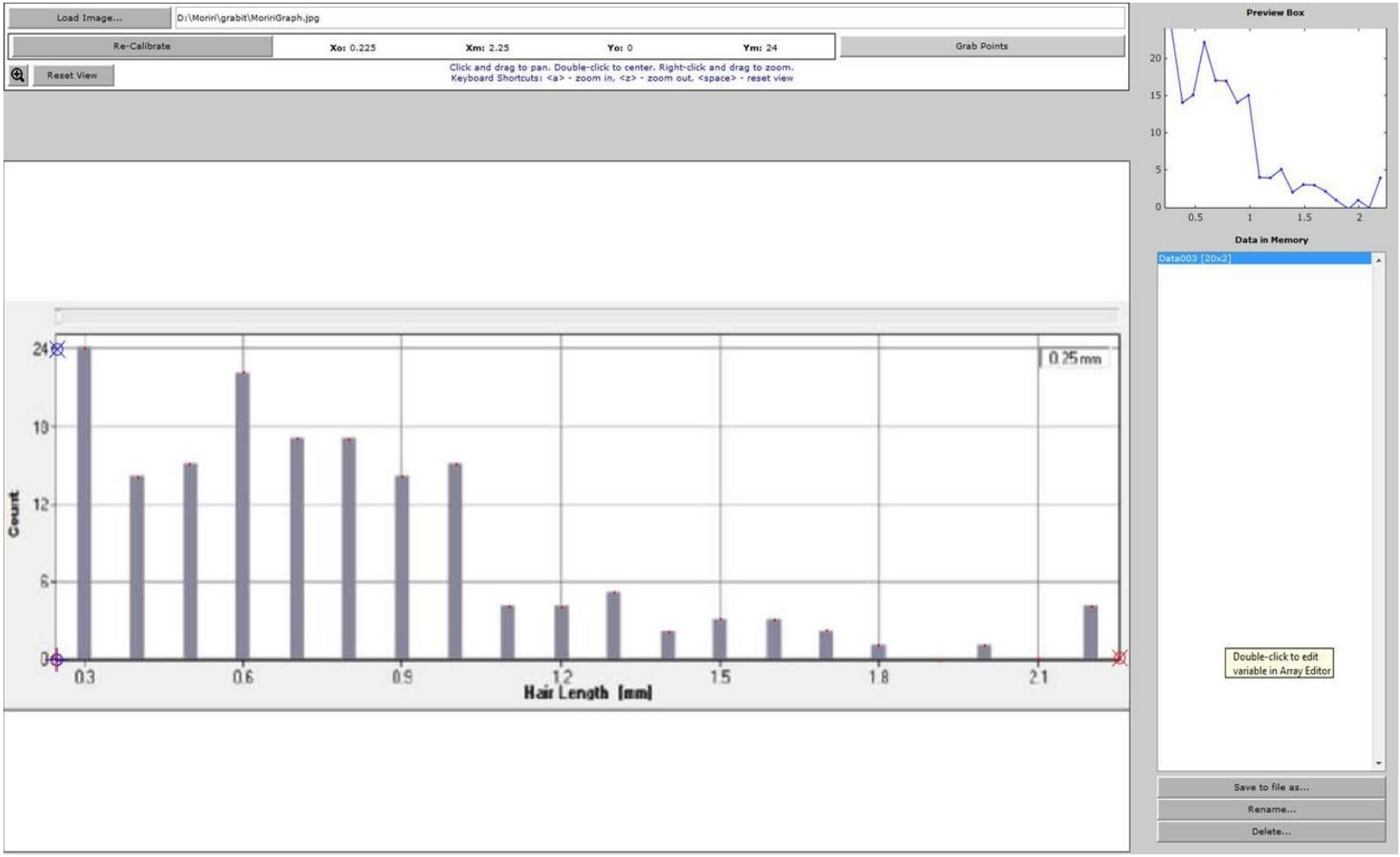

Appendix 4-2

Statistical significance observed in the mechanical properties of 8 hair groups. Statistical significance was assessed using the Kruskal-Wallis and Dunn's Multiple tests.

Dunn's Multiple Comparison Test for 8 hair curl groups		
	Comparison	**Level of Significance***
Cross sectional area	I vs II	***
	I vs III	***
	I vs VII	*
	II vs V	*
	II vs VI	*
	III vs V	**
	III vs VI	**
Elastic Modulus (MPa)	II vs VI	**
	III vs VI	***
	III vs VII	*
	IV vs VI	***
	IV vs VII	*
	VI vs VIII	*
Yield Extension (% strain)	I vs VII	***
	I vs VIII	***
	II vs VII	***
	II vs VIII	**
	III vs VII	***
	III vs VIII	*
	IV vs VII	***
	IV vs VIII	**
	V vs VII	**
Break Extension (% strain)	I vs VI	***
	I vs VII	***
	I vs VIII	***
	II vs VI	**
	II vs VII	***
	II vs VIII	***
	III vs VI	**
	III vs VII	***
	III vs VIII	***
	IV vs VI	**
	IV vs VII	***
	IV vs VIII	***
	V vs VII	**
	V vs VIII	*

* Asterisks indicate different levels of significance; p-value between 0.01 and 0.05 (*), p- value between 0.001 and 0.01 (**) and $p < 0.001$ (***).

Appendix 4-3

Statistical significance observed between the 6 hair curl groups

Dunn's Multiple Comparison Test for 6 hair curl groups		
	Comparison	**Level of Significance***
Cross sectional area	1 vs 2	***
	1 vs 3	***
	1 vs 6	*
	2 vs 5	***
	3 vs 4	*
	5 vs 6	***
Elastic Modulus (MPa)	2 vs 5	*
	3 vs 5	***
	4 vs 5	***
Yield Extension (% Strain)	1 vs 6	***
	2 vs 6	***
	3 vs 6	***
	4 vs 6	***
	5 vs 6	**
Break Extension (% Strain)	1 vs 5	**
	1 vs 6	***
	2 vs 5	*
	3 vs 6	***
	3 vs 5	*
	3 vs 6	***
	4 vs 6	***
	5 vs 6	*

* Asterisks indicate different levels of significance; p-value between 0.01 and 0.05 (*), p- value between 0.001 and 0.01 (**) and $p < 0.001$ (***).

Appendix 4-4

Average tensile strength of 8 hair curl groups.

	Average Tensile Strength of 8 Hair Groups (MPa)		
Hair Group	**Mean**	**Std. Deviation**	**95% CI (LL - UL)**
I	200,5	22,86	191,8 - 209,2
II	205	27,16	197,1 - 212,9
III	204,5	19,43	198,8 - 210,2
IV	211,1	22,71	203,8 - 218,3
V	203,7	28,37	192,5 - 214,9
VI	190,4	25,34	182,3 - 198,5
VII	185,4	18,97	178,3 - 192,5
VIII	192,3	24,43	181,5 - 203,1

Average tensile strength of 6 hair groups

	Average Tensile Strength of 6 Hair Groups (MPa)		
Hair Group	**Mean**	**Std. Deviation**	**95% CI (LL - UL)**
1	200,5	22,86	191,8 - 209,2
2	205,0	27,16	197,1 - 212,9
3	204,5	19,43	198,8 - 210,2
4	211,1	22,71	203,8 - 218,3
5	195,7	27,20	189,1 - 202,4
6	188,3	21,50	182,3 - 194,3

CHAPTER FIVE

5 DISCUSSION

The interest in human scalp hair extends beyond cosmetic applications. Hair is increasingly being used for diagnoses[107,108,115], detection of drug use and abuse[5,8,112] and as a substrate to bio mark disease progression[15,16,19].

Some of the most recent investigations include testing for antiretroviral drug levels to monitor treatment compliance[9–13]. Interpretation of hair testing results continue to be based on race as a surrogate for hair morphology, however racial categorizations is limited, subjective and could misconstrue findings[120,169]. Further, variations in hair morphology are usually associated with other hair characteristics such hair growth rate, hair density and biochemical composition. The extent of these variations is possibly masked in subjective racial categorization.

The first geometric classification of hair morphology was by Daniel Hrdy, an anthropologist who assessed the variation of hair form in 7 populations[71]. Unlike other researchers before him, Hrdy systematically studied hair morphology using direct curling variables and attempted to apply quantitative and statistical methods to describe observed variations. Other workers used variables such as hair diameter, medullation scale count or cross-sectional index. Further, Hrdy devised 4 additional curling variables (average curvature, ratio of maximum to minimum curvature, crimp and ratio of natural to straight hair length) to accurately measure hair curl[71].
Hrdy's work was followed by Bailey& Schliebe who focused on average curvature for describing hair morphology[70].

Recently, a new geometric system that classifies hair based on hair curvature was proposed. This new classification used 3 geometric parameters (curve diameter, curl meter and number of waves), adopted from Hrdy, Bailey & Schliebe, to objectively classify hair as I (least curvature) to VIII (greatest curvature). The curve diameter is comprised of circles of known radii and the curl meter is a simplified assessment of the ratio of natural to straight hair length[71] for curly hair groups[63,69] .

Geometric classifications of human scalp hair are a welcomed move away from using race as a surrogate for hair morphology. However to date no study has published data on the reliability of the most recent geometric classification.

The aims of this dissertation were therefore to, firstly evaluate the reliability of the geometric classification and explore whether its reliability could be improved.

Secondly, I sought to elucidate the relationships between the hair morphology and biochemical characteristics, focusing on internal lipid content and FTIR absorption.

Lastly, I investigated the relationships between the physical characteristics of hair with varying degrees of curvature in order to understand associations between hair morphology and mechanical properties, hair growth rate, hair density. Ultrastructural details were elucidated to understand correlations between cortical cell distributions and hair curvature.

Geometric classification of human scalp hair curl: reducing groups from 8 to 6 improves reliability

Natural hair samples from 128 volunteers (83% female and 17% male) were collected to assess the reliability of the new geometric classification. Hair geometry was initially classified using a published template that classifies the variation in hair curvature into 8 groups using 3 parameters; curve diameter, curl meter and counting the number of waves[63,69].

Six centimetre long strands of hair were place on top of the curve diameter template and a glass slide placed on the hair without shifting or altering its natural curl. The hair was then classified as hair curl group I, II, III or IV by superimposing it to the best fit half-circle. For hair with curls too tight to fit in the curve diameter template, both the curl meter and the number of waves calculated were used for classification. The curl meter was a circle with a diameter of 0.98cm. Hair samples that did not fit into the curl meter were classifiable as V and VI and those that completely fit as VII and VIII. Counting the number of waves present in a 5cm strand that was constricted to 4cm further differentiated the high curvature hair groups; up to 3 for V; ≥4 for VI; up to 5 for VII and ≥ 6 for VIII.

Ten strands of hair were assessed from 48 volunteers by 3 evaluators at 2 occasions in order to investigate the reliability of the published classification. The most frequently occurring hair curl group for each set of 10 strands was reported on each occasion. In instances where there was more than one frequently occurring hair curl group, the group with the higher degree of curvature was assigned because I considered this group to be representative for the volunteer than straighter hair that could have straightened due to mechanical damage or extension.

Temporary hair curl change as a result heat and/or cosmetic physical curling would not persist beyond the sample preparation steps. Chemically altered hair (straightened or curled) was excluded from the study.

Further, hair samples were washed in between evaluators in order for the hair to regain its natural non-extended hair form. Lastly, the overall hair curl for each of the 48 volunteers was based on the most frequently occurring hair group of the 6 evaluations (i.e. from 60 hairs).

The last step (counting the number of waves) of 8-group classification was found by the 3 evaluators to be laborious and impractical for the purposes of rapidly classifying hair curl. This classification categorized hair curl groups 1 to 4 similarly as I to IV in th 8-group classification. For differentiating high curvature hair groups, the curl meter circle was still used. Hair group 5 was those hairs that did not fit inside the curl meter and was equivalent to V and VI (in the 8-group classification), while hair group 6 was comprised of hair groups VII and VIII, hair fibres that fitted perfectly inside the curl meter.

In chapter two, the results of the investigation of the reliability of a published geometric classification were presented. Kappa statistics reflecting the level of agreement between the 3 evaluators was 0.447. The reproducibility of the classification was assessed by comparing each evaluator's scores at the two occasions and the intra-observer scores ranged from k = 0.444 (95% CI; 0.334 – 0.553) to k = 0.648 (95% CI; 0.525 – 0.771)].

The Kappa coefficient measures chance corrected agreement between two or more raters and can range between +1 and -1[127]. Kappa values < 0.20 reflect poor

agreement and 0.41-0.60 reflect moderate agreement. Kappa values between 0.61-0.80 are regarded as good agreement, while very good agreement is reflected by kappa values ranging from 0.81 to 1.00[127,129,130]. A kappa value below 0 reflects worse than expected agreement[128].

Improvements were seen in both the reliability and reproducibility of the geometric classification when the 6-group classification was used. The level of agreement between the 3 evaluators was 0.7291. The reproducibility (intra-observer) of the classification ranged from 0.599 (95% CI: 0.422 – 0.776) to 0.836 (95% CI; 0.691 – 0.981). The intra-observer kappa statistic for the one evaluator who classified the additional 80 volunteers was 0.754 (95% CI; 0.669 – 0.839), reflecting good agreement.

The main findings of this study were that the 6-group geomentric classification is more reliable both between three different evaluators and within the same assessor at two different time points.

The Relationship between Biochemistry and Hair Morphology

It has long been largely accepted that the biochemical characteristics of different hair phenotypes are uniform and tend to overlap[93]. This has been illustrated by most amino acid analysis quantification studies, particularly those using whole hair fibre. Investigations of different components of hair proteins have also come to similar conclusions[136,170]. Variations have however been reported in the total internal lipid content of hair from healthy volunteers of different racial groups[73]. Changes in lipid content have also been reported as possible indicators of breast and colon cancer [107,115].

The biochemical characteristics of hair groups in the current study were investigated using 2 approaches;

Total internal lipids were extracted from pulverized hair using organic solvents and non-destructive assessment of whole fibre was profiled using attenuated total reflectance Fourier Transform Infrared Microspectroscopy (ATR-FTIR).

Although an attempt was made to collect similar numbers of samples from each group, the 8-group method that was used initially employed was later shown to be unreliable (chapter 2), contributing to unequal numbers of participants in hair groups.

Total internal content was assessed using the SPV assay and a minimum of two volunteers per hair group were included for comparison were included. The Vanillin Assay has been used to quantify total lipids in serum[149,150] and Meibomian gland secretions[153] and it was adapted for use in a microplate to allow for rapid quantitative analysis by Cheng et al[148]. The assay requires the presence of a carbon-carbon double bond [149] and the unsaturated free internal lipids from the hair shaft that would have been quantified are; ceramide, cholesterol ester (ChE), cholesterol sulphate (ChS) and free fatty acids such as linoleic, oleic and alpha linoleic acids[149,155,171].

Although no distinction of exact lipid class was made in the current study, the observed higher internal lipid content for high curvature hair groups could be attributed to contributions from FFAs, cholesterol esters and cholesterol sulphate. This is consistent finding by Cruz *et al.*, where African hair samples were richer in these lipids than Caucasian or Asian hair samples[73].

Unlike other comparisons of lipid content from FTIR spectra[107,118] that assess absorption of lipids in the 1500 – 1400 cm^{-1} or 1739 – 1740 cm^{-1}, this study focused on the lipid band at 2850 - 2960 cm^{-1} region. This region was discernible from unprocessed spectra (expect for background correction) and did not require derivatization to separate it from other peaks. This was thought to be an important requirement for applications of rapid hair classification of hair. Further, Zhang *et al*[114] observed higher lipid content in the cuticle, so although the evanescent wave of IR radiation did not reach the cortex region, variations in lipid content could still be observed. Indications of spectra in the cortex are; Amide I at approximately 1652 cm^{-1} and Amide II at approximately 1548 cm^{-1}, reflecting α-helical conformation of tertiary proteins[114,146]. An Amide I band at 1630 cm^{-1} with an Amide II band between 1515 – 1525 cm^{-1} indicate proteins that have a β-sheet conformation[146,157]. The keratin conformation observed in the current study was closer to the ranges of the β-sheet form, indicating that the evanescent wave did not did not reach the hair cortex.

Together with the outcomes of the SPV assay, this corroborates reports that African hair has higher lipid content with contribution from both the cortex and cuticle layers.

Further, for the FTIR spectra of hair samples from different geometric groups; curly hair groups also tended to have higher lipid content. Lower amide I and amide II absorption was also observed in these groups.

When the variations in baseline corrected spectra were compared, observations were more haphazard with no clear correlation between biochemistry for the 8 group classification. Trends were however observed trends (although no consistent correlation) between the biochemical characteristics and different hair groups for the 6-group geometric classification.

When an 8-group classification was used, 78% of the variations in the spectra were explained by hair morphology, while for the 6-group classification, hair morphology explained 81% of the variation.

Further, the prediction model for the 6-group classification was better than that of the 8-groups. Using general discriminant analysis, the important wavenumbers that were used to explain the variation between 6 groups were close to bands of interest in biological tissue. Six out of the 9 wavenumbers could be correlated to discernible peaks in the FTIR-spectra of scalp hair. Two of the selected wavenumbers were in the range of O-H absorption and two other wavenumbers were in the Amide I region.

Hair lipid levels were investigated in the current study using the Vanillin assay and FTIR in order to understand baseline levels of lipids across different geometric hair groups for accurate comparisons of diseased hair samples in the future. It is acknowledged that factors such as dietary habits could have a confounding effect on these lipids.

The Relationships between Hair Morphology and Physical Characteristics Mechanical Properties

The mechanical properties of hair fibres were assessed using a miniature tensile tester. For the analysis, single hair fibres were crimped and loaded onto a rotatory carrousel for automated mechanical testing instrument. The setup included a laser scanning micrometre for measuring hair diameter. Mechanical properties quantifiable with this instrument were cross-sectional area, minimum, mean and maximum diameter, elastic modulus, gradient and extension, plateau load and stress, load and work and load at different % strains (15% and 25%), yield and break extensions, post yield gradient, break load and stress, total work and toughness.

The chosen variables for assessments of variations in mechanical properties across groups in the current study were; hair diameter, cross-sectional area, elastic modulus, yield extension, break extension and break stress. Stress & strain curves were generated for all hair groups. These variables are widely used for descriptions of hair strength[92,160,172].

The hair group with the straightest hair (group 1), comprising of Asian volunteers, had the greatest average diameter; as expected, however this variation was not statistically significant from that observed for hair groups 4 to 6. Hair curl groups 2 and 3 were significantly thinner than those of all other groups. This was not surprising because Caucasian hair samples are sometimes reported to be fine or thinner than Asian or African hair samples[22,93].

All hair groups had a yield extension below 30% strain similar to published reports that hair is perfectly elastic up to 30% extension [165], after which point it will not regain its original shape even if the exerted mechanical energy is lifted. The yield strengths observed in the current study were higher than those reported in literature. All yield strengths were above 100MPa. The reported average yield strength for Asian, Caucasian and African hair is 100 MPa, 67 MPa and 58 MPa respectively[160].

The elastic modulus of the hair group 3 was statistically higher than that of all hair groups with a higher degree of curvature; this could be related to the smaller average

diameter for this hair group. No significant differences were observed between hair groups 1 to 3 and 5 to 6. These observations give indications of two major groups; those with low curvature and those with high curvature, masking variations that could be observed for intermediate hair groups.

The lower tensile properties of hair groups with high curvature have been attributed to the kinks present along the hair shafts of such hair groups. These kinks become areas where the applied stress gets concentrated, leading to premature breakage or failure[62].

The tensile strength is the maximum stress that each single fiber was able to withstand. The average tensile strength of the group with the highest curvature (hair group 6) was statistically lower than hair groups 2 to 4.

Hair Growth Parameters

Hair growth rate

Hair growth rate was calculated from the TrichoScan® platform and interscale distance. The TrichoScan platform calculates hair growth parameters and is widely used in dermatology for assessment of hair loss and response to treatments[166,167].

Although the relationship between hair morphology and hair growth was not directly proportional, the growth rate of the curliest hair group was the slowest, as previously reported by other workers[161]. In the current study, significant differences in hair growth rate were observed between the straightest hair groups (1 and 2) and the curly hair groups (4 –6).

Hair growth rate is reported to be related to the distance between cuticle layers for straight hair on scanning electron microscopy[159]. Quantifying interscale distance is similar to the scale count assessment that researchers used to describe hair morphology[71].Using ISD and hair shaft diameter, Baque *et al*. showed that for straight hair from Asian and Caucasian volunteers, a thick hair fibre corresponded with a high growth rate[159].

This study is the first (we are aware of) to report the relationship between ISD and hair growth rate for hair groups with high curvature. The results observed in the current study were similar to those obtained by Baque *et al*. for the ISD of straight hair; however, the anticipated trend that the curliest hair ought to have the longest ISD was not observed. The curliest hair group (6) had shorter inter scale distances than straight hair groups (1 and 2).

Hair growth rates based ISD had no association with hair curl .Hair group 5 had an average hair growth rate that was statistically higher than that of hair groups 1 and 4, which was unexpected because the inverse was observed for hair growth rates based on the TrichoScan ® platform. Further, ISD based growth rates were also observed to be higher than TrichoScan® based results ; 1.1 ± 0.2cm/month (group 1) to 1.4 ± 0.5 cm/month (group 6) versus 0.72 ± 0.2 cm/month (group 1) to 0.39 ± 0.1 (group 6).

The growth rate based on the TrichoScan® approach was fastest for the straightest hair (group1, 0.72 ± 0.3 cm/month), while hair groups with the greatest curvature were significantly slower (5 and 6, 0.39 ± 0.2 and 0.39 ± 0.11 cm/month).

Of the two growth rate assessments, the TrichoScan was observed to be more reliable, having growths that were similar to those reported by other workers (Asian: 0.73 – 1.8 cm/month, Caucasian: 0.50 – 1.5cm/month, African: 0.5 – 0.6 cm/month)[158,162].

The rate of hair growth could influence amounts of drug incorporation into the growing hair shaft. Interestingly, hair testing studies assume a blanket growth rate of 1cm per month for all racial groups[3,6,17,126]. Variations in growth rate across, ages, races and nutritional states should be taken into consideration for all hair groups in order to correctly interpret results obtained for various hair analyses[120,126].

Ultrastructure

Several researchers have visualized the variation in the ratios and distributions of cortical cells within the cortex of different hairs using TEM[77,168]. To our knowledge, the current study is the first to show the distribution cortical cells of more than 2 hair groups using the FLM dual staining protocol.

The arrangement of cortical cells was imaged by FLM using a dual staining protocol has been used for Japanese hair[90]. Straight hair from Japanese volunteers was found to be predominantly composed of paracortical cells[90]. In the current work, the straight hair cortex of samples representing hair groups I to III was observed to be composed of paracortical cells. For curlier hair groups, there were variations in the distributions of orthocortical and paracortical. Samples from hair groups IV to VII were observed to have an almost 1:1 distribution of these cells types, while hair groups VIII cross sections were observed to have lower proportions of orthocortical cells.

This new dual staining techniques by FLM have been used for visualizing cortical cell in straight hair and were found to give similar results to TEM. This study is the first (that we are aware of) to confirm that this is also the case for African hair; FLM techniques are cheaper and more efficient than TEM.

LIMITATIONS

One of the major limitations of the current study was recruitment of volunteers with natural scalp hair. In spite of much advertisement only 128 participants could be included in the study. After geometric classification the hair curl groups were unequal, with the least number of volunteers in group 1 which is the straightest hair group and the most were the curliest hair groups. The biggest contributors to these groups were Asian and African volunteers respectively. Further, although an attempt was made to collect similar numbers of samples from each group, the 8-group method that was used initially was later shown to be unreliable (chapter 2) also contributing to unequal numbers of participants in hair groups.

However, in spite of a small sample size, to our knowledg this is the first thesis to test the reliability of a geometric classification and correlate hair curl with biochemistry and other parameters.

CONCLUSIONS

This thesis is the first to comprehensively investigate the characteristics of human hair using multiple approaches on the same sample pool. Understanding the variation in

human hair morphology is the doorway to elucidating the mechanism involved in substance incorporation as well correct interpretations of hair analyses results.

This thesis supports a geometric classification with fewer groups (6 based kappa statistics and 4, based on biochemistry); it is also the first to report correlations between hair geometry, biochemistry and physical properties.

SUGGESTIONS FOR FUTURE WORK

Improvements on the current work could be to include more volunteers for the assessments of other hair characteristics, particulary biochemistry (internal lipid content and absorption of relavent FTIR bands of interest) in order to expand components that were only explored in the current study. Additionally, an FT-IR prediction model that correlates hair spectra with hair biochemistry would make the use of destructive hair analysis technique for quantifying hair chemistry obsolute. This would allow for rapid scientific classification of hair that would more reliable for use in Medicine and Forensic Science.

REFERENCES

1. **Robbins, C. R. in *Chem. Phys. Behav. Hum. Hair* 177 – 204 (2012).**

2. **Stenn, K. S. & Paus, R. Controls of Hair Follicle Cycling. *Physiol. Rev.* 81, 449–494 (2001).**

3. **Piraccini, B. M., Pazzaglia, M. & Tosti, A. in *Hair growth Disord.* (Blume-peytavi, U., Tosti, A. & Trueb, R. M.) (Springer, 2008).**

4. **Banirashaid, A. Forensic Research and Technology. *J. Forensic Res.* 4, 82 (2013).**

5. **Nakahara, Y. Hair analysis for te abused and therapeutic drugs. *J Chromatogra B Biomed Sci Appl* 733, 161–80 (1999).**

6. **Umweltbundtsesamt. Hair Analysis in Environmental Medicine. *Bundesgesundheitsbl-Gesundheitsforsch-Gesundheitsschutz* 48, 246–250 (2005).**

7. **Appenzeller, B. M. R. & Tsatsakis, A. M. Hair analysis for biomonitoring of environmental and occupational exposure to organic pollutants : State of the art , critical review and future needs. *Toxicol. Lett.* 210, 119–140 (2012).**

8. **Boumba, V. ., Ziavrou, K. . & Vougiouklakis, T. Hair as a biological indicator of drug use, drug abuse or chronic exposure to environmental toxicants. *Int. J. Toxicol.* 143 – 63 (2006).**

9. **Bartelink, I. H. *et al.* Pharmacokinetics of Lopinavir/Ritonavir and Efavirenz in Food Insecure HIV-Infected Pregnant and Breastfeeding Women in Tororo,Uganda. *J. Clin. Pharmacol.* XX, 1 –12 (2013).**

10. **Gandhi, M. *et al.* Atazanavir concentration in hair is the strongest predictor of outcomes on antiretroviral therapy. *Clin. Infect. Dis.* 1267 – 75 (2011).**

11. **Gandhi, M. & Greenblatt, R. . Hair it is: The long and short of monitoring antiretroviral treatment. *Ann. Intern. Med* 137, 696–697 (2002).**

12. **Van Zyl, G. . *et al.* Low lopinavir plasma or hair concentrations explain second protease inhibitor failures in a resource-limited setting. *J. Acquir. Immune Defiency Syndr.* 333 (2011).**

13. **Olds, P. . *et al.* Assessment of HIV antiretroviral therapy adherence by measuring drug concentrations in hair among children in rural Uganda. *AIDS Care* 1 – 4 (2014).**

14. **Staufenbiel, S. M., Penninx, B. W. J. H., Spijker, A. T., Elzinga, B. M. & van Rossum, E. F. C. Hair cortisol, stress exposure, and mental health in humans: a systematic review. *Psychoneuroendocrinology* 38, 1220–35 (2013).**

15. **Karlén, J., Ludvigsson, J., Frostell, A., Theodorsson, E. & Faresjö, T. Cortisol in hair measured in young adults - a biomarker of major life stressors ? *BMC Clin. Pathol.* 11, 12 (2011).**

16. **Sauve, B., Koren, G., Walsh, G., Tokmakejian, S. & Uum, S. Van. Measurement of cortisol in human hair as a biomarker of systemic exposure. *Clin Invest Med* 30, E183–91 (2007).**

17. **Kirschbaum, C., Tietze, A., Skoluda, N. & Dettenborn, L. Hair as a retrospective calendar of cortisol production —– Increased cortisol incorporation into hair in the third trimester of pregnancy. 32–37 (2009). doi:10.1016/j.psyneuen.2008.08.024**

18. **Wołowiec, P., Michalak, I., Chojnacka, K. & Mikulewicz, M. Hair analysis in health assessment. *Clin. Chim. Acta* 419, 139–171 (2013).**

19. **Oimomi, M., Masuda, S., Igaki, N. & Nakamichi, T. Glycation of Hair Protein in the Assessment of Long-term Control of Blood Glucose. *Japanese J. Med.* 27, 277–280 (1988).**

20. **Hijazy, M. in *Princ. Pediatr. Dermatology* (2008).**

21. **Ebling, F. J. The activity of the hair follicle. *J. Soc. Cosmet. Chem.* 15, 447 – 457 (1964).**

22. **Robbins, C. R. in *Chem. Phys. Behav. Hum. Hair* 1 – 104 (2012). doi:10.1007/978-3-642-25611-0**

23. **Hardy, M. H. The secret life of the hair follicle. *Trends Genet.* 8, 55–61 (1992).**

24. **Paus, R. *et al.* A Comprehensive Guide for the Recognition and Classification of Distinct Stages of Hair Follicle. 523–532 (1999).**

25. **Botchkarev, V. A. & Paus, R. Molecular biology of hair morphogenesis: development and cycling. *J. Exp. Zool. B. Mol. Dev. Evol.* 298, 164–180 (2003).**

26. **Chi, W., Wu, E. & Morgan, B. A. Dermal papilla cell number specifies hair size, shape and cycling and its reduction causes follicular decline. *Development* 140, 1676–83 (2013).**

27. **Higgins, C. A., Chen, J. C., Cerise, J. E., Jahoda, C. A. B. & Christiano, A. M. Microenvironmental reprogramming by three-dimensional culture enables dermal papilla cells to induce de novo human hair-follicle growth. *Proc. Natl. Acad. Sci. U. S. A.* 110, 19679–88 (2013).**

28. **Rogers, G. E. Hair follicle differentiation and regulation. *Int. J. Dev. Biol.* 48, 163–70 (2004).**

29. **Fukuyama, K., Inuoe, N., Suzuki, H. & Epstein, W. Keratinization. *Int. J. Dermatol.* 15, 473 – 489 (1976).**

30. **Philpott, M. & Paus, R. in *Mol. basis Epithel. appendage Morphog.* (Chuong, C. .) 75 – 103 (Landes Bioscience Publication, 1998).**

31. **Birbeck, M. S. & Mercer, E. H. The electron microscopy of the human hair follicle. Part 1. Introdcution and the hair cortex. *J. Biophys. Biochem. Cytol.* 3, (1957).**

32. Feughelman, M. & South, N. The physical properties of alpha-keratin fibers. 406, **385–406 (1982).**

33. Zahn, H. Progress report on hair keratin research. *Int. J. Cosmet. Sci.* 24, **163 – 169 (2002).**

34. Cooper, G. . & Sunderland, M. . *The Cell: A Molecular Approach*. (Sinauer Associates, 2000).

35. Yang, F., Zhang, Y. & Rheinst, M. C. The structure of people ' s hair. (2014). doi:10.7717/peerj.619

36. Langbein, L. The Catalog of Human Hair Keratins. I. EXPRESSION OF THE NINE TYPE I MEMBERS IN THE HAIR FOLLICLE. *J. Biol. Chem.* 274, **19874–19884 (1999).**

37. Dunn, S. M., Keough, R. a, Rogers, G. E. & Powell, B. C. Regulation of a hair follicle keratin intermediate filament gene promoter. *J. Cell Sci.* 111 (Pt 2, **3487–96 (1998).**

38. Hoffmann, R. & McElwee, K. J. Hair follicle mesenchymal stem cells and use thereof. (2013).

39. Robbins, C. R. *Chemical and Physical Behaviour of Human Hair*. (1994).

40. Thibaut, S., Gaillard, O., Bouhanna, P., Cannell, D. . & Bernard, B. Human hair shape is programmed from the bulb. *Br. J. Dermatol.* 152, **632–8 (2005).**

41. Blount, M., Goff, S. & Slusarewicz, P. In vitro degradation of the inner root sheath in human hair follicles lacking sebaceous glands. *Br. J. Dermatol.* 158, **22 – 30 (2008).**

42. Alonso, L. & Fuchs, E. The hair cycle. *J. Cell Sci.* 119, **391–393 (2006).**

43. Kealey, T., Philpott, M. & Guy, R. The regulatory biology of the human pilosebasecous unit. *Baillieres. Clin. Obstet. Gynaecol.* 11, **205 – 227**

(1997).

44. Shimomura, Y. & Christiano, A. M. Biology and Genetics of Hair. *Annu Rev Genomics Hum Genet.* 11, 109 – 32 (2010).

45. Morioka, K. Hair Cortex and Hair Cuticle. *Hair Follicle Differ. Under Electron …* (2005). at <http://link.springer.com/content/pdf/10.1007/4-431-27179-1_3.pdf>

46. Bernard, B. A. Hair biology: an update. *Int. J. Cosmet. Sci.* 24, 13 –16 (2002).

47. Krause, K. & Foitzik, K. Biology of the Hair Follicle: The Basics. *Semin. Cutan. Med. Surg.* 25, 2–10 (2006).

48. Paus, R. Principles of hair cycle control. *J. Dermatol.* 25, 793–802 (1998).

49. Schneider, M. R., Schmidt-Ullrich, R. & Paus, R. The hair follicle as a dynamic miniorgan. *Curr. Biol.* 19, R132–42 (2009).

50. Rogers, G. E. Electron microscopy of wool. *J. Ultrastruct. Res.* 2, 309 – 330 (1959).

51. Panteleyev, A. A., Jahoda, C. A. B. & Christiano, A. M. Hair follicle predetermination. *J. Cell Sci.* 114, 3419 – 3431 (2001).

52. Stenn, KS., Parimoo, S and Prouty, S. *Growth of the hair follicle: a cycling and regenerating biological system. In: Molecular Basis of Epithelial Appendage Morphogenesis*. (1998).

53. Araújo, R., Fernandes, M. & Cavaco-paulo, A. Biology of Human Hair : Know Your Hair to Control It. (2010). doi:10.1007/10

54. Paus, R., Muller-Rover, S. & Botchkarev, V. A. Chronobiology of the hair follicle: hunting the ‘ hair cycle clock’. *J. Investig. Dermatol. Symp. Proc.* 4, 338–345 (1999).

55. Wolfram, L. J. Human hair: a unique physicochemical composite. *J. Am. Acad. Dermatol.* 48, S106–14 (2003).

56. Randall, V. A. Androgens and hair : a biological paradox. 207–232

57. Trotter, M. A review of the classifications of hair. *Am. J. Phys. Anthropol.* 24, 105–126 (1938).

58. Schlake, T. Determination of hair structure and shape. *Semin. Cell Dev. Biol.* 18, 267–273 (2007).

59. Lindelof, B., Forslind, B., Hedblad, M. & Kaveus, U. Human hair morphology revealed by light and scanning electronmicroscopy and computer aided three-dimensional reconstruction. *Arch Dermatol* 124, 1359–63 (1988).

60. Thibaut, S., Barbarat, P., Leroy, F. & Bernard, B. A. Human hair keratin network and curvature. 46, 7–10 (2007).

61. Robbins, C. R. *Chemical compositon of different hair types*. (Springer Berlin Heidelberg, 2012). doi:10.1007/978-3-642-25611-0

62. Porter, C. E. *et al.* The behavior of hair from different countries. 109, 97–109 (2009).

63. De La Mettrie, R. *et al.* Shape Variability and Classification of Human Hair: A Worldwide Approach. *Hum. Biol.* 79, 265–281 (2007).

64. Davis-Sivasothy, A. *The Science of Black Hair: A Comprehensive Guide to Textured Hair:* (Saja Publishing, 2011). at <https://books.google.co.za/books?id=WQAZAgAAQBAJ>

65. http:/www.andrewalkerhair.com/v/vspfiles/templates/140/Hair-Typing-System.asp.

66. Webpage. www.healthyhairdimensions.com/?page_id=71.

67. Bigby, M. & Thaler, D. Describing patient's 'race' in clinical presentations should be abandoned. *J. Am. Acad. Dermatol.* 54, 1074 – 6 (2006).

68. Khumalo, N. P. Yes, let's abandon race - It does not accurately correlate with hair form. *J. Am. Acad. Dermatol.* 56, 709–710 (2007).

69. Loussouarn, G. *et al.* Worldwide diversity of hair curliness : a new method of assessment. (2007).

70. Bailey & Schliebe, S. *The Presicion of average curvature meaurement. In Human Hair:Proceedings of the Symposium on Forensic Hair Comparisons, Federal Bureau of Investigation, ed. Washing, DC: US Govenment Printing Office.* (1985).

71. Hrdy, D. Quantitative hair form variation in seven populations. *Am. J. Phys. Anthropol.* 39, 7 –18 (1973).

72. Ogle, R. J. & Fox, M. J. *Atlas of Human Hair Microscopic Characteristics*. (CRC Press LLC, 1999).

73. Cruz, C. F. *et al.* Keratins and lipids in ethnic hair. *Int. J. Cosmet. Sci.* 35, 244–9 (2013).

74. Wolfram, L. J. & Lindemann, M. . Some observations of the hair cuticle. *J. Soc. Cosmet. Chem.* 22, 839 – 856 (1971).

75. Areida, S. K., Ismail, M. F., Hady, E. K. A. & Osman, A. O. Molecular Characterization of the Hair Cuticle and its Extracted Proteins in Seven Mammalian Species. *Egypt. J. Hosp. Med.* 23, 287–308 (2006).

76. Robbins, C. R. in *Chem. Phys. Behav. Hum. Hair* 537 – 640 (Springer-Verlag Berlin Heidelberg, 2012). doi:10.1007/978-3-642-25611-0

77. Leon, H. Structural aspects of keratin fibres. 445, (1972).

78. Bradbury, J. H., Chapman, G. ., Hambly, A. . & King, N. L. . Separation of chemically unmodified histological components of hair fibres and

analyses of cuticles. *Nature* 210, **1333 – 1334 (1966).**

79. Swift, J. A. & Bews, B. . The chemistry of the human hair cuticle: part 3: Isolation and amino acid analysis of sufractions of cuticle obtained by pronase and trypsin difestion. *J. Cosmet. Sci.* 27, **289 – 300 (1976).**

80. Robbins, C. R. & Crawford, R. Cuticle damage and the tensile properties of human hair. *J. Soc. Cosmet. Chem.* 42, **59 –67 (1991).**

81. Fraser, R. D. ., MacRae, T. . & Rogers, G. E. in *Keratins , Thier Compos. Struct. Biosynthesis.* (1972).

82. Popescu, C. & Hocker, H. Hair - the most sohpisticated biological composite. *Chem. Soc Rev.* 36, **1282 – 1291 (2007).**

83. Kassenbeck, P. in *Hair Res.* (Orfanos, C. ., Montagna, W. & Stuttgen, G.) 52 – 64 (Springer-Verlag Berlin, 1981).

84. Mowat, I., Parmar, R. ., Speakmann, P. . & Woodhouse, M. Crimp, Amino-acid Composition, and the Proportion of Orthocortical, Paracotival and Mesocortical Cells in Wool from Different Breeds of Sheep. *J. Text. Inst.* 73, **246 – 248 (1982).**

85. Harland, D. P., Vernon, J. A., Walls, R. J. & Woods, J. L. Transmission electron microscopy staining methods for the cortex of human hair : a modified osmium method and comparison with other stains. 243, **184–196 (2011).**

86. Takizawa, T., Takizawa, T., Uchiwa, H. & Arai, S. Ultrastructural Localization of Hair Keratins in Human Scalp Hair Shafts as Revealed by Rapid-Freezing Immunocytochemistry. *Acta Histochem. Cytochem.* 31, **237–242 (1998).**

87. Orwin, D. F. ., Woods, J. L. & Ranford, S. . Cortical cell types and thier distribution in wool fibres. *Aust. J. Biol. Sci.* 37, **237 – 255 (1984).**

88. Caldwell, J. P., Mastronarde, D. ., Woods, J. L. & Bryson, W. G. The three dimensional arrangement of intermediate filaments in Romney wool

cortical cells. *J. Struct. Biol.* 151, **298 – 305 (2005).**

89. Harland, D. P., Caldwell, J. P., Woods, J. L., Walls, R. J. & Bryson, W. G. Arrangement of trichokeratin intermediate filaments and matrix in the cortex of Merino wool. *J. Struct. Biol.* 173, **29 – 37 (2011).**

90. Bryson, W. G. *et al.* Cortical cell types and intermediate filament arrangements correlate with fiber curvature in Japanese human hair. *J. Struct. Biol.* 166, **46–58 (2009).**

91. Harland, D. P. *et al.* Three-dimensional architecture of macrofibrils in the human scalp hair cortex. *J. Struct. Biol.* 185, **397–404 (2014).**

92. Kamath, Y., Hornby, S. & Weigmann, H. Mechanical and fractographic behavior of negroid hair. *J Soc Cosmet Chem* 43, **21–43 (1984).**

93. Robbins, C. R. in *Chem. Phys. Behav. Hum. Hair* 105 – 176 (Springer-Verlag Berlin Heidelberg, 2012).

94. Khumalo, N., Dawber, R. & Ferguson, D. Apparent fragility of African hair is unrelated to the cystine-rich protein distribution : a cytochemical electron microscopic study. 311–314 (2005).

95. Hutchinson, P. E. & Thompson, J. R. The size and form of the medulla of human scalp hair is regulated by the hair cycle and cross-sectional size of the hair shaft. *Br. J. Dermatol.* 140, **438–445 (1999).**

96. Yoshida, H. *et al.* Keratins of the human occipital hair medulla: androgenic regulation of in vitro hair keratin K37 expression. *Br. J. Dermatol.* 169, **218–21 (2013).**

97. Clay, R., Cook, K. & Routh, J. I. Studies in the composition of human hair. *J Am Chem Soc* 62, **2709–2710 (1940).**

98. Curry, K. V. & Golding, S. Hair lipids -I. The extraction of fatty materials from hair clippings. *J. Soc. Cosmet. Chem.* 22, **681 – 699 (1971).**

99. Coderch, L. *et al.* Lamellar rearrangement of internal lipids from human hair. *Chem. Phys. Lipids* 155, 1–6 (2008).

100. Masukawa, Y., Narita, H. & Imokawa, G. Characterization of the lipid composition at the proximal root regions of human hair. *J. Cosmet. Sci.* 56, 1–16 (2005).

101. Lee, W.-S. Integral hair lipid in human hair follicle. *J. Dermatol. Sci.* 64, 153–158 (2011).

102. Koch, J., Aitzetmuller, K., Horf, G. . & Waibel, J. Hair lipids and their contribution to the perception of hair oiliness: part 1: surface and internal lipids in hair. *J. Soc. Cosmet. Chem.* 33, 317 – 326 (1982).

103. Evans, D. . & Lanezki, M. Cleavage of intergral surface lipids of wool by aminolysis. *Textilw Res. J.* 67, 435 – 444 (1997).

104. Bhushan, B. & Chen, N. AFM studies of environmental effects on nanomechanical properties and cellular structure of human hair. *Ultramicroscopy* 106, 755–764 (2006).

105. Duvel, L., Chun, H., Deppa, D. & Wertz, P. W. Analysis of hair lipids and tensile properties as a function of distance from scalp. 193–197 (2005).

106. Lyman, J. D. & Murray-Wiljelath, J. Fourier transform infrared attenuated total reflection analysis of human hair: comparison of hair from breast cancer patients with hair from healthy subjects. *Appl. Spectrosc.* 59, 26 – 32 (2005).

107. Lyman, J. D. & Fay, G. S. The effect of breast cancer on the Fourier transform infrared attenuated total reflection spectra of human hair. *eCancer Med. Sci.* 405, (2014).

108. James, V., Kearsley, J., Irving, T., Amemiya, Y. & Cookson, D. Using hair to screen for breast cancer. *Nature* 398, 33–34 (1999).

109. Ajose, F. O. A. Diseases that turn African hair silky. *Int. J. Dermatol.* 51, 12 – 16 (2012).

110. **Schräder, J., Rothe, M. & Pragst, F. Ethyl glucuronide concentrations in beard hair after a single alcohol dose: evidence for incorporation in hair root. *Int. J. Legal Med.* 126, 791–9 (2012).**

111. **Measurement of Cortisol in Hair : Some Recent Investigations. 2–6**

112. **Pragst, F. & Balikova, M. . Sate of the art in hair analysis for the detection of drug and alcohol abuse. *Clin. Chim. Acta* 370, 17 – 49 (2006).**

113. **James, V. J. A place for fiber diffraction in the detection of breast cancer ? *Cancer Detect. Prev.* 30, 233–238 (2006).**

114. **Zhang, G., Senak, L. & Moore, D. J. Measuring changes in chemistry, composition, and molecular structure within hair fibers by infrared and Raman spectroscopic imaging. *J. Biomed. Opt.* 16, 056009 (2011).**

115. **James, V. Fibre diffraction from a single hair can provide an early non-invasive test for colon cancer. *Med Sci Mon It* 7, MT79 – 84 (2003).**

116. **Barton, P. M. J. A Forensic Investigation of Single Human Hair Fibres using FTIR-ATR Spectroscopy and Chemometrics. (2011).**

117. **Lin, S.-Y., Li, M.-J. & Cheng, W.-T. FT-IR and Raman vibrational microspectroscopies used for spectral biodiagnosis of human tissues. *Spectroscopy* 21, 1 – 30 (2007).**

118. **Lyman, J. D. & Schofield, P. Attenuated total reflection Fourier transform spectroscopy analysis of human hair fibre structure. *Appl. Spectrosc.* 62, 525 – 535 (2008).**

119. **Little, J. . & Kridel, S. . Fatty acid synthases are expressed in cancer. *Subcell Biochem* 49, 169 – 94 (2008).**

120. **Mieczkowski, T. The Further Mismeasure : The Curious Use of Racial Categorizations in the Interpretation of Hair Analyses. *Int. J. Drug Test.* 2, 1–20 (1999).**

121. Gray, J. *Human hair diversity*. (Wiley, 2001).

122. Ogle, R. J. & Fox, M. J. *Atlas of Human Hair: Microscopic Characteristics (Google eBook)*. (CRC Press LLC, 1999). at <http://books.google.com/books?id=-WdtFZoZVOgC&pgis=1>

123. Wickenheiser, R. A. & Hepworth, D. G. Further evaluation of probabilities in human scalp hair comparisons. *J. Forensic Sci.* 35, 1323–1329 (1990).

124. Khumalo, N. P., Gumedze, F., Lehloenya, R. & Ward, G. Folliculitis keloidalis nuchae is associated with the risk for bleeding from haircuts. *Int. J. Dermatol.* 50, 1212 – 1216 (2011).

125. Khumalo, Nonhlanhla P., Callender, V. D. in *Hair growth Disord.* 483 – 497 (Springer US, 2008).

126. Russell, E., Koren, G., Rieder, M. & Uum, S. Van. Hair cortisol as a biological marker of chronic stress : Current status , future directions and unanswered questions. *Psychoneuroendocrinology* 37, 589–601 (2012).

127. McHugh, M. L. Interrater reliability: the kappa statistic. *Biochem. Medica* 22, 276 – 82 (2012).

128. Viera, A. J. & Garret, J. M. Understanding the Interobserver Agreement: The Kappa Statistic. *Fam. Med.* 37, 360 –3 (2005).

129. Cohen, J. . A coefficient of agreement for nominal scales. *Educ. Psychol. Meas.* 20, 37 – 46 (1960).

130. Landis, J. . & Koch, G. . The measuremenet of observer agreement for categorical data. *Biometrics* 33, 159 – 74 (1977).

131. Bryant, H., Porter, C. & Yang, G. Curly hair: measured differences and contributions to breakage. *Int. J. Dermatol.* 51, 8 – 11 (2012).

132. Gandhi, M. *et al.* Protease inhibitor levels in hair samples strongly predict

virologic responses to HIV treatment. *AIDS* 471 (2009).

133. Shah, S. . *et al.* Simultaneous analysis of antiretroviral drugs abacavir and tenofovir in human hair by liquid chromatography-tandem mass spectrometry. *J. Pharm. Biomed. Anal.* 308 – 13 (2013).

134. Thibaut, S. *et al.* Hair keratin pattern in human hair follicles grown in vitro. 160–164 (2003).

135. Dekoi, S. & Jidoi, J. Amounts of fibrous and matrix substances in hairs of differenet races. *J. Dermatol. Sci.* 17, 62– 4 (1990).

136. Dekoi, S. & Jidoi, J. Hair low-sulphur protein composition does not differ electrophoretically among different races. *J. Dermatol. Sci.* 15, 393 – 6 (1988).

137. Franbourg, A., Hallegot, P., Baltenneck, F., Toutain, C. & Leroy, F. Current research on ethnic hair. *J. Am. Acad. Dermatol.* 48, S115 – 9 (2003).

138. Jones, L. . Hair structure anatomy and comparative anatomy. *Clin. Dermatology* 19, 95 – 103 (2001).

139. Allen, A. ., Ellis, J. & Rivett, D. . The presence of glycoproteins in the cell membrane complex of a variety of keratin fibres. *Biochem. Biophys. Acta* 1074, 331 – 333 (1991).

140. Kreplak, L. *et al.* Profiling lipids across Caucasian and Afro-American hair transverse cuts , using synchrotron infrared microspectrometry. 369–374 (2001).

141. Jones, L. . & Rivett, D. . The role of 18-methyleicosanoic acid in the structure and formation of mammalian hair fibres. *Micron* 28, 469 – 485 (1997).

142. Bertrand, L., Doucet, J., Simionovici, A., Tsoucaris, G. & Walter, P. Lead-revealed lipid organization in human hair. *Biochim. Biophys. Acta - Gen. Subj.* 1620, 218–224 (2003).

143. Bramanti, E. *et al.* A new approach to the study of human hair by means of FT-IR microspectroscopy. 296, **285–296 (1992).**

144. Doyle, W. M. Principles and Applications of Fourier Transform Infrared (FTIR) Process Analysis.

145. Staurt, B. *Infrared Spectroscopy: Fundamentals and Applications*. (2004).

146. Gallagher, W. FTIR Analysis of Protein Structure. 662–666 (1997).

147. Panayiotou, H. & Kokot, S. Matching and discrimination of single human-scalp hairs by FT-IR micro-spectroscopy and chemometrics. *Anal. Chim. Acta* 392, **223–235 (1999).**

148. Cheng, Y.-S., Zheng, Y. & VanderGheynst, J. Rapid Quantitative Analysis of Lipids Using a Colorimetric Method in a Microplate Format. *Lipids* 46, **95–103 (2011).**

149. Knight, J. A., Anderson, S. & Rawle, J. M. Chemical basis of the sulfo-phospho-vanillin reaction for estimating total serum lipids. *Clin. Chem.* 18, **199–202 (1972).**

150. Johnson, K. R., Ellis, G. & Toothill, C. The sulfophosphovanillin reaction for serum lipids: a reappraisal. *Clin. Chem.* 23, **1669–1678 (1977).**

151. Kyriacou, K. COASTAL RESOURCES AND NUTRITION AMONG MIDDLE STONE AGE HUNTER-GATHERERS IN THE SOUTHWESTERN CAPE. (2014).

152. Centerchem, I. *Sunflower Oil*.

153. McMahon, A., Lu, H. & Butovich, I. A. The Spectrophotometric Sulfo-Phospho-Vanillin Assessment of Total Lipids in Human Meibomian Gland Secretions. *Lipids* 48, **513–525 (2013).**

154. Mishra, S. K. *et al.* Rapid quantification of microalgal lipdis in aqueous medium by a simple colorimetric method. *Bioresour. Technol.* 155, **330 –**

333 (2014).

155. Takahashi, T. & Yoshida, S. Distribution of Glycolipid an Unasturated Fatty Acids in Human hair. *Lipids* 49, 905 – 917 (2014).

156. Ning, Y.-C. *Interpretation of Organic Spectra*. (John WIley & Sons (Asia) Pte Ltd, 2011).

157. Zhang, G., Moore, D. J., Zhang, G., Senak, L. & Moore, D. J. Measuring changes in chemistry , composition , and molecular structure within hair fibers by infrared and Raman spectroscopic imaging Measuring changes in chemistry , composition , and molecular structure within hair fibers by infrared and Raman spectrosc. doi:10.1117/1.3580286

158. Loussouarn, G., Rawadi, E. & Genain, G. Diversity of hair growth profiles. *Int. J. Dermatol.* 44, 6 – 9 (2005).

159. Saint Olive Baque, C. *et al.* Relationships between hair growth rate and morphological parameters of human straight hair: A same law above ethnical origins? *Int. J. Cosmet. Sci.* 34, 111–116 (2012).

160. Seshadri, I. P. & Bhushan, B. Effect of ethnicity and treatments on in situ tensile response and morphological changes of human hair characterized by atomic force microscopy. *Acta Mater.* 56, 3585–3597 (2008).

161. Loussouarn, G. African hair growth parameters. *Br. J. Dermatol.* 145, 294–7 (2001).

162. McMicheal, A. Ethnic hair update: past and present. *J. Am. Acad. Dermatol.* 48, S127–33 (2003).

163. L.M. Dowling, R. D. R. K. F. L. A Novel Route to the Isolation of Ortho and Para Cortical Cells from Merino Wool. in *Proc. 8th Int. Wool Text. Res. Conf.* I, 214 –224 (1990).

164. Abramoff, M. D., Magalhaes, P. J. & Ram, S. J. Image processing with ImageJ. *Biophotonics Int.* 11, 36 – 42 (2004).

165. Swift, J. a. The mechanics of fracture of human hair. *Int. J. Cosmet. Sci.* 21, 227–239 (1999).

166. Hoffmann, R. TrichoScan: A Novel Tool For The Analysis of Hair Growth In Vivo. *J Investig Dermatol Symp Proc* 8, 109–115 (2003).

167. Gassmueller, J., Rowold, E., Frase, T. & Hughes-Formella, B. Validation of TrichoScan technology as a fully-automated tool for evaluation of hair growth parameters. *Eur. J. Dermatol.* 19, 224–231 (2009).

168. Swift, J. A. in *Form. Struct. Hair* (Jolles, P., Zahn, H. & Hocker, H.) 171 (Birkhauser Verlag, Basel, 1997).

169. Marques, P. R. Factors To Consider When Using Hair as a Cocaine-Exposure Measure for Mothers or Newborns. 183–197 (1991).

170. Menefee, E. Component distributions in keratins and their estimation from amino acid analyses. 30, 17–30 (1985).

171. Barba, C., Martí, M., Carilla, J., Manich, A. . & Coderch, L. The effect of internal lipids on the water soprtion kinetics of keratinized tissues. *J Therm Anal Calorim* (2015).

172. Lee, J. & Kwon, H. J. Measurement of stress-strain behaviour of human hair fibres using optical techniques. *Int. J. Cosmet. Sci.* 35, 238–243 (2013).

ADDENDUM 1:

Absorption of cancer associated lipid band across hair groups

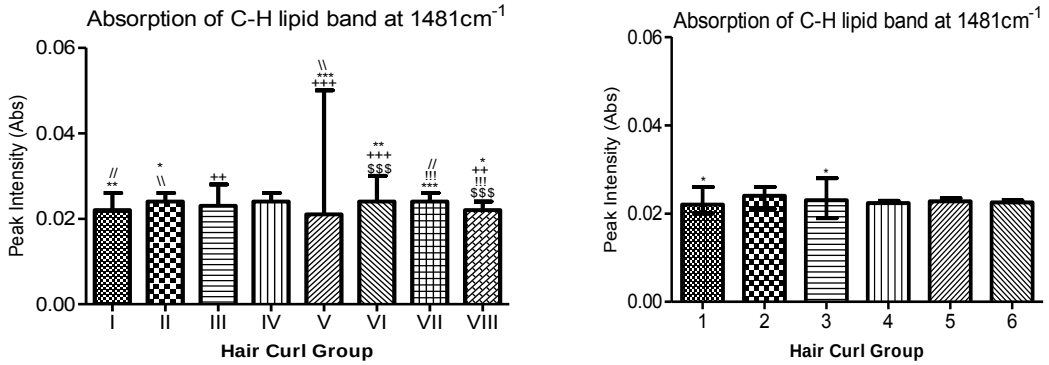

When the absorption of the cancer associated lipid peak (1400 – 1500 cm^{-1}) was investigated, spurious results were observed for the 8-group classification. The absorption of this C-H band was observed to be uniform for the 6-group classification, although hair group 3 was significantly higher than 1. The absorbance for this band ranged from 0.0220 to 0.00240 across the 6 groups. No major differences were observed for the adsorption of the C-H 1481 cm^{-1} with variations in hair morphology for the 6-group classification.

This uniformity of this peak (at 1481 cm^{-1}) in healthy patients confirms that this band is suitable region for indications of baseline characteristics of lipids. Elevated peak intensities in this region have been reported in hair samples from patients with breast cancer[107]. Interestingly, this peak did not require derivatization to separate it from other peaks, as reported in the cancer study[107]. Other peaks might however be present in this range (1400 – 1500 cm^{-1}) that might require spectral processing.

ADDENDUM 2:

Kappa statistics for 4-group classification

Following indications from FTIR data analysis that a 4-group classification might be more reliable, the reliability of this classification was investigated. The 8-group classification was merged into 4 groups (I & II (A), III & IV (B), V & VI (C) and VII & VIII (D)). Improved inter and intrarater statistics for this merged classification were observed and are shown in Table 1 and Table 2 below.

An improved inter-rater agreement was observed for the 4-group classification, k = 0.610 (95% CI 0.513 – 0.707), compared to the 8-groups (k = 0.380, 95% CI 0.313 – 0.447). The intra-rater agreement ranged for the between evaluators for the 4 groups was k =0.581 (95% CI: 0.421 – 0.741) to k = 0.701 (95% CI 0.525 – 0.8277) while that for the 8 groups had been k = 0.444 (95% CI; 0.334 – 0.553) to k = 0.648 (95% CI; 0.525 – 0.771). The results for the 8-group classification are reported in Chapter Two (Tables 2-1 and 2-2).

Table 1: Inter-rater agreement when 8-group classification n is reduced to 4 groups: 3 evaluators

Hair Group	**Kappa**	**95% CI**
A	**0.699**	**0.533 – 0.866**
B	**0.658**	**0.491 – 0.825**
C	**0.447**	**0.281 – 0.614**
D	**0.601**	**0.435 – 0.787**
Combined	**0.610**	**0.513 – 0.707**

Table 2: Intra-rater agreement (3 evaluators, 4-group classification)

	Agreement	Exp. Agreement	Kappa	95% CI
Evaluator 1	75.00%	25.35%	0.665	0.503 - 0.827
Evaluator 2	68.75%	25.43%	0.581	0.421 - 0.741
Evaluator 3	79.17%	30.25%	0.701	0.525 - 0.877